Experimental and Theoretical Studies on Microalgal Cell Adhesion and Interactions on Membranes

Negar Khosravi Zadeh, MSc in Environmental Engineering

Supervisors: Dr. Baoqiang Liao and Dr. Pedram Fatehi

August 2021

Contents

Abstract

Microalgae Cell adhesion is global and plays a critical role in different scientific and engineering problems especially in wastewater treatment. This study focused on both experimental and theoretical studies on microalgal cell adhesion and interactions on membrane surfaces. Microalgal cells (*Chlorella vulgaris* (C.V.)) were cultivated and characterized for cell adhesion study on various hydrophobic membrane surfaces (PDMS, PU and PTFE). Microalgal cell adhesion kinetics were studied using a Quartz Crystal Microbalance D (QCM-D). Furthermore, a quantitative scale to predict cell adhesion was suggested by identifying the major interaction between microalgae and membrane surface. This thesis reports the total interaction energy between algae cells and membrane surfaces in the different group of membranes based on the Extended Derjaguin, Landau, Verwey, Overbeek (XDLVO) method using the Physiochemical particle and surface properties. The simulation and calculation were on membrane and two different shapes of microalgae (Circle and ellipse). The results of cell adhesion kinetic studies using QCM-D showed that the properties of membranes had a significant impact on cell adhesion. A more hydrophobic membrane led to a fast and large quantity biofilm formation. The modelling results indicated that membrane asperity height and particle asperity number were more and less effective factors in the range of total interaction energy and adhesion. Also, the results show that membrane material is another significant factor in interaction energy because proximity was observed between the results of two sensors. The interaction energy trends were consistent with the experimental results in that a stronger attractive interaction energy favored a fast and large quantity of microalgal biofilm formation on more hydrophobic membrane surface.

1. Introduction

The United Nations (UN) acknowledged in 2010 that access to potable water is a fundamental human right (Meier et al. 2012). With global industrialization and population growth, the demand for clean water has increased dramatically. It is estimated that over two billion people have no access to safe and clean water, and over two million tons' human wastes are discharged to the water body daily, and over 70% wastewater from developing countries are not appropriately treated before entering the aquatic system (Massoud et al., 2009). Thus, it calls the scientific communities to develop low cost, highly efficient, and robust water, and wastewater purification technology to need the need of human being and industries.

Significant progresses have been made in developing new technologies for water and wastewater purification. Physical, chemical, and biological technologies for water and wastewater purification have been widely developed(Qu and Fan 2010). Among these technologies, flocculation, sedimentation, adsorption, membrane technology, activated sludge processes, biofilm processes, and microalgae processes are excellent examples of full-scale applications in water and wastewater purification (Alsheyab et al. 2010). Although these technologies have many advantages, the disadvantages of these technologies, such as excess sludge production, high energy consumption, addition of chemicals (causes secondary pollution), and high capital and operating costs, have limited its wide full-scale application and economic benefits. Thus, it is highly desirable to continuously search for novel technologies for water and wastewater purification.

In recent year, the purpose of algae and microalgae for wastewater treatment has received much attention, due to its high capability of nutrients (N and P) uptake and the high value of microalgae feedstock for food and biofuel. Extensive studies have been conducted in using microalgae for nutrients removal(Travieso et al. 1996) and cultivating microalgae as feedstock for food and biofuel(Lum et al. 2013). Microalgae for wastewater treatment for nutrients removal can be classified as suspended growth and immobilized growth (biofilm). The suspended growth (microbial flocs) processes are associated with a high cost of microalgal harvest and dewatering, due to the low concentration (0.2-1g/L) in the photo bioreactors(Ugwu et al. 2008). On the other hand, the immobilized growth (biofilm) processes have increased the microalgae concentration significantly (10-50 g/L) and thus can reduce the harvesting and dewatering costs of the microalgae processes significantly(Fasaei et al. 2018).

6

Compared to the widely studies of microalgal microbial floc processes, limited studies have been conducted on the microalgal biofilm processes(Irving and Allen 2011). The wide application of the microalgal biofilm processes has been limited, due to a lack of fundamental understanding of the biofilm formation and detachment process and how the microalgae and substratum properties, process conditions, and environmental conditions will affect the microalgal biofilm formation and detachment.

The overall objective of this study is to develop an increased fundamental understanding of the microalgal biofilm formation and detachment. More specifically experimental studies on microalgal cell adhesion on hydrophobic membranes and theoretical studies on the interactions of microalgal cells and hydrophobic membranes would be studies. Specific objectives are listed below:

1.) Characterize the properties (size, zeta potential, and contact angle) of microalgal cells (*Chlorella vulgaris*) and membrane properties (contact angle and zeta potential).
2.) Investigate cell adhesion of *Chlorella vulgaris* on hydrophobic membranes using QCM sensors.
3.) Modeling the interactions of *Chlorella vulgaris* and flat hydrophobic membranes using extended DLVO theory.
4.) Correlate the cell adhesion experimental results with the extended DLVO theory modelling results

2. Literature review

Microalgae is a promising technology for wastewater treatment. Three distinct advantages of using microalgae for wastewater treatment are: 1.) microalgae has a high capability of nutrients (N and P) uptakes from wastewater for nutrients recovery and reuse; 2.) microalgae uses CO_2 as a carbon source for growth and thus plays a vital role in greenhouse gas emission reduction; and 3.) microalgae is an excellent feedstock for foods, biofuels, and various bioproducts. The following sections provide a literature review on the recent advances of microalgae for wastewater treatment and its applications.

2.1 What are Microalgae?

Microalgae is a kind of microorganisms that are invisible to the eyes that they are found in fresh and mineral water systems that they are alive in the water and sediment. Microalgae are unicellular that are individually or in the group. Depending on the variety, algae sizes can change from a few micrometers to a few hundred micrometers. Microalgae, are able to perform photosynthesis, that is important for life on earth; they produce about half of the oxygen of atmospheric and use at the same time the gas carbon dioxide of the greenhouse to produce photo autotrophic ally(Spolaore et al. 2006a).
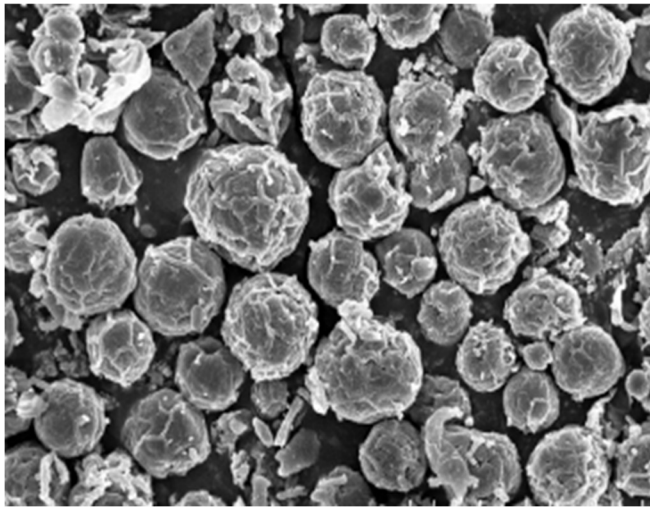
Figure 2.1. *Chlorella vulgaris* Microalgae cells (Liang et al. 2012).

2.2 Characteristics of microalgae

Microalgae is a form of photosynthetic microorganism, grow up quickly and naturally in plenty overwater areas for instance ponds, lakes, and rivers are considered as one of the most promissory renewable feedstocks for biofuels production. Several comparative benefits of microalgae are comparing with other energy crops, in conditions of faster growth, quicker rotation, greater oil content, better photosynthetic productivity, higher efficiency, advanced biochemical activity, as well as the smaller obligation of agricultural land(Amaro et al. 2011). Also, microalgae acknowledge the direct creation of products desired, for instance bio-oil, hydrogen, and by-products(Posten and Schaub 2009). Although separating microalgae from water mixtures con-strains their large-scale usage as an alternative fuel for energy supply, has huge cost and research on valued and high-quality fuels obtained from microalgae species is worthwhile for future achievements. *Chlorella vulgaris*, a genus of unicellular green microalgae that have the spherical

shape of 2.0–10.0µm in diameter, living both in fresh and marine water, can generally be found in the freshwater of ponds and ditches, moist soil, or other damp situations such as the surface of tree trunks, water pots and damp walls (Posten and Schaub 2009). *Chlorella* has eight species, and *Chlorella vulgaris* is one among them, growing in freshwater.

2.3 Applications of microalgae

In general, microalgae used by the cosmetic and pharmaceutical industry, in wastewater managing, in human nutritional supplements, and in animal feeds supplement. Photosynthetic organisms include chlorophylls that are used for cosmetic and food purposes (Spolaore et al. 2006b). Some species of algae include an active mixture with critical pharmaceuticals purposes for instance antiviral and antibacterial activity. Other combinations have been separated with anti-inflammatory and antitumor activity (Spolaore et al. 2006b). Moreover, "high-value products can be produced by microalgae, such as carotenoids, astaxanthin, antioxidants, and the long-chain polyunsaturated fatty acids: docosahexaenoic acid (DHA), eicosapentaenoic acid (EPA), and arachidonic acid (AA)"(Borowitzka 2013). Another use of microalgae is in the food industry, and they are utilized as food dyes in chewing gums, candies, or beverages (Adarme-Vega et al. 2012). In the last two decades, a significant quantity of studied has been shown to generate biodiesel from lipids extracted from algal biomass and other biofuels such as ethanol.

Figure 2.2 Applications of Microalgae (Spolaore et al. 2006c).

2.3.1 Microalgae in wastewater treatment

Primary treatment and secondary treatment processes have been introduced in a growing number of places to eliminate quickly settled materials (primary treatment) and oxidize the organic material that are in wastewater (secondary treatment). The result is a clear, clean effluent that is

discharged into natural water. The secondary waste is loaded with inorganic nitrogen (Ni) and phosphorus (Pi) and affects eutrophication and more long-term difficulties because of refractory organics and heavy metals that are discharged (Posten and Schaub 2009) This condition calls for a tertiary treatment stage that will remove those inorganic ions. Biological processes seem to perform well compared to the chemical treatment and physical treatment processes, which are, in general, too costly to be implemented in most places and may lead to secondary pollution. Generally, Algae feed on light, temperature, and nutrients (Nitrogen, phosphorous) to grow, so they can destroy nutrients. Still, besides it, some algal blooms result from the higher concentrations of these nutrients in the water. As a result, increase algae, which provide food for aquatics, But, if algae grow too uncontrollably, levels of oxygen in the water will be decreased, and fish will die so, Nitrates have the same impact on aquatic plant growth as phosphates and therefore the same negative effect on water quality(Crini and Lichtfouse 2019; Mata et al. 2010).
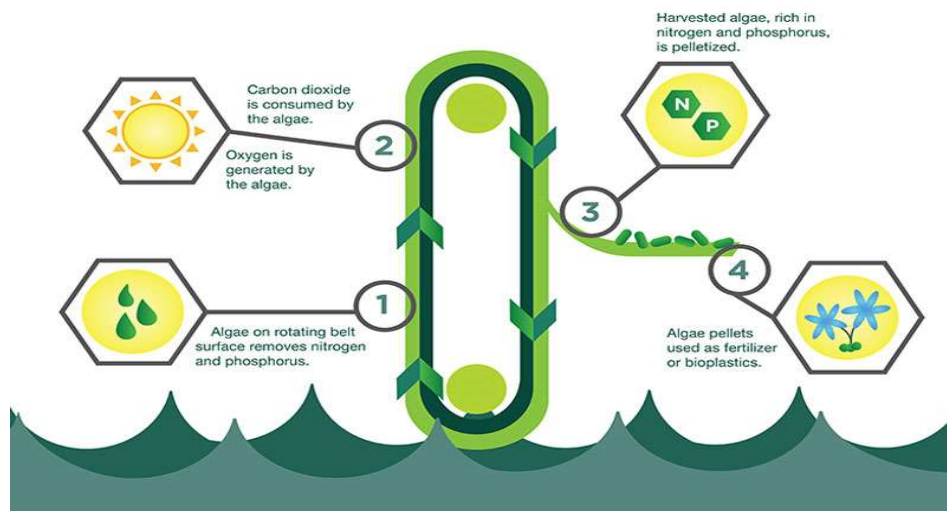
Figure 2.3. Application of Microalgae in wastewater treatment(Posten and Schaub 2009).

2.3.2 Microalgae for Biofuel

Microalgae of marine sequester carbon dioxide (CO_2) all through photosynthesis and may be used to create biogas, including methane and hydrogen, by anaerobic processing (Hughes et al. 2012). While certain microalgae species were known in the 1940s to have cellular lipids in high amounts in selective growth pressures, it was not until the 1950s when algae were seen as a source of

potential energy and were tested for methane gas production via anaerobic digestion of their cell carbohydrates (Oswald and Golueke 1960). Microalgal species' flexibility and (or) adaptively to water and cultural conditions allow us to spare fresh water and arable land for crop production. The land-use productivity of microalgae for biofuel production, growing with 30% oil content with weight, was 130 and 338 times more significant than the typical biodiesel feedstock soybean and corn, respectively (Chisti 2007).

2.3.3 Microalgae as animal feed

Microalgae using as the animal feed has long been studied, dating as far back as in the1950's; only recent literature has shown struggles to supplement lipid-extracted microalgae in animal diets (Austic et al. 2013). At first, researchers sought out methods to culture algae in ponds, and studies on algae supplementation quickly followed the developments into animal diets as a protein source (Oswald and Gotaas 1957). Different sources of cultivated algae effectively maintained animal growth performing and, in some cases, improved daily body weight achieve. Sewage-grown Chlorella and Scenedesmus. They have gained consideration as potential nutrient sources because of their high crude protein and carotenoid subjects. In1952, Combs stated that supplementing 10%Chlorellasp. Into a diet lacking in riboflavin and vitamin A increased chicks' feed efficiency and growth (Grau and Klein 1957).. Later work showed no adverse growth response by chicks to diets containing 20% sewage-grown, aluminum-free Chlorella and Scenedesmus, compared with those fed a corn-soybean meal-based diet (Grau and Klein 1957).

2.4 Cultivation of microalgae

One of the microalgae growing is immobilized. One of the limitations for the development of wastewater treatment systems based on microalgae is the biomass harvest at the end of the treatment process, so the immobilization of cells can represent an alternative for solving the problem as well as providing advantages, such as an increase in the cell retention time within bioreactors and higher metabolic activity.

2.4.1 Open raceway ponds

In most existing full-scale microalgae cultivation plants the open raceway ponds are preferred, and they can only maintain low biomass productivities, which increases the biomass harvesting expenses (Wang et al. 2012). Microalgal growth is also limited to the pond's surface, causing in

low volumetric productivity and a minimal overall biomass concentration. Using high-rate algal ponds (HRAP), a maximum biomass concentration of only 0.6 g/L was reached. Closed PBRs, in contrast, are additional complex in operation but have greater volumetric productivity. To date, the most popular large-scale, commercial cultivation of microalgae methods are based on open-ponds technique(Christenson and Sims 2012).

2.4.2 Closed photobioreactors (PBRs)

The washout problem is one of the most disadvantageous limitations of PBRs, that restricts their implementation as a microalgal-based technology to produce biomass. Since the achievable concentrations from this cultivation system are deficient (0.3–1 g/L), therefore requiring a >99% volumetric reduction element of the culture before it can be applied for further processing. Furthermore, microalgae are tiny and have a slight relative density to water that makes them hard to settle and which affects them to form an almost homogeneous suspension, become stable by negative charges on the outer surface of the microalgal cells (Bhave et al. 2012). Therefore, simple sedimentation cannot decouple microalgal biomass retention time (MRT) from dilution ratio (D) in a normal photobioreactor. Consequently, the PBR is usually run at its optimal D to achieve maximum efficiency, often negligible. Also, due to the small D, PBRs can only reach small biomass concentrations, leading to lower production levels and lower nutrient uptake. Moreover, high costs are correlated with harvesting the microalgal biomass at low concentrations, mainly for the early concentration stage, then most of the liquid should be removed.
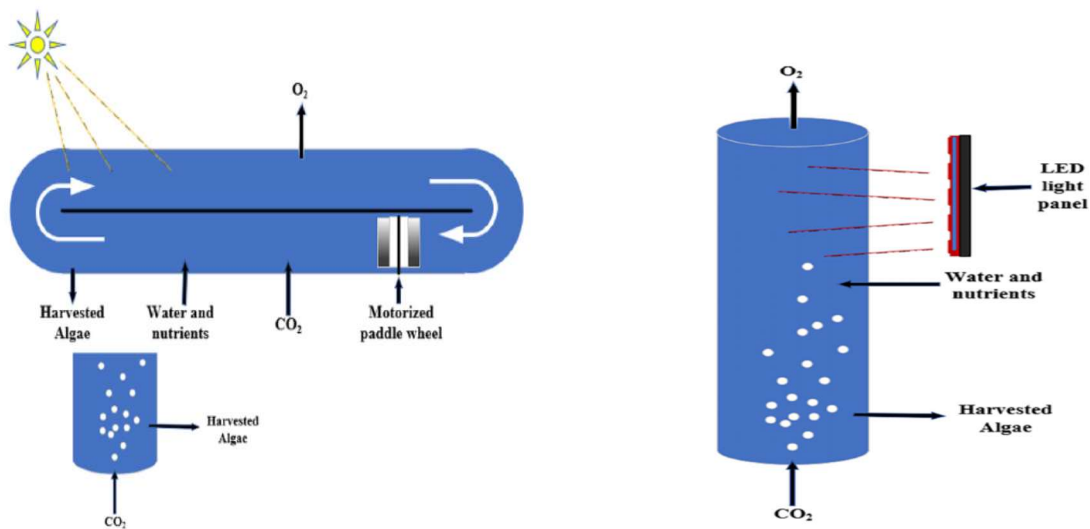
Figure 2.4. Open raceway ponds Microalgae cultivation at the left and PBR Microalgae cultivation at the right side (Pankratz et al. 2019).

2.5   Membrane photobioreactor (MPBR)

The common MPBR is generally an operating technique that incorporate an enclosed PBR with a submerged or side-stream membrane filtration procedure using micro or ultrafiltration membranes for separation of solid-liquid. MPBR is designed and utilized to rise light access (high surface/volume ratio) and proposition favorable for algal growth conditions that for instance, adequate mixing, easy access to carbon source, and degassing as reduce the costs of construction are the good samples. (Alcántara et al. 2015). The utilization of a membrane target to provide keeping of algae cells, therefore challenging the issue of microalgae washout, and allowing separate control of solids retaining time (SRT) and hydraulic retention time (HRT). (Marbelia et al. 2014). MPBRs have also shown higher productivity of biomass, greater efficiency of nutrient removal and less space requirement (Bilad et al. 2014). The advantages of MPBRs and the recent application of membrane bioreactor (MBR) systems in the municipal and industrial wastewater can be compared together. Producing high-quality treated waste with low amount of organic substances, pathogen, and suspended solids are the typical MBRs behavior (Melin et al. 2006; Sun et al. 2006). MBRs, or MPBRs based on microalgae, have been planned as another bio-treatment process to eliminate nutrients from wastewater. Difference between these two methods is the demand for biomass making. In MBRs, production of minimum biomass is supported to decrease sludge control and removal costs, although MPBR operation targets at more biomass manufacture for following consumption. Hence, MBRs and MPBRs are supposed to be operated by different circumstances to achieve this relative purpose. The elimination of nitrogen and phosphorus is generally achieved by various metabolic methods, during MPBR treatment. These methods are impacted through some of factors, same as wastewater characteristics, operational factors, and environmental elements(Bamba et al. 2021). Also for nutrient removal, MPBRs are capable to reach CO_2 sequestration and removal of heavy metals and micro pollutants (Luo et al. 2017). The MPBRs are subject matter to membrane fouling in operation, exactly same as MBRs. In MPBR, membrane fouling grows as algae cells, organic material including derivative of both algal cells or bacteria, and inorganic matters gather inside the membrane pores and on the membrane surface (Low et al. 2016; Villacorte et al. 2015).
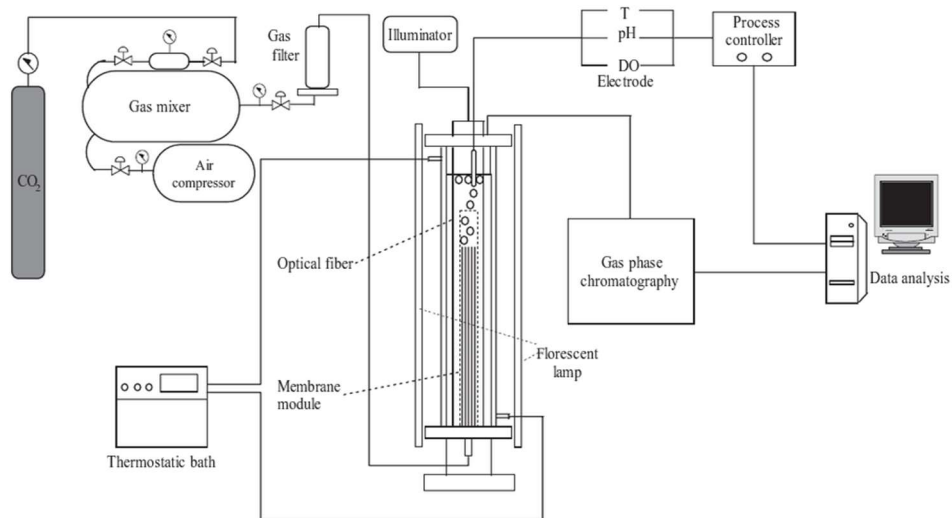
Figure 2.5. schematic diagram of membrane photobioreactor (L. Fan et al. 2007).

2.6 PBRs VS MPBRs

The new and practical concept is suggested for microalgae cultivation and pre-harvesting using a membrane photo bioreactor (MPBR). The bioreactor is coupled to membrane filtration by cultivating *Chlorella vulgaris*. The basic simulation was primary performed to understand the behavior of the hybrid system. The effectiveness of the MPBR for cultivation and pre-harvesting was proven (Fan et al. 2007). The membrane ultimately retained the biomass, which was partly reused into the bioreactor to maintain a high biomass concentration, so enhancing the flexibility and robustness of the system. The MPBR can run at higher dilution and growth rates, resulting in a 9 times higher biomass productivity. In addition, pre-harvesting can be achieved by applying varying concentration factors in the filtration phase. The membrane permeate was used to the reactor as a feed medium without affecting the algae growth, which offers a substantial reduction of 77% in the water footprint (Rossignol et al. 2000).

The PBR was initially operated batch-wise for one week until the microalgae reached the stationary phase in a 25 L bioreactor. The 25 L cylindrical PBR was then operated continuously under different dilution rates (D= 0.08–0.340 d-1) for 45 days, corresponding to a 2.0–7.5 L/day feed flow rate(Rossignol et al. 2000). Afterward, the filtration system was included, and the operation turned into an MPBR using a similar bioreactor. Like the PBR, the MPBR was originally cultivated in batch-mode after being inoculated through a fresh inoculum, followed by continuous operation at a constant dilution ratio of 0.3 d-1. In the MPBR, the culture broths were circulated into a 4 L

filtration tank(Fan et al. 2008; Zhen-Feng et al. 2011). They were split into retentive (product) and permeate streams with a volumetric concentration factor (t) of 4.4 L. The retentive became the pre-concentrated/harvested product, and the permeate was collected and later recycled as a feed medium after the addition of the required concentrated stock substrates. The volumetric mass balance of both systems is presented in Figure 2.6 (Bilad et al. 2014). Pressurized air sources supplied CO2 into the culture medium after being filtered at a fixed flow rate (5 L/min). The PBR and MPBR were operated under constant light (no dark phase) without temperature or pH control. To maintain high biomass concentrations in the bioreactor and prevent washout, the retentive was also partly recycled using a recirculation ratio of R= 50%. Some fresh demineralized water was introduced to make up the volume harvested as the retentive, which disappeared through evaporation. 40 mL of sample was taken from the feed, bioreactor, retentive, and permeate daily by temporarily opening the bioreactor lid (Fan et al. 2008; Zhen-Feng et al. 2011).
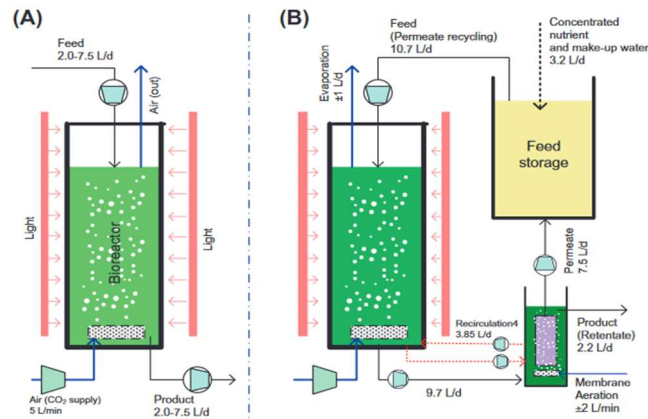
Figure 2.6. Schematic illustration of (A) PBR and (B) MPBR set-up (Bilad et al. 2014)

2.7 MPBR configuration

The separated MPBR system consists of a photobioreactor and a membrane module in two separate chambers. It is a system in which a pump can be used to deliver the microalgae suspension from the photobioreactor to the membrane module. The retentive water from the membrane module is recirculated to the photobioreactor, and thus the degradation and filtration processes occur in the two separate chambers. The separated MPBR system can be operated in both closed-loop mode and continuous flow-through mode. In a closed-loop manner, the permeate water is recycled to the photobioreactor. In the constant flow-through way, the permeate water is discharged continuously. In the meantime, fresh feed water is constantly fed into the photoreactor to maintain a constant

working volume of the photoreactor. The transmembrane pressure (TMP) and permeate flux can be auto recorded at predetermined time intervals by a data logging system (Wang et al. 2013).

The combined MPBR system is with the membrane module incorporated in the photo-bioreactor, the so-called submerged membrane photobioreactor (MPBRs) system. A UV blocking baffle can be used to prevent the polymeric membrane from deterioration by UV irradiation. Although ceramic membrane can be a favorable choice over the polymeric membrane regarding the UV or OH attacks, it is remarkably costlier. A pump can be used for the permeate water suction. The combined MPBR system can also be operated in both closed-loop mode and continuous flow-through mode. In addition, the TMP and permeate flux can be auto-recorded by a data logging system (Wang and Lim 2012). Removing low-concentration nitrate from water is desirable because it may cause eutrophication when discharged, but it is challenging using current technologies. Membrane photobioreactor (MPBR) technology (which is the combination of membrane and microalgae cultivation) emerges as a suitable option to efficiently reduce the nutrient load from wastewater.

2.8 Factors affecting the performance of MPBR

The MPBR performance for biomass production, membrane fouling, and nutrient removal is depending on the characteristics of biomass and operating conditions (hydraulic and solids retention time, aeration, lighting condition, temperature, membrane flux and PH). This part review of factors affecting on efficiency of MPBR process.

2.8.1 Hydraulic and solids retention time (HRT, SRT)

The HRTs used for MPBR operation are from 6 h to 5 d so generally they are shorter than PBRs that is between 2–5 days and high-rate algal ponds (HRAPs) that is between 2–9 days (Yoon et al. 2004). Choosing an applicable HRT for cultivation of microalgae is reliant on various reasons, such as wastewater characteristics, environmental conditions, and treatment goals. Quicker HRTs rise nutrient load up that helps microalgae growth, but longer HRTs may be the reason of higher nutrient removal and nutrient restriction (Arbib et al. 2013). Thus, RT is a critical effective circumstance and effects on microalgae efficiency (Matamoros et al. 2015a).

2.8.2 Lighting condition

Considering the dependency of microalgae on light, the accessibility of light energy is important. Optimizing efficiency of light energy use improves the productivity of biomass so nutrient uptake efficient face/volume ratio to encourage light utilization. Light intensity, light wavelength, and light cycle are essential factors for efficient microalgae growth in bioreactor. The light intensity has affect on biomass cultivation and nutrient exclusion from effluent (Zhen-Feng et al. 2011). Considering the algal species and concentrations change, the need for light intensities changes too. That rise in light intensity lead to production of biomass (Simionato et al. 2013). Some studies shows that nutrient absorption by S. obliquus are related to the biomass interior nutrient content not light intensity and the effect of light is only important after the maximum amount for nutrient storage is reached (Ruiz et al. 2014). So, the demand for light intensity in the bioreactors is species dependent. Furthermore, biomass concentrations affect the light amount distribution in algal systems. In specific concentration of biomass, light strength is decreased along the light passing through a culture so, light attraction may be limited at high biomass concentrations.

2.8.3 Aeration

It is vital to have appropriate aeration during MPBR operation in order to successfully combine the algal suspension, deliver CO_2, and reduce membrane fouling. Moderate aeration is optimal for ammonia removal by stripping, and it also has the added benefit of lowering the oxygen concentration in the system (Park et al. 2010). When it comes to microalgal cultures, both under- and over-aeration of the cultures can be detrimental to the growth and viability of the cells. Immoderate aeration causes an unwanted increase in energy consumption. For sustainable & achievable operation of MPBRs, it's important to have complete knowledge of the impact of aeration. One of the main objectives of applying aeration in MPBR is to ensure the supply of carbon sources for microalgae. Microalgal biomass constitutes almost 50% carbon, which is conventionally extracted from CO_2 (Chisti 2007). Some common sources of carbon for microalgal biomass production are concentrated or pure CO_2, fuel gas, air, and soluble carbonate. In terms of common choice, Gaseous carbon sources have an edge over aqueous sources (Sutherland et al. 2015). Generally, concentrated CO_2 is found to be more favorable for biomass productivity contrary to atmospheric air (0.04% CO_2). Furthermore, numerous studies have showed that CO_2 values between 6 and 15 percent are nearly ideal for the formation of *Chlorella sp.*, *Scenedesmus*

obliquus, Spirulina sp., and *N. occulta* (Razzak et al. 2015); furthermore, swelling CO_2 levels to 30–50% may improve the build-up of total lipids and polyunsaturated fatty acids (Tang et al. 2011) that's why it's subjected to further examination.

2.8.4 PH

pH is an important parameter throughout the MPBR technique because it influences the growth and harvesting of microalgal biomass (Yoo et al. 2014). It has been observed that different photosynthetic activities of microalgae can increase the pH drastically (Muñoz and Guieysse 2006). Comparative research between an MPBR and a PBR finds that the pH of the MPBR (9.0) is lower than the pH of the PBR (up to 10.5), and that the pH of the MPBR has more benefits for microalgae growth (Gao et al. 2014). The optimal pH for the production of microalgae varies depending on the strain. It has also been demonstrated that the highest production of Chlorella sp. in PBRs fed with dairy effluent was achieved between the pH ranges of 6.3 and 7.5 (Posadas et al. 2015). Likewise, when we analyze the productivity of *S.obtusiusculus*, it also fluctuates at changing pH in a PBR, with the maximum productivity of 0.97 g/L d seen at pH 8 (Cabello et al. 2015). Analyzing the PBR mentioned in this research, we can jump to the conclusion that managing pH between the range of 7 and 8 may be the ideal point for the growth of most microalgae in MPBRs, barring some exceptional cases. However, the scope of this research is still very restricted, and it requires more investigation to appropriately know about the effect of pH on MPBR. In order to modulate the pH of the microalgal wastewater treatment systems, CO_2 can be supplied to the systems. For example, during the culturing of *Desmodesmus sp.* in a PBR, the pH of the cultures aerated with CO_2 was much lower (pH 8) than the pH of the cultures aerated with air (up to 10.5) (Cabello et al. 2015). In addition to CO_2, acetic acid can be used to alter the pH of a solution. For instance, there was a significant amount of lipid content present. When acetic acid was used to regulate the pH of the water, the algae *Chlorella Zofingiensi* was discovered (Huo et al. 2012). Another result was that the addition of acetic acid reduced the nutrient removal efficiency (N: 79.6 percent; P: 42.0 percent) when compared to the use of CO_2 (N: 97.5 percent; P: 51.7 percent), presumably because the initial CO_2 provided an adequate amount of carbon source for the microalgae (Huo et al. 2012). Overall, a cost-benefit analysis would've been performed to determine whether the higher operational costs associated with maintaining a healthy pH in order to increase microalgae productivity were justified.

2.8.5 Temperature

Change in temperature may also affect both enzyme activity and microalgal metabolic processes (Chinnasamy et al. 2009). According to the literature, the last MPBR examinations were often conducted at a temperature of roughly 25 degrees Celsius; as a result, the influence of temperature on MPBR is not completely recognised. Many microalgae species thrive at temperatures between 25 and 30 degrees Celsius, which is considered excellent for their growth (Bamba et al. 2015b). There is every chance that high temperatures (35 °C or above) harm the development of some species, such as *Chlorella vulgaris* (Chinnasamy et al. 2009). The effect of temperature on the productivity of S. was also studied in another investigation. When illuminated with a light source of 11.334 Klux (about 153 mol/m2 s) in a mineral media, obliquus appears (Chinnasamy et al. 2009): At 30 degrees Celsius, the greatest critical biomass growth (1.84 mg/L h) was achieved. In contrast to this, the lowest biomass production (1.1 mg/L h) was seen at 35 degrees Celsius. However, when grown at 35 degrees Celsius under 620 mol/m2 s of light in a flat panel PBR fed with BG11 media, *Scenedesmus obtusiusculus* demonstrated the highest photosynthetic activity and biomass production when grown under the same conditions (Cabello et al. 2015). This shows us that the ideal temperature for productivity keeps on changing among different species and the most suited temperature for the growth of most microalgae ranges between 25 and 30 °C. Temperature hampers microalgae's capacity to get rid of impurities, like nutrients and micropollutants, from wastewater (Matamoros et al. 2015b). It was discovered that the filtration of nitrogen, phosphorus, and trace organics is done more effectively by using warm water and high intensity of light (Converti et al. 2009).

Due to the fact that the permeate flux number imposed on the MPBR system is closely related to the fouling rate, it is another important issue for the process's long-term viability. In contrast to the normally high fluxes (N40 L/m2 h) employed for membrane-based harvesting approaches, the fluxes for this technique are very low (Boonchai and Seo 2015), It should be noted that practically all of the MPBR studies were carried out at relatively moderate changes (2.6 – 15 L/m2 h) in order to minimise the limit of membrane fouling. Exactly as predicted, fouling mechanisms found during MPBR operation were strikingly comparable to those observed during MBR operation (Low et al. 2016), In order to detach suspended particles, colloids, and dissolved organic materials, both of these procedures are required; however, biofouling generated by *Chlorella vulgaris* was found to

have a lower potential for damage when compared to fouling caused by activated sludge (Xu et al. 2014). Membrane fouling in MPBRs is not straightforward, and a variety of parameters, including algae species, microalgae broth qualities, operating conditions (as previously noted), and membrane properties, all influence the process.

2.8.6 Wastewater characteristics (TN, TP)

The total accumulation of nitrogen (TN) of MPBR feeds ranges from 7.5 mg/L to almost 40.0 mg/L (Honda et al. 2012). If alternative compositions for synthetic wastewaters are used, and if site-specific elements are taken into consideration, then the results will differ from one another. There is normally ammonium nitrogen (NH3-N) in the wastewater, nitrite nitrogen (NO2-N), nitrate nitrogen (NO3-N), and nitrogen that has been biologically bound in the effluent. Because of the decreased energy demand for ammonia uptake, ammonia-nitrogen is the very first choice nitrogen source for microalgae and cyanobacteria (Markou et al. 2014). When ammonium, nitrite, and nitrate are present in wastewater in a similar proportion, algae will tend to preferentially utilise ammonia, and absorption of nitrite and nitrate will not begin to a significant level until ammonia has been nearly completely utilised (Cai et al. 2013). As an illustration, during the culturing of *Chlorella vulgaris* in an MPBR supplied with aquaculture wastewater, it was noted that ammonia was nearly completely filtered out, and that nitrate and nitrite were also utilized to a minor extent throughout the cultivation. Another MPBR study found that while nitrate was present in the feed (processed effluent from MBR) in a considerably higher quantity than ammonium, nitrate was given precedence by *Chlorella vulgaris* over ammonium. *Botryococcus braunii*, and *Spirulina* platensis. In addition, some microalgae species, such as *Scenedesmus*, have been shown to be non-specific in their nitrogen preferences when exposed to various types of nitrogen (Park et al. 2010). As a result, the rate of N assimilation is dependent on both the species and the concentrations of feed.

Microalgae cultivation necessitates the use of additional nutrients, such as total phosphorus (TP). Phosphorus trihydrate (TP) is a mixture of multiple different types of phosphorus, comprising orthophosphate, polyphosphate, pyrophosphate, metaphosphate, and associated organic structures, that occurs in wastewaters. Cell physiology, cell hunger, TP levels, chemical forms of phosphorus, as well as other environmental conditions such as light intensity, pH, and temperature can all have an impact on algae's ability to absorb phosphorus from the environment. It has been discovered

that the elimination of TP has a significant beneficial relationship with the productivity of microalgal biomass (Choi and Lee 2014). For example, the most recent studies revealed that the P removal ratio (1.33 percent) to biomass production corresponded to the molecular formula of microalgae $CO_{0.48}H_{1.83}N_{0.11}P_{0.01}$. Similar results were obtained in a short-term PBR study (running for 15 days) utilising primary treated wastewater, where a mixotrophic culture containing C. Vulgaris ended up producing significantly more (nearly three grammes per litre per day), achieving high P removal (N90 percent), as opposed to P removal of b50 percent when the show was b1 grammes per litre per day (Choi and Lee 2014). It was also hypothesised that the formation of Scenedesmus in secondary effluent from PBRs had a relationship with P consumption to a certain extent (correlation coefficient = 0.5). It should be emphasised that, depending on the circumstances, abiotic phosphorus removal can account for a significant fraction of overall phosphorus removal. The role of abiotic nutrient removal in MPBRs, on the other hand, has been found to be insignificant, and assimilation by algae is thought to be the most important pathway for nutrient removal. It has also been discovered that microalgal absorption accounts for more than 90 percent of the overall elimination of phosphorus from MPBRs. As a result, algal absorption is a significant mechanism for the removal of phosphorus from wastewater in municipal solid waste treatment plants.

2.8.7 Membrane flux

In MPBR system the permeate flux value imposed is directly correlated to the fouling rate so, membrane flux is another critical factor in the sustainability of the process. Not same as the usually high fluxes (N40 L/m^2 h) used for membrane-based of harvesting methods (Boonchai and Seo 2015), all the MPBR studies are assumed at rather low changes as a strategy to extent of membrane fouling. As would expect, during MPBR operation, the fouling mechanisms show similarities with viewed for MBRs (Low et al. 2016), both methods try to filter a complicated mixture of colloids, biologically active suspended solids, dissolved organic matters and biofouling caused by C. vulgaris was seen to be less compared to fouling with activated sludge (Xu et al. 2014). In MPBRs the membrane fouling is complicated, and is affected by algae variety, microalgae broth properties, operating conditions, and membrane properties.
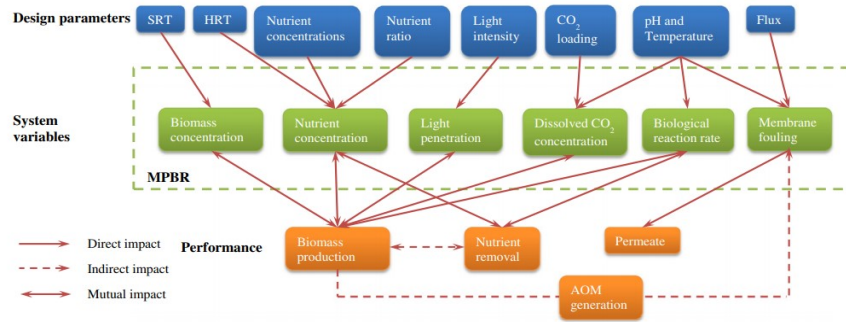
Figure 2.7. Interrelation among system and parameters(Luo et al. 2016a).

2.9   Membrane Fouling

Membrane systems can be operated at constant permeate flux (flow rate per unit membrane area, L/m2 h) with variable transmembrane pressure (TMP) or constant TMP with variable permeate flux. The former model is the common one. Based on the operating TMP, water treatment and reuse membranes can be broadly categorized as low-pressure membranes (LPMs) and high-pressure membranes (HPMs) (Li and Elimelech 2004). (LPMs include Microfiltration (MF) and loose ultrafiltration (UF) membranes, operated at relatively low TMPs, typically less than 100–200 kPa. On the other side, HPMs such as tight UF, Nanofiltration (NF), and reverse osmosis (RO) membranes are worked at relatively high TMPs (>200 kPa) (Carey and Migliaccio 2009). Membrane fouling occurs during a rise in TMP to maintain a particular flux or during a reduction in flux when the system is operated at constant pressure. Membrane fouling classification can be as reversible fouling and irreversible fouling, which the distinction is entirely dependent on the context in which membranes are operated and cleaned(Carey and Migliaccio 2009). Reversible fouling (including back washable and non-back washable) occurs due to the cake layer or concentration polarization of materials at the membrane rejection surface (Li and Elimelech 2004). Membrane with back washable, reversible fouling can be restored through appropriate physical washing protocol such as backwashing or hydrodynamic scouring (surface washing). In contrast, the non-back washable, reversible fouling only can be removed by chemical cleaning. Irreversible fouling occurs by chemisorption and pore plugging mechanisms (Pearce 2007). In case of irreversible fouling, the loss in transmembrane flux cannot be recuperated hydrodynamically or chemically. This means that the membranes must go across extensive chemical cleaning or be replaced. Fouling of membranes is caused by complex physical and chemical interactions between the various fouling constituents in the feed and between these constituents and the membrane

surface(Li and Elimelech 2004). Mass transport can lead to the attachment, accumulation, or adsorption of materials onto membrane surfaces and within membrane pores. Previous studies have demonstrated that membrane fouling and the characteristics of foulants are determined by feed water composition, the concentration of the major constituents, water chemistry (pH, ionic strength, and divalent cation concentration), membrane properties (surface morphology, hydrophobicity, charge, and molecular weight cut-off), temperature, mode of operation and hydrodynamic conditions (initial permeate flux and crossflow velocity) (Li and Elimelech 2004). Hence, any factors that could change the hydrodynamic characteristics of membrane modules and the chemical elements of feed waters would affect the overall membrane performance (Carey and Migliaccio 2009). Consequently, the combined physical and chemical effects will control the degree of attachment and determine how severe the fouling is and what strategies will prevent it. Commonly, foulants can be classified into the following four categories (Pearce 2007):

- Particulates: inorganic or organic particles/colloids act as foulants that can physically blind the surface of the membrane and block the pores or hinder transport to the surface by developing a cake layer.
- Organic: dissolved components and colloids, which would attach to the membrane by adsorption.
- Inorganic: dissolved components tend to precipitate onto the membrane surface due to pH change (scaling) or oxidation. Coagulant/flocculent residuals may be present as inorganic foulants.
- Micro-biological organisms: the microbiological category covers vegetative matter such as algae and microorganisms such as bacteria which can adhere to the membranes and cause biofouling.

2.10 Membrane Fouling Classification

Fouling can be classified into reversible and irreversible fouling based on the attachment strength of particles to the membrane surface(Pearce 2007). A strong shear force or backwashing can remove reversible fouling. The formation of a strong matrix of fouling layer with the solute during a continuous filtration process will result in reversible fouling being transformed into an irreversible fouling layer (Pearce 2007). Irreversible fouling is the strong attachment of particles that cannot be removed by physical cleaning. Raw waters contain a wide distribution of fine

particles, dissolved organic compounds, colloids, less soluble salts, and biological growth that can cause membrane fouling. Fouling by different foulants can be considered to occur by other mechanisms. Recent research has identified four principal fouling mechanisms: Figure 2.8a: pore blocking stemming from the deposition of particles which are larger than the membrane pore size; Figure 2.8b: partial pore blocking caused by adherence of particles adsorbed on the membrane surface which then block the membrane pores partially or adhere to the inactive area; Figure 2.8c: internal pore blocking, which happens when smaller particles regarding their diameter reach bigger pores; and Figure 2.8d: cake filtration forms due to the precipitation of particles on membrane surface those neither enter the pores nor block them, with scanning electron microscopy of the surface of the membrane(Carey and Migliaccio 2009).
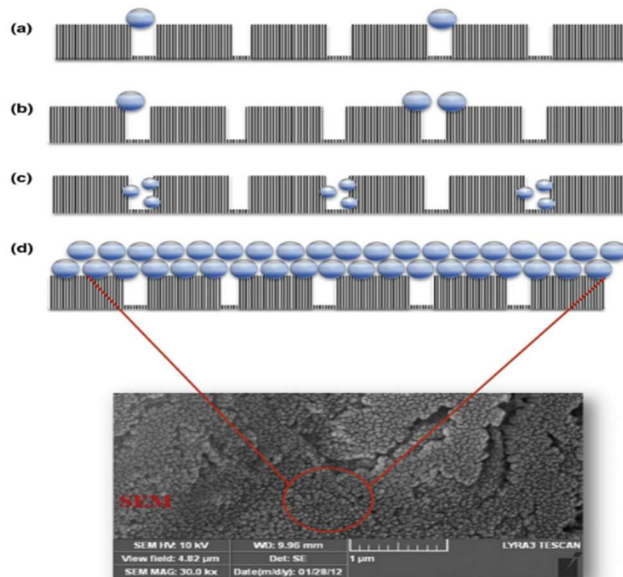

Figure 2.8. Fouling mechanisms of porous membranes. (Rezakazemi et al. 2018)

Recent vital studies indicate that membrane fouling is influenced by various factors such as system hydrodynamics, operating conditions, membrane properties, and material properties. At low pressure, low feed concentration, and high feed velocity, concentration polarisation effects are minimal, and flux is almost proportional to trans-membrane pressure difference.

2.11 Factors affecting microalgae cell adhesion to membrane

adhesion onto abiotic surfaces can be influenced by multiple factors, such as the surface properties of microorganism and abiotic surfaces, including their surface free energy (SFE), ζ potential,

hydrophobicity, roughness, morphology , the characteristics of the cultivating liquid medium, including its surface tension, pH, ionic strength, temperature, hydrodynamics, and some biotic factors, including the properties of cell membrane, production of extracellular polymeric substances, the chemotaxis of cells, and the presence of pili and flagella. Overall, it has been established that these factors can influence cell adhesion mainly by affecting the physicochemical interactions between cells and surfaces(Yang et al. 2000; Guillen-Burrieza et al. 2014).

2.11.1 Microalgae properties

2.11.1.1 Cell morphology
Biofilm formation on present day antifouling (AF) coatings is receiving increasing attention due to their persistence on the newer tin-free alternatives. A biofilm layer of 1 mm thickness can cause an 80% increase in skin friction coefficient and a 15% loss in ship speed compared to a clean hull (Schultz and Swain 2000). Differences in biofilm thickness and morphology have been shown to increase local skin friction coefficients between 33 and 187% (Schultz and Swain 1999). Additionally, biofilms on fouling release (FR) coatings may be difficult to remove even when a ship is underway. This poses a challenge to the shipping industry as the formation of biofilms on ship hulls will lead to increases in drag, consumption of fuel, emission of exhaust gas, and higher operational costs (Schultz et al. 2010).

2.11.1.2 Zeta potential
The Zeta potential is an important parameter which characterizes the physicochemical properties of the algal cells envelope and plays an important role in aggregation and disaggregation processes (Cieśla et al. 2011). The Zeta potential can easily be estimated from the mobility of the charged particles in an electric field; therefore, it is a useful indicator of the degree of repulsion between charged particles in a suspension. If the Zeta potential is relatively high (>20 mV, positive or negative), electrical repulsion between interacting particles is strong and the suspension is highly stable. Once the Zeta potential is close to zero, interacting particles can approach each other to the point where they will be attracted by van der Waals forces and consequently aggregate into heavy flocs allowing flocculation to occur (Vandamme et al.2013).

2.11.1.3 Hydrophobicity
Bacterial surface hydrophobicity is one of the key physio-chemical parameters which fundamentally affect the interactions between bacteria and inert or living surfaces. Hydrophobicity

of bacterial cells significantly influences the processes of flocculation, sedimentation, and dewatering in activated sludge (AS) during wastewater treatment. Thus, a change of bacterial hydrophobicity in AS may cause serious operational problems in wastewater treatment plants. For example, the sludge foaming process is due mainly to the excessive growth of filamentous bacteria with extremely hydrophobic surface. Moreover, for the attached growth biological treatment processes, such as trickling filters or rotating biological contactors, bacterial hydrophobicity could also largely influence the biofilm formation, including bacterial initial attachment as well as subsequent development of bacterial colony and the maturation of biofilm on substrata. Therefore, to facilitate the optimization of the biological waste-water treatment processes of WWTPs. it is necessary to understand the hydrophobicity of bacteria cells present in the AS and biofilms.

2.11.2 Membrane and substratum surface properties

Membrane properties, such as hydrophobicity and zeta potential, play a vital role in cell adhesion. The hydrophobicity and zeta potential of membranes affects the initial adhesion and development of microalgal biofilm formation. Thus, various studies were conducted to develop a better understanding of the role of membrane or substratum surface properties on microalgal cell adhesion. The following paragraphs will summarize the studies in this area. Ozkan and Berberoglu (2013a) found that a hydrophobic surface of substratum, such as ITO (Indium Tin Oxide), favored the formation of *Chlorella vulgaris* biofilm, as compared to hydrophilic surfaces. The rate of biofilm formation on the more hydrophobic surfaces was three times higher than that on the hydrophilic surface in the first 40 minutes' adhesion. Eventually, the density of *Chlorella vulgaris* biofilm on the hydrophobic surfaces was 2.7 times that on the hydrophilic surfaces (Ozkan and Berberoglu 2013c). Furthermore, in another study, Ozkan and Berberoglu (2013b) found that a hydrophilic microalgae and hydrophilic substratum should be used to reduce microalgal biofouling or biofilm formation during microalgae cultivation (Ozkan and Berberoglu 2013d). A general trend that has been observed is that a higher adhesion density (quantity of biofilm) is associated with a more hydrophobic surface.

Zeta potential is another surface property of membrane and substratum that affects the rate and density of microalgal biofilm formation. Zhang et al. (2013) found out that *Chlorella sp*. was more easily attached to the substratum surface to form biofilm with a positive zeta potential, as compared to the substratum surface with a negative zeta potential (Zhang et al. 2013). This might be due to

the charge neutralization effect. Furthermore, Yuan et al (2019) found that the pH of the solution affects the zeta potential of both microalgal cells and substrata (Qin et al. 2019). An increase in pH led to a more negative zeta potential of both microalgal cells and substrata. Eventually, cell adhesion would be decreased by increasing zeta potential of substrata and microalgal cells. Thus, studies suggest that an opposite zeta potential of microalgal cells and substrata or membrane or a smaller zeta potential of both microalgal cells and substrata or membrane should be selected to enhance microalgal biofilm formation rate and density.

2.11.2.1 Materials and texture

The adhesion involves an interaction between cells and membrane surfaces and is related to the properties of algal cells and especially the membrane. Among membrane properties, surface roughness plays a significant role in cell adhesion (Blanken et al. 2014). Greater roughness enhancing the deposition of algal cells to surface is widely reported (Huang et al. 2018). An increase in surface roughness also promoted the *Chlorella vulgaris* deposition to the surfaces of manmade carriers in rocking condition. Nevertheless, the mechanism of material surface roughness affecting the algal short-term cell adhesion under dynamic flow condition is still unknown. According to the findings of Boutt et al.(2006) and Shen et al. (2015), material surface roughness mainly affected the bacteria cells/colloids deposition via its created hydro-dynamic conditions under dynamic flow condition. The surface roughness of the fracture had a significant impact on the flow path and flow direction, further influencing the migration of colloids. Some researchers reported that fracture roughness tends to increase fluid velocity in the fracture locally(Boutt et al. 2006) and creates hydrodynamic conditions including recirculation areas and low flow velocity areas to trap colloids. In addition, surface roughness could lead to un-even distribution of shear stress on the carrier surface, which was acritical factor controlling the attachment and detachment of *Legionella pneumophila* cells (Shen et al. 2015).

2.11.2.2 Zeta potential

The zeta potential is a combination of the surface charge on the body of a cell or particle plus any adsorbed layer at the interface and is specific to the medium in which the surface is immersed. Along with other surface properties, such as hydrophobicity, the zeta potential is important in determining the likelihood that single celled algae and bacteria will adsorb to surfaces.

2.11.2.3 Surface free energy

Recently, some researchers proposed several criteria to quantitatively predict cell adhesion. Based on the thermodynamic approach, Zhang et al. found that bacterial adhesion was mediated by the SFE difference between cells and surfaces, with a lower SFE difference indicating a higher degree of adhesion(Zhang et al. 2015). Furthermore, by considering the components of SFE, Cui and Yuan reported that, for microalgae that have a dispersive component of SFE higher than that of water and a polar component of SFE lower than that of water, adhesion would be more favorable on surfaces with a higher dispersive component of SFE but a lower polar component of SFE. Moreover, some researchers showed that cell adhesion would decrease with increasing electron-donor characters. Overall, these criteria have important implications in predicting the cell adhesion. Meanwhile, these criteria indicated that the physicochemical interactions between cells and surfaces, including EL, LW, and AB interactions, might play different roles in cell adhesion under different conditions(Zhang et al. 2015). However, to date, few studies have been conducted to understand and quantify the dominant physicochemical interactions in various cell adhesions.

2.11.3 Environmental conditions

The density of adhering cells increases when the pH of the suspending medium was brought near the isoelectric point (IEP) of the substrate surface (Yuan et al. 2019). To date, many studies have analyzed the effect of pH on cell adhesion. Sekar et al. found that the adhesion of *Chlorella. vulgaris*, onto hydrophobic, hydrophilic, and toxic substrata was higher at pH 7 and above (Sekar et al. 2004). Hamadi et al. reported that the adhesion of *Staphylococcus aureus* to glass and indium tin oxide-coated glass was strong in the pH range 4.0–6.0 and weak at highly acidic pH (< 4.0) and alkaline pH (> 7.0) (Hamadi et al. 2012).

2.11.4 Hydrodynamic conditions

Hydrodynamic conditions can alleviate membrane fouling results from algae suspensions by increasing the shear rate at the membrane surface. Vibration membranes have been observed to optimize transport conditions for improving membrane filtration performance and can lead to a decline in fouling, because they can create a shear rate at the liquid-membrane interface with high vibration frequencies or amplitudes(Yuan et al. 2019).

2.12 XDLVO theory

In aqueous solutions, NOM usually bonds together in aqueous solutions to form colloidal aggregates of tens or hundreds of nanometers in size. The attachment of a colloidal particle to a surface can be described by the XDLVO theory (Brant and Childress 2002), which considers the following three interactions (as membrane fouling contributors): van der Waals (LW) interactions, electrostatic (EL) interactions, and short-ranged acid-base (AB) interactions. The positive interaction force between organic colloids and the UF membrane surface represents a repulsive action to reject membrane fouling, while a negative one causes an attraction that aggravates fouling (Feng et al. 2009). Previous studies have shown that the XDLVO theory can be used to predict membrane fouling. There is, however, a lack of available information on the interactions between NOM and UF membranes at different pH values about the XDLVO theory.

2.13 Model of cell adhesion

The microalgae, a promising source of biofuel, convert carbon dioxide and sunlight into algal biomass. Engineered algae bioreactors can also be used for carbon dioxide extraction and reduce greenhouse gas emissions and wastewater treatment. Thanks to their ability to generate many valuable bioproducts and biofuels, to particular nutrients (N and P) from wastewater, and to minimize CO_2 (greenhouse gas) from the atmosphere and industrial waste gasses, microalgae have attracted growing interest in recent years. Membranes are commonly used in closed or partially closed photobioreactor systems to enhance microalgae cultivation efficiency. Traditional methods such as coagulation, flocculation, float, and centrifugation have historically been used to separate microalgae. However, membrane filtration has been given greater prominence thanks to its high efficiency and easy operation. These membrane-led processes, MF and UF, are unfortunately prone to fouling and energy-intensive. Continuous work is being carried out to search for an optimum algae separation technology with high separation efficiency and low inputs (Ozkan and Berberoglu 2013a).

3   Materials and Methods

3.1 Algae Cultivation

Chlorella vulgaris algae samples were grown in the MSM nutrient medium in the clear container (1 Liter) under the light bulbs using a bubble pump (Heredia-Arroyo et al. 2011). Mixed liquid suspended solids (MLSS) concentration was monitored every four days to follow the cultivation

process. It was apparent that the concentration of algae samples increased with cultivation time. After two weeks, the fluid color inside the container changed from light green to dark green. The composition and quantify of the MSM medium is shown in Table 3.1, which follows what was reported previously (Muñoz et al. 2005) and each of MSM solution prepared as much as we need to use in algae cultivation that come from literature. It should be stated that all of the chemicals used in this thesis were obtained from Sigma Canada. After algae cultivation, measuring the concentration of the algae solution is with using the vacuum filter, filter paper, oven and the scale. The final concentration of the microalgae reached to 1.16 g/L.

Table 3.1. Preparation of Mineral Salt Medium (MSM) (Muñoz et al. 2005)

Name	Reagent	Weight/g	Volume	
MSM-A	$CaCl_2. 2H_2O$	11.05		
	$MnCl_2. 4H_2O$	1.44		
	$COCl_2. 6H_2O$	0.4	100 ml	1 ml
MSM-B	$FeSO_4. 7H_2O$	4.98	100 ml	1 ml
MSM-C	$Na_2MOO_4. 2H_2O$	1.18	100ml	1 ml
MSM-D	$ZnSO_4. 7H_2O$	8.82	100ml	1 ml
	$CuSO_4. 5H_2O$	1.57		
MSM-E	H_3BO_3	11.42	500 ml	5 ml
	$MgSO_4. 7H_2O$	62.5		
MSM-F(P)	KH_2PO_4	31.235	500 ml	10 ml
	K_2HPO_4	66.255		
ADD THIS AT FINAL IN 1 L	EDTA-Na	0.64		
ADD THIS AT FINAL IN 1 L	NH_4Cl	3.82		

3.2 Characterization of the morphological properties of algal cells

Algae cells were characterized in terms of concentration, size, and surface area. The morphological characteristics of algae cells were quantified from images obtained by an inverted microscope (Manual version 1.04). The diameters of the cells were determined using Image-pro plus 7.0 analysis software. Based on their sizes under the microscope, the equivalent spherical diameters of the cells were determined for the cells. The projected area of the equivalent spheres represents the same size as that of the ellipsoidal cell with the specified major and minor diameters. Also, the

circularity of the cells was determined where Acell and Pcell are the imaged area and the cell's perimeter, respectively, as per equation 3.1. (Jiang et al. 2020).

$$\text{Circularity} = 4\pi \frac{A_{Cell}}{P^2\ cell} \tag{3.1}$$

3.3 Measurement of the contact angle of algal cells

The surface energy of the algae cell was quantified based on contact angle (θ) measurements using a Tensiometer instrument (Biolin Scientific Finland) and drop technique (Ozkan and Berberoglu 2013a; Busscher et al. 1984). In this analysis, 20 mL of algae solution was filtered using 0.45 μm filter papers. Then, the filter papers containing algae were pressed between two glass slides for 1 week (Figure 3.1). After that, the contact angle of diodomethane, formamide, and water was measured on the prepared filter papers. Also, the contact angle of these three solvents was measured on PDMS, PU and PTFE sensors (QSX900, QSX999, QSX33, respectively) of QCM instrument. The contact angle (θ) is the angle that a droplet of liquid makes when contacting a solid surface. It quantifies the wettability of a solid surface by a liquid via the Young equation. A given system of solid, liquid, and vapor at a given temperature and pressure has a unique equilibrium contact angle. The contact angle depends upon the medium above the free surface of the liquid, and the nature of the liquid and solid in contact. It is independent of the inclination of solid to the liquid surface. It changes with surface tension and hence with the temperature and purity of the liquid.

Figure 3.1 surface of filter paper covered with algae.
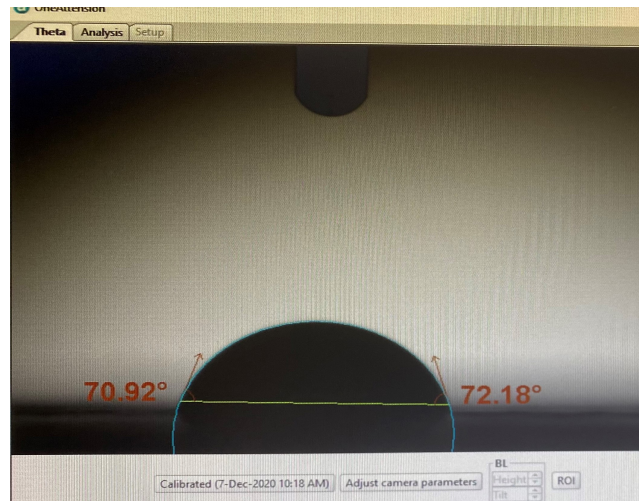
Figure 3.2 Contact angle of water on cake layer algae.

3.4 Measurement of surface tension

Surface tension (γ) is the tendency of liquid surfaces at rest to shrink into the minimum surface area that was calculated by the Tensiometer (Attention sigma 700) equipped with a platinum loop (Ponnusamy et al. 2012; Ozkan and Berberoglu 2013b). Surface tension of liquids were measured following the ring method at 22 °C using a platinum loop. Surface tension is what allows objects with a higher density than water such as razor blades and insects to float on a water surface without becoming even partly submerged (Ozkan and Berberoglu 2013b. The cohesive force a molecule is pulled equally in every direction by neighbouring liquid molecules, resulting in a net force of zero. The molecules at the surface do not have the same molecules around them and therefore are pulled inward (Ponnusamy et al. 2012). This creates some internal pressure and forces liquid surfaces to contract to the minimum area. There is also a tension parallel to the surface at the liquid-air interface, which will resist an external force, due to the cohesive nature of water molecules. The forces of attraction acting between the molecules of same type are called cohesive forces while those acting between the molecules of different types are called adhesive forces. Surface tension is responsible for the shape of liquid droplets. Although easily deformed, droplets of water tend to be pulled into a spherical shape by the imbalance in cohesive forces of the surface layer. In the absence of other forces, the drops of virtually all liquids would be approximately spherical.

3.5 Adsorption studies

The Quartz crystal microbalance (QCM) with dissipation, a well-known, sensitive technique, results in a mass variation per unit area by measuring changes in the resonant frequency of a quartz crystal (QCM-D 401, E1, Qsense Inc. Gothenborg, Sweden). Three different sensors of PDMS (QSX900), PU (QSX 999) and PTFE (QSX 331) were used in this experiment. Duration of tests was 45 minutes with 5 min buffer solution with 0.150 ml flow rate in 25°. Then, the algae solution (0.2 g/L) was injected into the QCM chamber for absorption. This instrument can monitor the simultaneous adsorbed mass and adsorbed layer properties of algae on solid-liquid surfaces throughout the adsorption experiment. The QCM can be used to monitor the deposition rate in thin film deposition systems or in liquid environments, that it is highly effective at controlling the affinity of molecules to surfaces functionalized with recognition sites. This method is used to measure greater entities for example viruses or polymers and biological assemblies with a sensor surface, in air or liquid, label-free and in real-time based on the change in the resonant frequency of a sensor when it is covered with a thin film of liquid.

4   Results and Discussion of Statistical analysis

4.1 Algae cell characterization

The morphological characteristics of algae cells were quantified from images (Figure 4.1) obtained by an inverted microscope, and their diameters were determined. It is seen that the cells were spherical with the average diameter smaller than 3 µm. Also, their surface area and circularities are similar (Table 4.1). The images show that the morphology of *Chlorella vulgaris* cells was spherical with a circularity of 0.96-0.99 (almost perfect sphere).
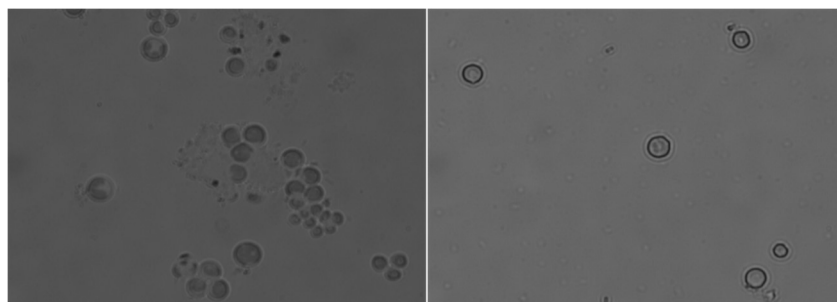

Figure 4.1 Algae cells under inverted microscope

Table 4.1 Morphological properties of algae cells in 30 single cells.

Average of cells measurements	Length (µm)	Angle	Area (µm^2)	Perimeter (µm)	Circularity
First 10 cells Average	2.70	180°	23.88	17.32	0.99
	2.81	90°			
Second 10 cells Average	2.92	180°	20.46	16.32	0.96
	2.23	90°			
Third 10 cells Average	2.54	180°	20.51	16.06	0.99
	2.57	90°			

4.2 Surface tension measurement

The surface tension of the three solvents of water, formamide and diiodomethane were measured in 50 min, and Figure 4.2 shows the results of this analysis. It can be seen that the average surface tension was 72.8 mN/m for water, 56.8 mN/m for formamide and 50.3 mN/m for diiodomethane.
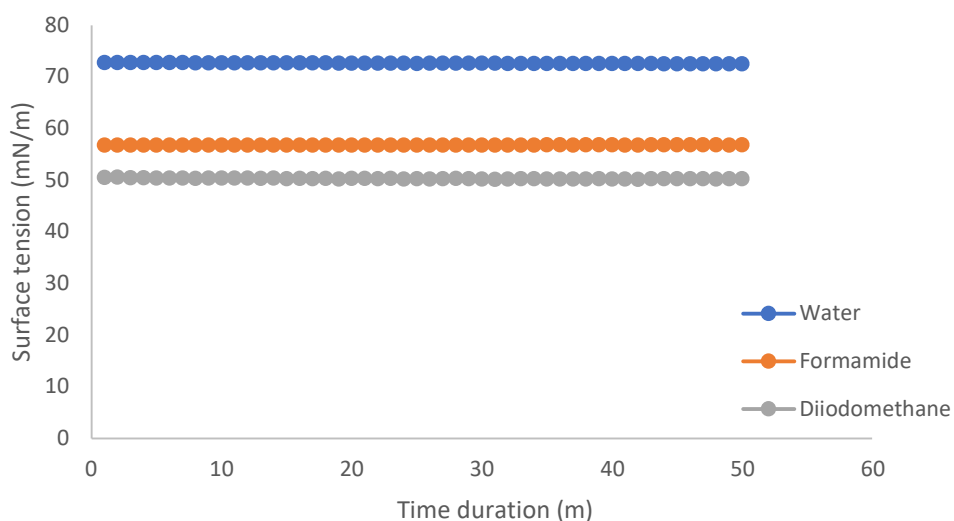
Figure 4.2 Surface tension of algae and water, formamide and diiodomethane.

4.3 Contact angle measurement of the cake layer of *Chlorella vulgaris* cells

Figure 4.3a. shows the contact angle of different solvents on the cake layer of *Chlorella vulgaris* cells on a filter paper. It is obvious that water made the largest contact angle, and contact angle dropped as time elapsed, especially for water and formamide. In the same vein, the largest contact angle was observed for water on cake layer of *Chlorella vulgaris* cells on filter papers, and the

smallest contact angles were observed for diiodomethane. As the surface tension of water was larger than other solvents (Figure 4.2), it made the largest contact angle on the cake layer of *Chlorella vulgaris* cells on the coated filters. The drop in contact angle is an indication of the diffusion of solution in the cake layer of *Chlorella vulgaris* cells on the filter paper and soaking of algae with the solution (Zhang et al. 2019). With comparing the figure 4.3 b, c and d, we can recognize that these three sensors with three different materials have not same properties. For example, the PTFE and PU are the most and less hydrophobic.
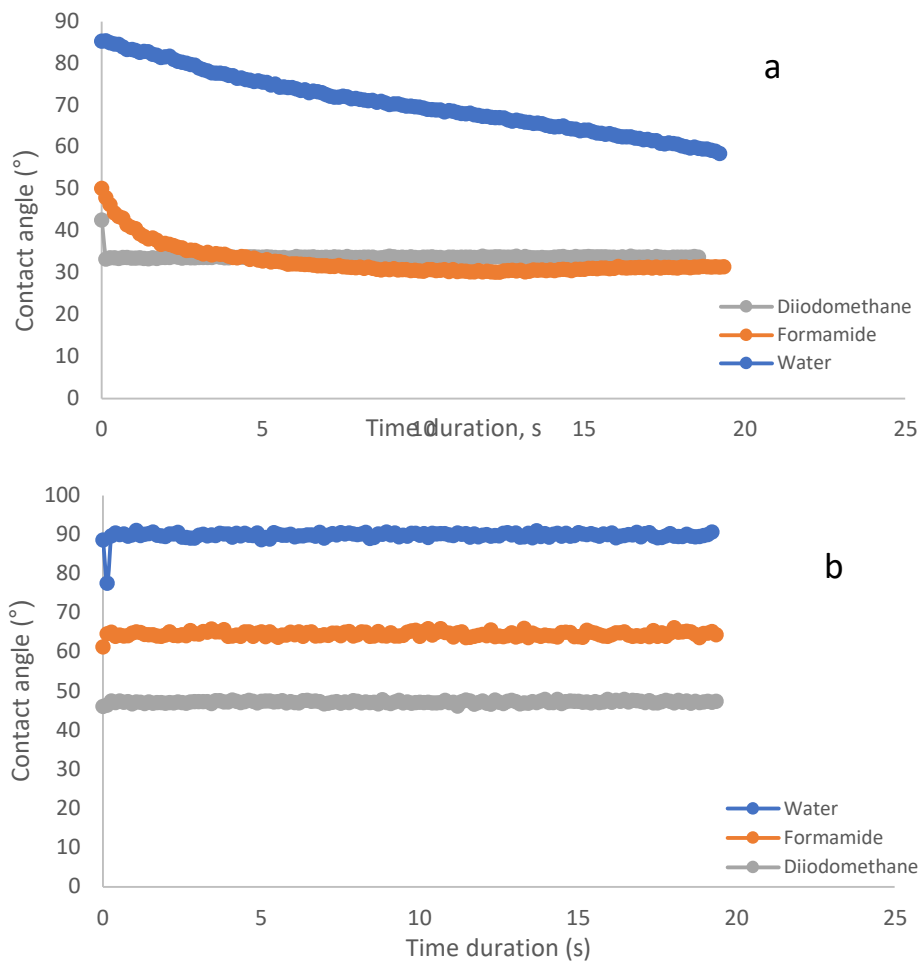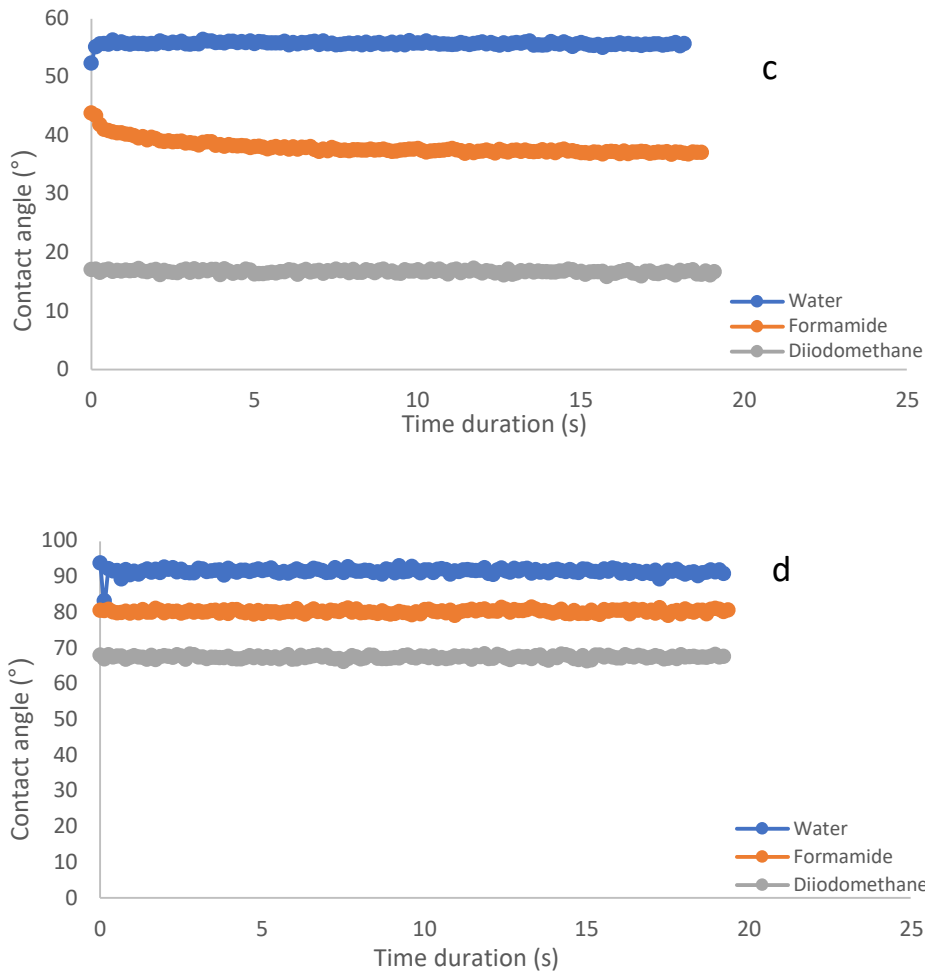
Figure 4.3. a) Contact angle of diiodomethane, formamide and water on the cake layer of C. V. cells on the filter paper; contact angle of diiodomethane, formamide and water on the b) PDMS, c) PU, d) PTFE sensore.

Table 4.3. lists the contact angle of solvents on sensors. It is seen the contact angle of water on the PDMS, and PTFE sensors were similar but larger than that of PU sensor. Therefore, PDMS and PTFE sensors were more hydrophobic than PU sensor. Also, other solvents made smaller contact angles on all sensors, but the contact angles were still larger for PDMS and PTFE sensors than the PU sensor. Also, PTFE sensors made larger contact angle than other surfaces, which reflects its more hydrophobic nature than other sensors (Table 4.2) (Morra et al. 1990).

Table 4.2 Contact angle of solvents on four surface after 2 s of experiment.

Contact angle (°)	Water	Diiodomethane	Formamide
Cake layer of C. V. Cells on Filter papers	81.5	33.6	37
PDMS	89.6	47	64.4
PU	55.7	17.1	39.5
PTFE	92.7	67.9	79.9

4.4 QCM Test

The frequency and dissipation of the sensors adsorbing algae is shown Figure 4.4. It is seen that all the sensors adsorbed water as their F dropped and D elevated slightly upon treating with water at the beginning of experiment. These results support the fact that the sensors became wet. Interestingly, PDMS and PFTE sensors had the larger frequency changes than PU sensor did, while all sensors developed close dissipation. Also, it is observable that by washing the sensor with buffer water after adsorption experiment, some algae were detached from the surface, implying their weak adsorption on the sensors. The dramatic increasing after 5 minutes' buffer rinsing for sensor PDMS is a good reason to prove the accuracy of the modeling. Because in the simulation, in all of properties impact, the most total interaction energy is with sensor PDMS (Figure 4.4).
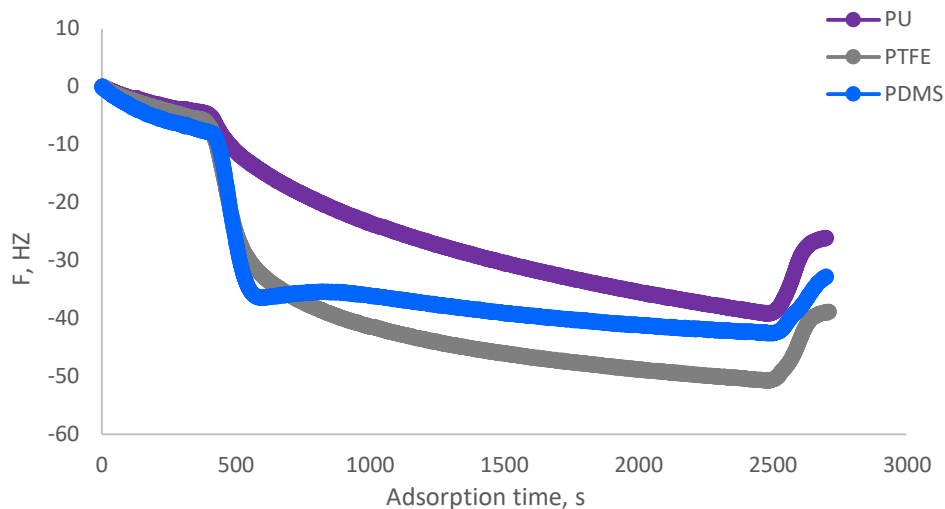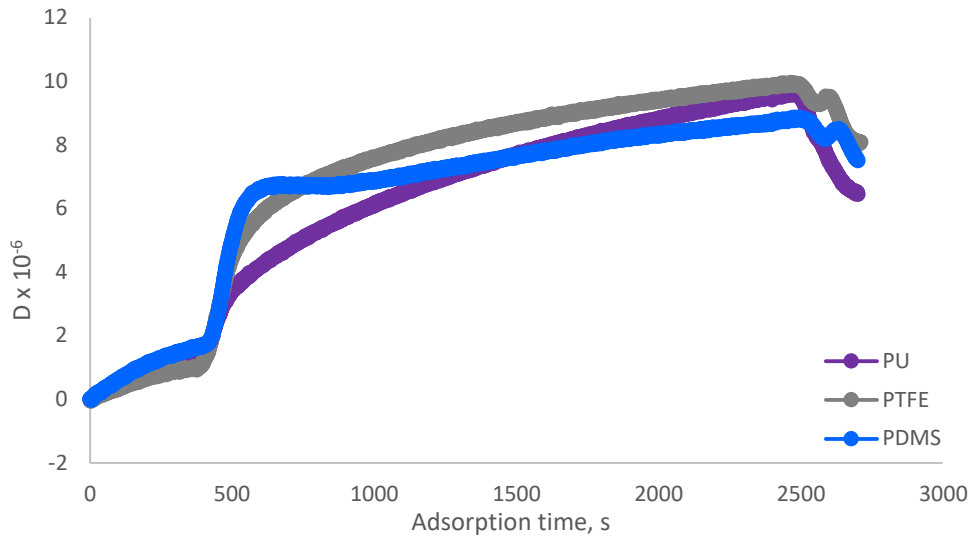
Figure 4.4. Frequency and dissipation of sensors of PDMS, PU and PTFE upon adsorbing algae.

The mass and thickness of adsorbed algae on the sensors are shown in Figure 4.5. It is observable that the PDMS sensor had the higher rate of mass adsorption, but PTFE sensor had a higher overall adsorbed mass at equilibrium. The PU sensor had the slowest rate of algae adsorption. The developed thickness of algae follows the same trend as adsorption mass (i.e., the higher mass generated a thicker adsorbed adlayer) (Figure 4.5). The lower adsorption of algae on the PU sensor supports the fact that the hydrophilic surfaces adsorb less algae (Table 4.2). Also, in figure 4.5 fast increasing of the PDMS exactly after first buffer rinsing would be the reason of the most interaction energy that PDMS has, rather that another two sensors.
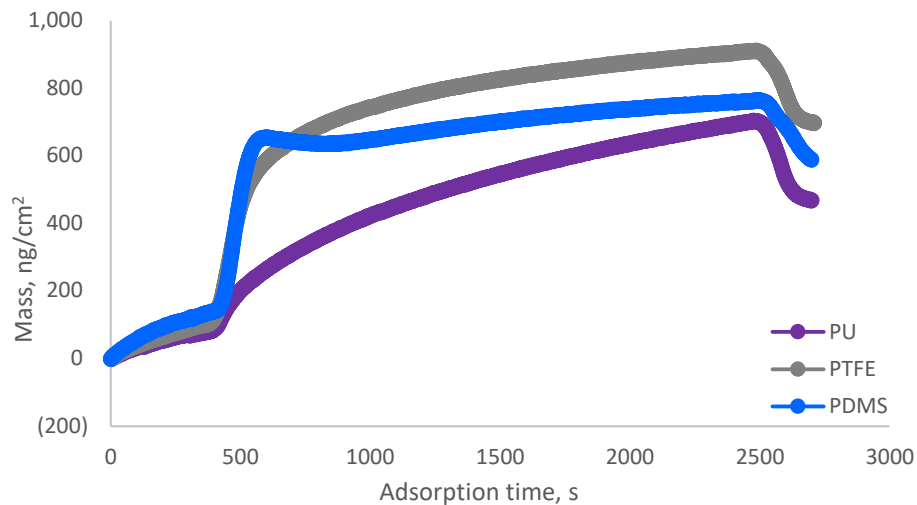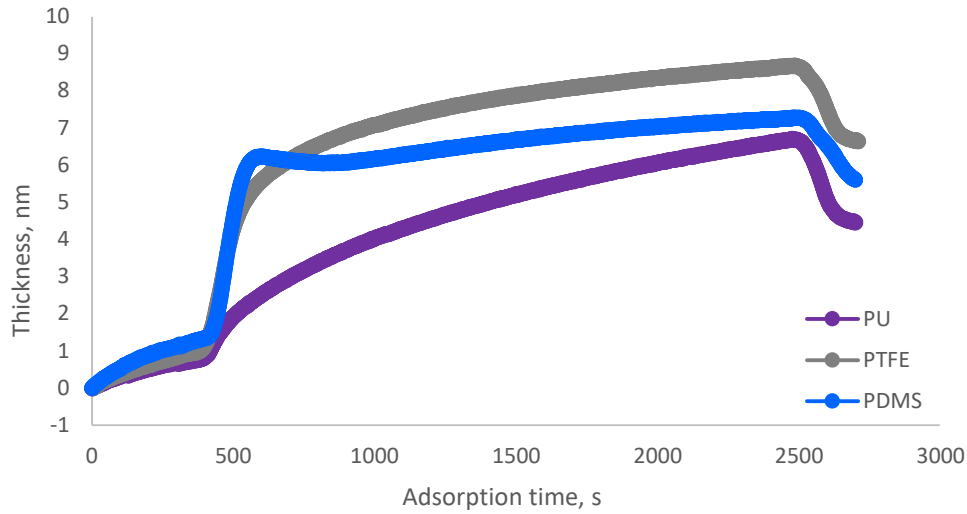
Figure 4.5. Mass and thickness of adsorbed mass of algae on sensors.

5 Theory and modeling

5.1 Abbreviations

Table 5.1. nomenclature

AB	Hydrophobic interaction	+	Electron acceptor
EL	Repulsion force	-	Electron donor
LW	Attraction force	k	Reciprocal debay (0.103)
m	membrane	h_0	Cut off distance (0.158)
W	water	T/λ_0	Decay length (0.6)
L	liquid	f	Foulant particle minimum equilibrium
S	solid	TO L	total
ΔG	Interaction energy per unit area (mj.m^{-2})	$\varepsilon_r \varepsilon_0$	Suspending liquid Permittivity (C.V^{-1}, m^{-1})
h	Separation distance (nm)	γ	Surface tension parameter(mj.m^{-2})
i	Unit vector along positive X-direction	θ	Contact angle
j	Unit vector along positive Y-direction	Z	Roughness of membrane
r	Radius of smooth part (nm)	ζ	Zeta potential(mv)
R	Radius of rough part (nm)	n	Asperity number
D	Closest distance (nm)	λ	Asperity ratio

5.2 Calculation of interaction energy following XDLVO theory

According to the XDLVO theory, the total interaction energy between colloidal particles (Equation 5.1) consists of Lifshitz-Vander Waals (LW), acid-base (AB) and electrostatic double layer (EL) interaction energies. The energy per unit area of these three interactions ($\Delta G^{LW}(h)$, $\Delta G^{AB}(h)$ and $\Delta G^{EL}(h)$) between two infinite planar surface can be described according to Equations 5.2 to 5.4 (Bhave et al. 2012).

$$\Delta G^{Total}(h) = \Delta G^{LW}(h) + \Delta G^{AB}(h) + \Delta G^{EL}(h) \tag{5.1}$$

$$\Delta G^{LW}(h) = -\frac{A_H}{12\pi h^2} = \Delta G_{h_0}^{LW}\frac{h_0^2}{h^2} \tag{5.2}$$

$$\Delta G^{AB}(h) = \Delta G_{h_0}^{AB}\exp\left(\frac{h_0-h}{\lambda}\right) \tag{5.3}$$

$$\Delta G^{EL}(h) = k\,\zeta_A\,\zeta_m\,\varepsilon_r\,\varepsilon_0\left(\frac{\zeta_A^2+\zeta_m^2}{2\,\zeta_A\,\zeta_m}(1\text{-coth }k\,h) + \frac{1}{\sin kh}\right) \tag{5.4}$$

Respectively, h_0 is the minimum equilibrium cut-off distance, which is assumed to be 0.158 nm (Bhave et al. 2012). Also, ε, ζ, and κ^{-1} are the permittivity of the medium, zeta potential, and the double-layer thickness, respectively; λ is the correlation length of molecules in a liquid medium, 0.6 nm (Luo et al. 2016b). In these equations, ε is usually expressed as the product of the permittivity of a vacuum ($\varepsilon_0 = 8.854 \times 10^{-12}$ C²/J·m) and the relative permittivity (also called the dielectric constant) of the medium ε_r, which is 80 for water at 20°C (Luo et al. 2016b).

The surface or interface tensions are expressed as the sum of an polar (Lifshitz–van der Waals) component (γ^{LW}) and a polar (acid-base) component (γ^{AB}). γ^{AB} can be separated into an electron-donating component (γ^-) and an electron-accepting component (γ^+) (Bilad et al. 2014). According to these parameters, the ΔG^{LW} and ΔG^{AB} can be calculated following Equations 5.5 and 5.6:

$$\Delta G_{h_0}^{LW} = -2\left(\sqrt{\gamma_A^{LW}} - \sqrt{\gamma_L^{LW}}\right)\left(\sqrt{\gamma_m^{LW}} - \sqrt{\gamma_L^{LW}}\right) \tag{5.5}$$

$$\Delta G_{h_0}^{AB} = 2\left[\sqrt{\gamma_A^+}\left(\sqrt{\gamma_m^-} + \sqrt{\gamma_A^-} - \sqrt{\gamma_L^-}\right) + \sqrt{\gamma_L^-}\left(\sqrt{\gamma_m^+} + \sqrt{\gamma_A^+} - \sqrt{\gamma_L^+}\right) - \sqrt{\gamma_m^-\gamma_A^+} - \sqrt{\gamma_m^+\gamma_A^-}\right]$$

$$\tag{5.6}$$

Where, subscript A means algae; subscript m means membrane; subscript L means liquid.

The properties of particle surface can be obtained by solving a set of three Young's equations (Equation 5.7) (Eroglu et al. 2015). The values of the surface tensions for liquid (γ_l^{LW}, γ_l^+, and γ_l^-) (l is liquid. means water, formamide and diiodomethane) and contact angles (θ) should be measured for at least three different liquids (e.g., water, formamide, and diiodomethane) to determine the surface free energy of a solid (γ_m^{LW}, γ_m^+, and γ_m^-) (m is membrane. means PDMS, PU and PTFE). In this modeling study, the above-mentioned parameters were collected from previous literature and summarized in Table S1 in appendix (Melin et al. 2006). Table 5.2 summarizes the parameter of surface tensions of the forementioned liquids (A is the symbol of the algae).

$$\frac{(1+cos\theta)}{2}\gamma_l^{Tol} = \sqrt{\gamma_l^{LW}}\sqrt{\gamma_m^{LW}} + \sqrt{\gamma_l^-}\sqrt{\gamma_m^+} + \sqrt{\gamma_l^+}\sqrt{\gamma_m^-} \tag{5.7}$$

Table 5.2 Surface tensions (mN/m) of three probe liquids.

Probe liquids	γ_l^{LW}	γ_l^-	γ_l^+
Water	21.8	25.5	25.5
Formamide	39.0	39.6	2.28
Diiodomethane	50.8	0.0	0.0

Table 5.3 Surface tension parameters of surface of membranes made of PDMS, PTFE, PU and algae

Membrane	Θ_W	Θ_F	Θ_D	γ_m^{LW}	γ_m^-	γ_m^+	ζ
Algae	81.5	37	33.6	42.641	0.230	2.965	-25.56
PDMS	89.6	64.4	47	35.88	1.974	0.113	-83
PTFE	92.7	79.9	67.9	24.01	5.135	0.00292	-75.2
PU	55.7	39.5	17.1	48.581	21.511	0.0259	-18.56

5.3 Total interaction energy calculation for circle shape particle and membrane surface

With the contributions of scanning electron microscope (SEM), the surface morphology of silica particles, polystyrene particles, and methyl methacrylate particles were revealed to have raspberry-like surface morphology with depressions and protrusions (Luo et al. 2016b; Marbelia et al. 2014; Bilad et al. 2014). In the present work, we applied the ripped rough particle theory to construct the rough particle that can help capture the details of peaks and valleys of the ripples on the particles

with similar structures. This construction method was successfully applied in modeling the rough flocs for simulating the interaction between flocs and membranes in the past (Matamoros et al. 2015a).

To simplify the calculation, the cartesian coordinates (χ, y) was replaced by spherical coordinates (R, θ) in this study.

$$x = R \sin \theta \tag{5.8}$$

$$y = R\cos \theta \tag{5.9}$$

The surface morphology of particles can represent the surface roughness of colloidal particles. This analytical image can be determined mathematically (Bilad et al. 2014; Melin et al. 2006). The rough surface and radius of rough particles were modeled following Equations 5.10 (Marbelia et al. 2014).

$$R_{circle} = r + r \times \lambda \times \cos(n\theta) \tag{5.10}$$

Where r is the radius of element particle (smooth), λ is the asperity ratio, n is the asperity number.

$$h = D + r + r \times \lambda - R\cos\theta + P - f(x) \tag{5.11}$$

where the D is the closest distance between particle and membrane, the P is the asperity height of membrane with rough surface. Also, W is the width of the asperity on membrane surface and $f(x)$ is the roughness of membrane surface, which was calculated following Equation 5.12.

$$f(x) = P\cos(\frac{\pi r \cos\theta}{2W}) \tag{5.12}$$

By combining Equations 5.10 to 5.12 , Equations 5.13 to 5.15 were developed to determine the individual LW, AB, and EL interactions between rough algae and rough membrane (Qu and Fan 2010; Zhao et al. 2016). Figure 5.1 shows the parameters considered for modeling the interaction of a circle and membrane surface.

$$U(h)^{AB} = \int_0^\pi \Delta G_{h_O}^{AB} \exp\left(\frac{h0-[D+R-R\times\cos\theta+P-f(x)]}{\lambda 0}\right) \, d\theta =$$
$$\Delta G_{h_O}^{AB} \int_0^\pi \exp\left(\frac{h0-[D+R-R\times\cos\theta+P-f(x)]}{\lambda 0}\right) \, r d\theta \tag{5.13}$$

$$U(h)^{EL} = \int_0^\pi k \, \zeta_A \, \zeta_{f2} \varepsilon_r \varepsilon_0 \left(\frac{\zeta_A^2+\zeta_m^2}{2\,\zeta_A\,\zeta_m} (1\text{-coth } k \, [D+R\text{-}R\times\cos\theta+P\text{-}f(x)]) + \frac{1}{\sin k[D+R-R\times\cos\theta+P-f(x)]}\right)$$
$$r d\theta \tag{5.14}$$

$$U(h)^{LW} = \int_0^\pi \Delta G_{ho}^{LW} \frac{ho^2}{[D+R-R\times\cos\theta+P-f(x)]^2} \; d\theta = \Delta G_{ho}^{LW} \int_0^\pi \frac{ho^2}{[D+R-R\times\cos\theta+P-f(x)]^2} r d\theta$$

(5.15)
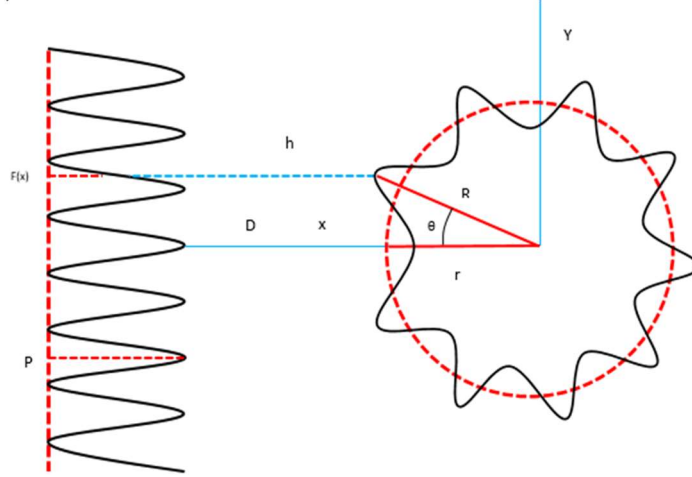
Figure 5.1. Parameters involved in the simulation of circle and membrane surface.

5.4 Total interaction energy calculation for ellipse shape particle and membrane surface

For ellipsoidal particles, the radius of the rough ellipse (R), the radius of the smooth ellipse (r), separation distance (h), and roughness of membrane *f(x)* should be considered for determining the interaction energy of the ellipse and membrane surface. The equation to represent a smooth ellipse in coordinate is shown in Equation 5.16.

$$r = \sqrt{\frac{1}{\frac{\cos^2\theta}{a^2} + \frac{\sin^2\theta}{b^2}}}$$

(5.16)

Where the a is the major hemi axes and b the minor axes.

Basically, the surface morphology can represent the surface roughness of the colloidal particles. To stimulate the surface roughness, one object with a rough surface should be built. In this case, one mathematical model applied to rippled rough particle theory is often used for constructing the rough surfaces of particles (Wood 1981). The rough surface and radius of rough ellipsoids were modeled following Equations 5.17 and 5.18.

$$\Delta r = r \times \lambda \times \cos(n\theta) \tag{5.17}$$

$$R = \sqrt{\dfrac{1}{\dfrac{\cos^2\theta}{(a+(\Delta r))^2} + \dfrac{\sin^2\theta}{(b+(\Delta r))^2}}} \tag{5.18}$$

Figures 4.2 shows the scenario for the interaction of one rough ellipse and a rough flat surface, e.g., membrane. As shown in this Figure, the separation distance (h) to the flat rough surface could be calculated following equation 4.19:

$$h = a + D + r \times \lambda - R\cos\theta + P - f(x) \tag{5.19}$$

As seen in Figure 5.2 the interaction of ellipse and a flat surface can follow two scenarios. It matters if the ellipse approaches the membrane horizontally or vertically (Yin et al. 2020). According to the SEI method, the total interaction energy of two particles (U(h)) can be calculated by considering the interaction energy per unit area ($\Delta G(h)$) of particles and projected surface area of the rough particles according to Equations 5.20 to 5.22.

$$U(h)^{AB} = \int_0^\pi \Delta G_{h_O}^{AB} \exp\left(\dfrac{h0-[a-R\cos\theta+D+P-f(x)]}{\lambda 0}\right) d\theta = \Delta G_{h_O}^{AB}$$
$$\int_0^\pi \exp\left(\dfrac{h0-[a-R\cos\theta+D+P-f(x)]}{\lambda 0}\right) r\, d\theta \tag{5.20}$$

$$U(h)^{EL} = \int_0^\pi k\, \zeta_{f1}\, \zeta_{f2}\varepsilon_r\varepsilon_0\left(\dfrac{\zeta_A^2+\zeta_m^2}{2\,\zeta_A\,\zeta_m}\right)(1\text{-coth } k[a\text{-}R\cos\theta+D+P-f(x)]) + \dfrac{1}{\sin k[a-R\cos\theta+D+P-f(x)]}$$
$$r d\theta \tag{5.21}$$

$$U(h)^{LW} = \int_0^\pi \Delta G_{h_O}^{LW} \dfrac{h0^2}{[a-R\cos\theta+D+P-f(x)]^2}\, d\theta = \Delta G_{h_O}^{LW} \int_0^\pi \dfrac{h0^2}{[a-R\cos\theta+D+P-f(x)]^2}\, r d\theta$$
$$\tag{5.22}$$
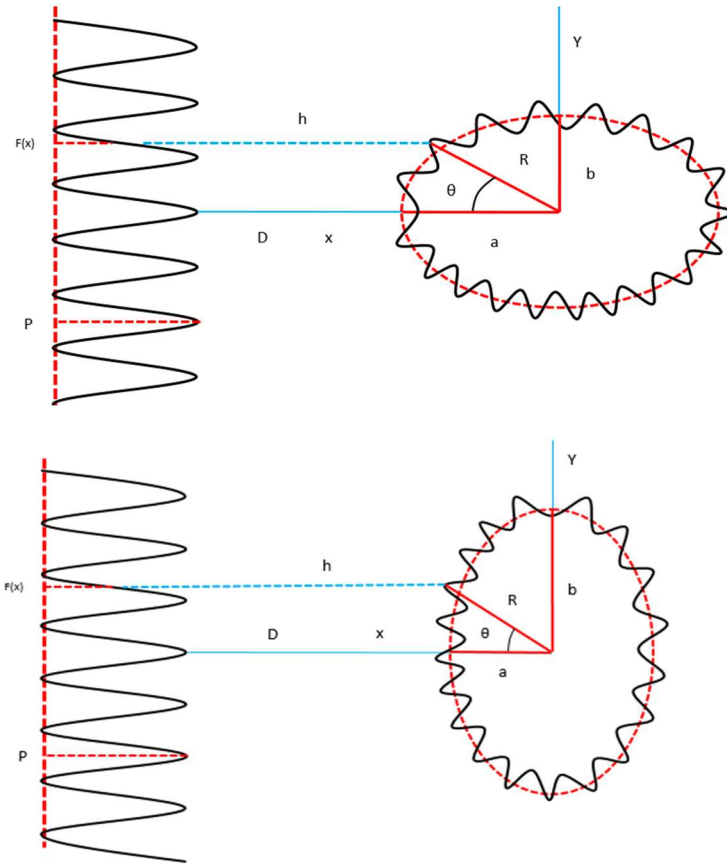
Figure 5.2 interaction parameters of an ellipsoidal particle and membrane surface.

5.5. Impact of various parameters in total energy calculation

5.5.1 The particle size

In this modeling study, the weight and density of particles were not changed, and only the size of particles is considered for analysis. The analysis range selected for particle size effects was the value of a (or b) from 1100 to 1500 nm.

5.5.2 The asperity number

In this part of modeling study, the size of particle and the asperity ratio were not changed, and only the number of particle asperity on the particle is considered for analysis. The analysis range selected for asperity number effects was the value of n between 3 and 10.

5.5.3 The asperity ratio

In this section of the modeling study, the size of particle and the asperity number were not changed, and only the ratio of particle asperity is considered for analysis. The analysis range selected for asperity ratio effects was the λ value between 0.00001 and 0.1 nm.

5.5.4 The membrane asperity height

In this modeling study, the particle properties and membrane asperity width were not changed, and only membrane asperity height was altered. The analysis range selected for membrane asperity height effect was the value of P between 500 and 2500 nm.

5.5.5 The membrane asperity width

In this modeling study, the particle properties and membrane asperity height were not changed, and only the membrane asperity width was altered for analysis. The analysis range selected for membrane asperity width effect was the value of w between 500 and 2500 nm.

5.5.6 The orientation angle of ellipse and membrane

In this modeling study, the membrane properties and the size and asperity properties of particle were not altered, and only the difference between 90° and 180° angle between ellipse and the membrane surface was considered for analysis.

6. Result and discussion of Modeling

6.1 Results and discussion on the interaction energy of circular particle and membrane surface

6.1.1 Particle size effect

In this set of analysis, the particle size effects on the total interaction energy between particles and membrane were modeled. Considering the actual average size of microalgae cell (Figure 4.1), the simulated particle size was selected to be between 1100 (nm) and 1500 (nm) (Table 4.1). It is seen that by enlarging the particle size, total interaction energy increases slightly as the interaction area between the particle and surface increase. Yin and Wang studied the effect of particle size of scheelite on their interaction efficiency and concluded that the total interfacial energy between the

particles was increased with enlarging the particles. As the size of particle enlarges, the interaction of particle and surface become more dominant, which will promote the adhesion of particles on the smooth surface (Erramilli and Genzer 2019; Al-Awady et al. 2015; Karunakaran et al. 2015). Interestingly, by including surface roughness, our results supported the previous simulation analysis (Bargozin et al. 2015). The results in Figures 6.1(a) and 6.1(c) are almost similar but are significantly lower than those in Figure 6.1(b) because the hydrophobicity of PDMS and PTFE surfaces are close, but both are larger than that of PU surface (Table 4.2) and algae interact/adsorb more with the PDMS and PTFE surfaces as it is a hydrophobic material (Table 4.2).
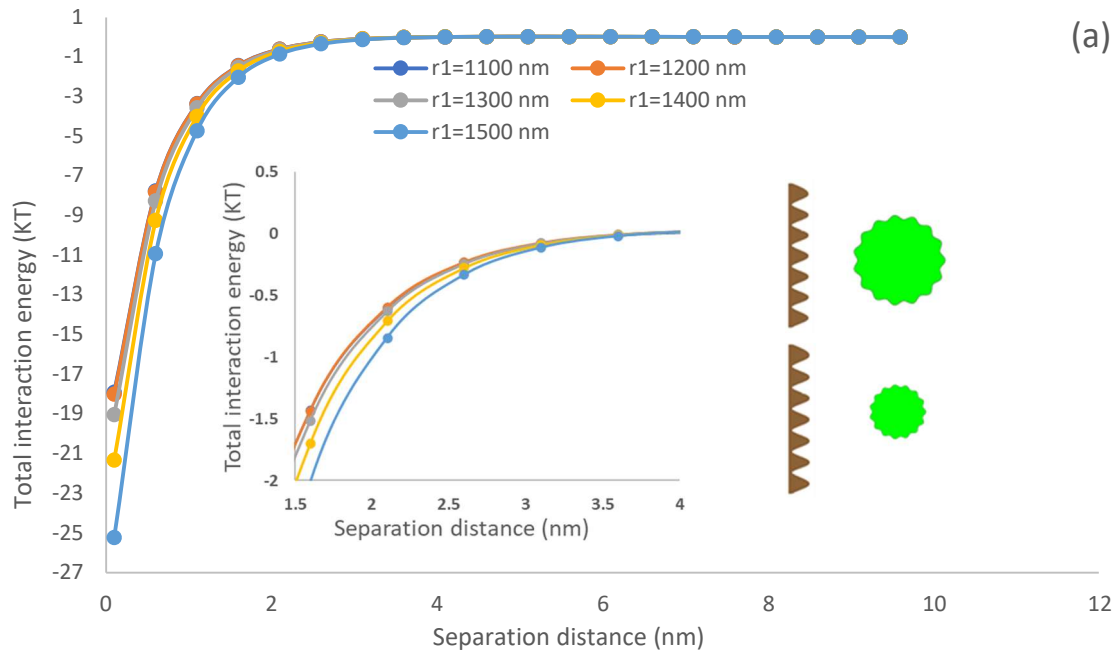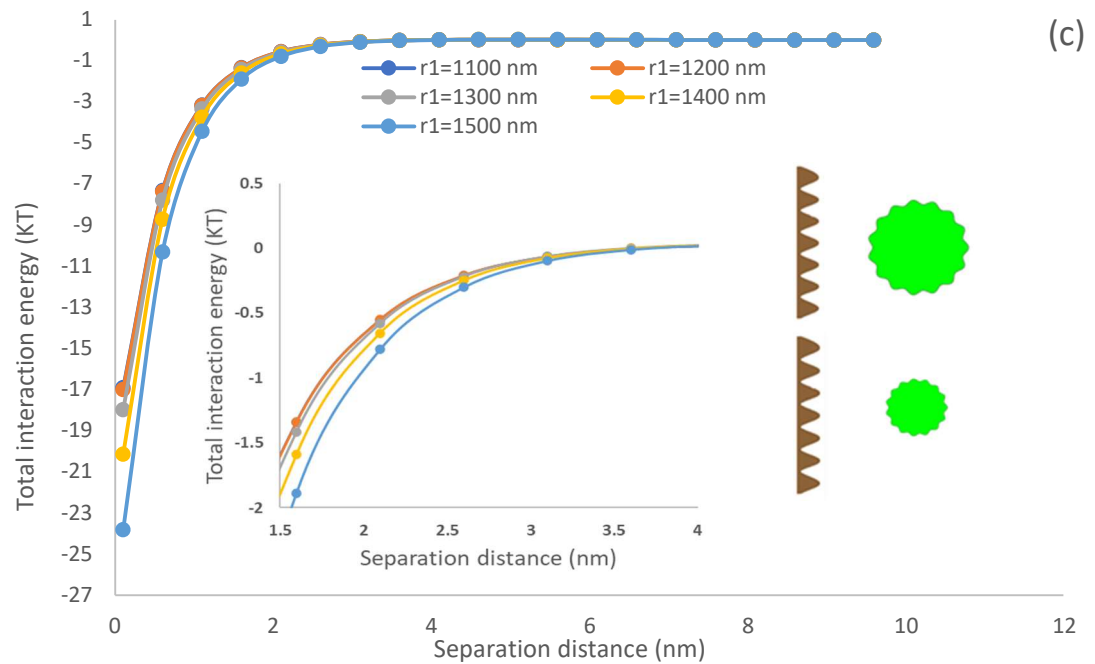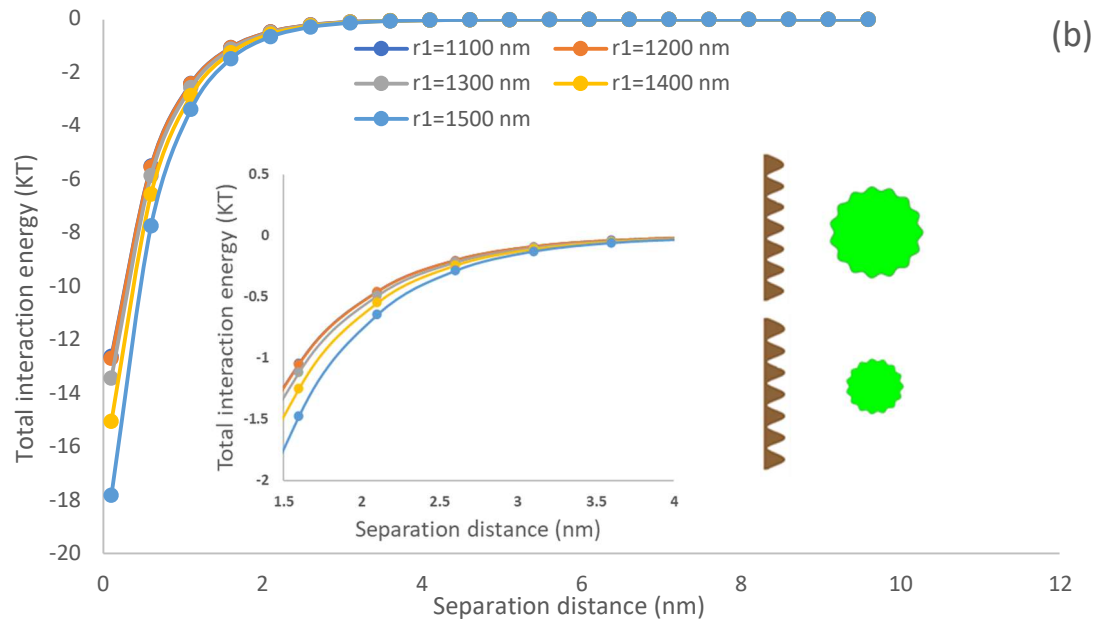
Figure 6.1. The effects of particle size on total interaction energy of circle particle and membrane surface (a) PDMS (b) PU (c) PTFE.

6.1.2 Asperity number effects

Figure 6.2 shows the impact of the asperity number of the particle on the interaction of the particle and membrane. The asperity number was considered between 2-8. Regardless of the membrane type, it is observable that with increasing the number of particle asperity, there was an insignificant change in the total interaction energy. According to equation 5.10, with increasing the asperity number (n), the separation distance (h) in equation 5.11 will increase and the total interaction energy will decrease. The primary minimum decreased slightly with raising the number of asperities (2 to 8) indicating a reduction in the attraction energy between algae and membrane (Figure 6.2). This fact is acceptable because the surface roughness reduced the adhesion force between particles (Luo et al. 2016b). Decrease in attraction energy happened at the closest distance, that led to a shallow primary minimum (Ruiz et al. 2014).
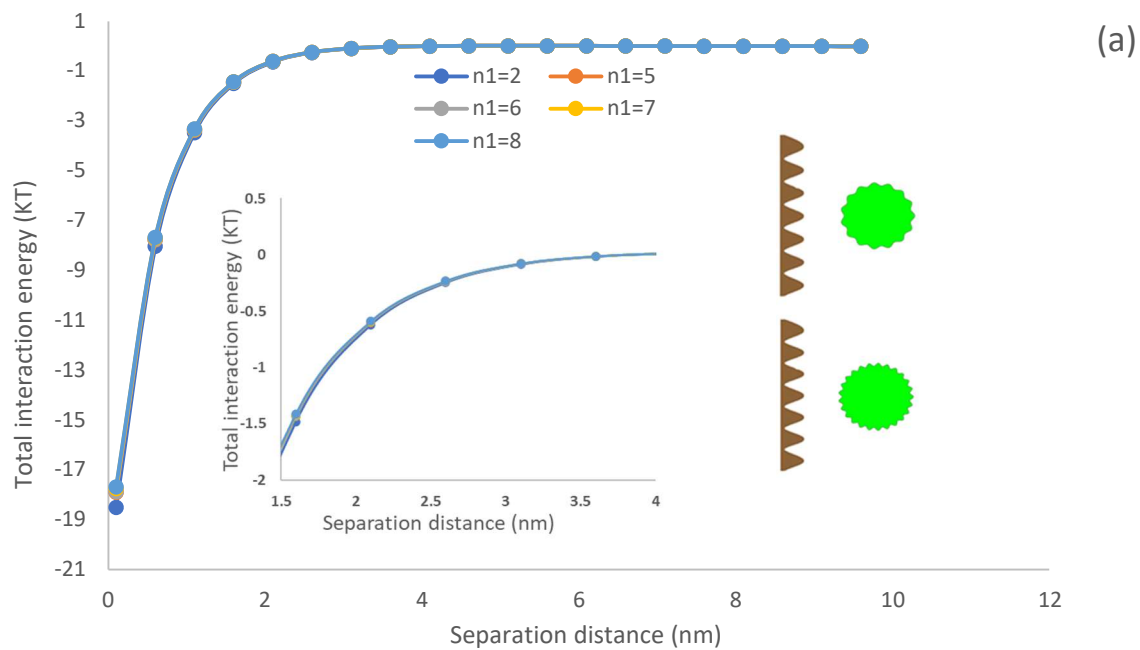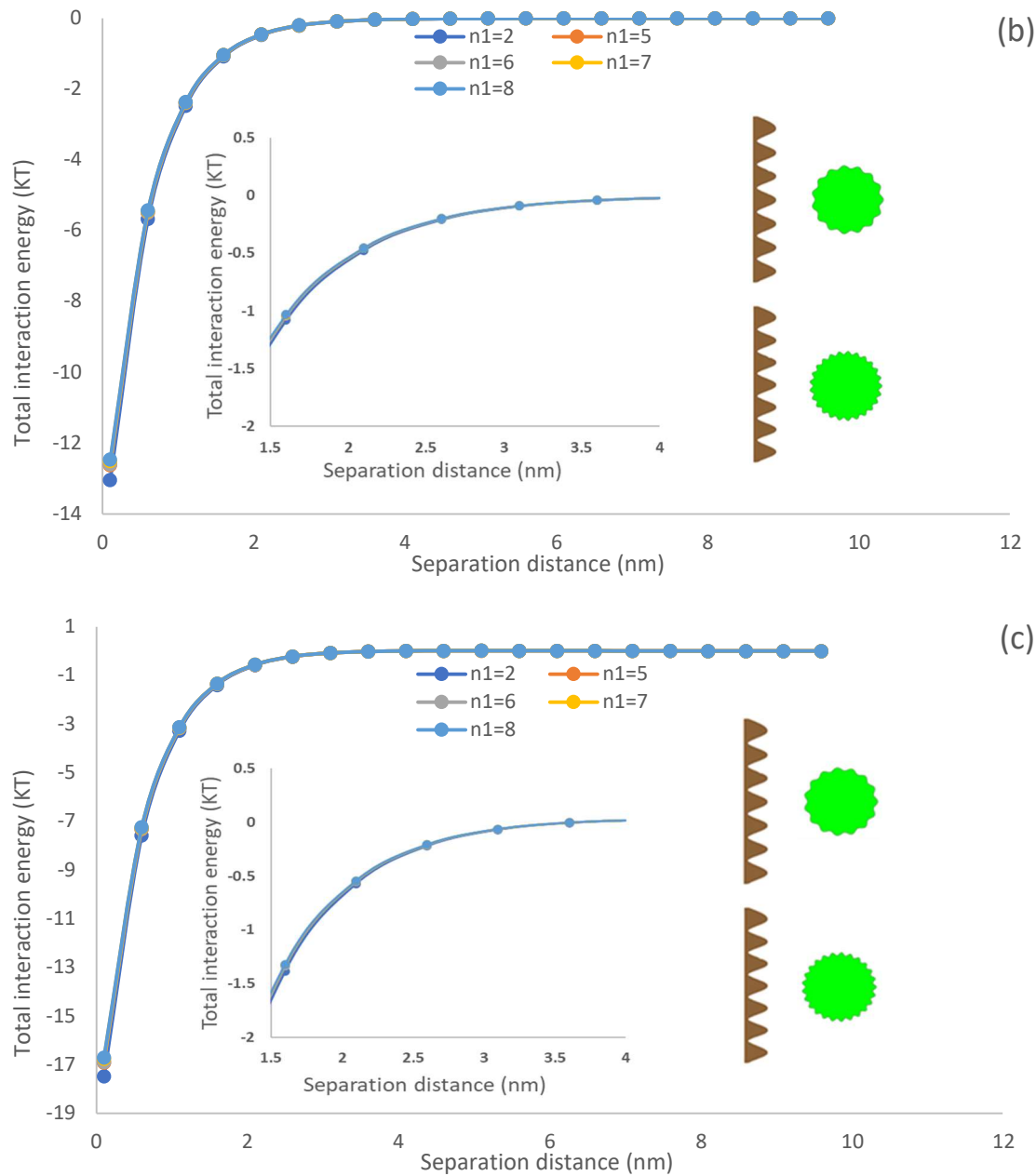
Figure 6.2 The effect of Asperity number on total interaction energy of particle and membrane surface. (a) PDMS (b) PU (c) PTFE.

6.1.3 Asperity ratio effects

Figure 6.3 shows the impact of the asperity ratio of the particles on the interaction energy of the particle and membrane surface. In this modeling study, the range between 0.1 and 0.00001 was considered. With decreasing the asperity ratio, the total interaction energy increases, regardless of

the membrane type. A particle (nanoscale) with a larger asperity ratio shows less total interaction energy and more separation distance (Ozkan and Berberoglu 2011). According to equation 5.11, as the asperity ratio (λ) increases, the separation distance (h) will increase and thus the total interaction energy will decrease. Based on the results, the asperity ratio of particles has a significant effect on the adhesion of algae on the membrane surface. The particles may adhere without adequate electric repulsion force to affect the attractions (Lum et al. 2013). On the other note, surface roughness decreases the particles contact area because the asperity size and height would increase with increasing the roughness (Muñoz et al. 2005; Luo, Le-Clech, and Henderson 2016b).
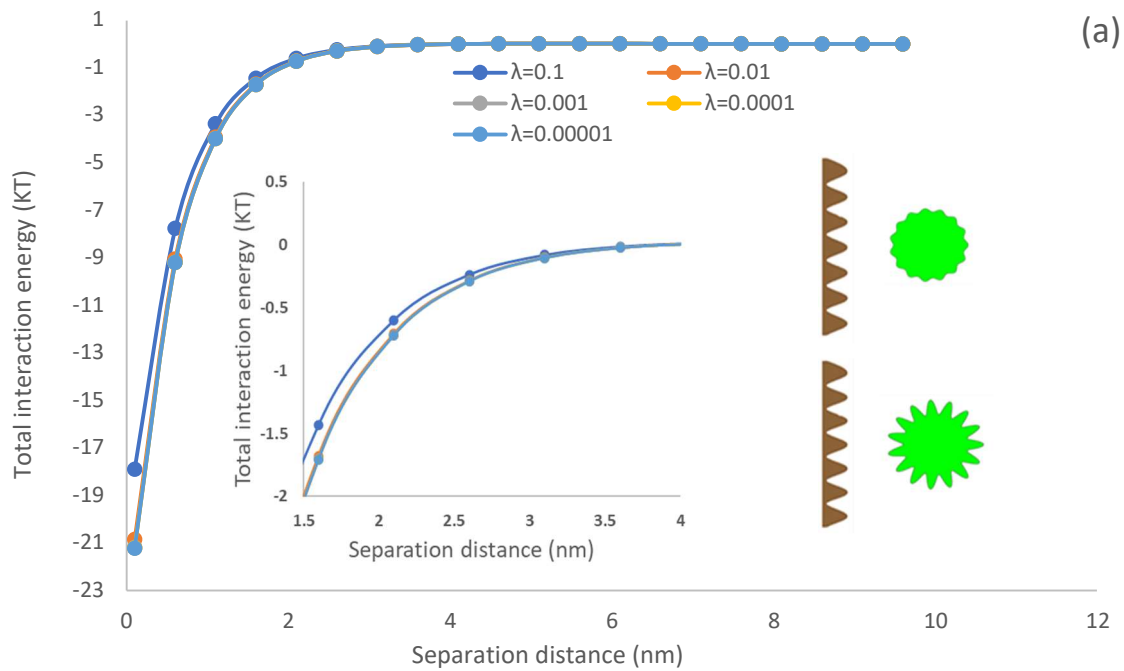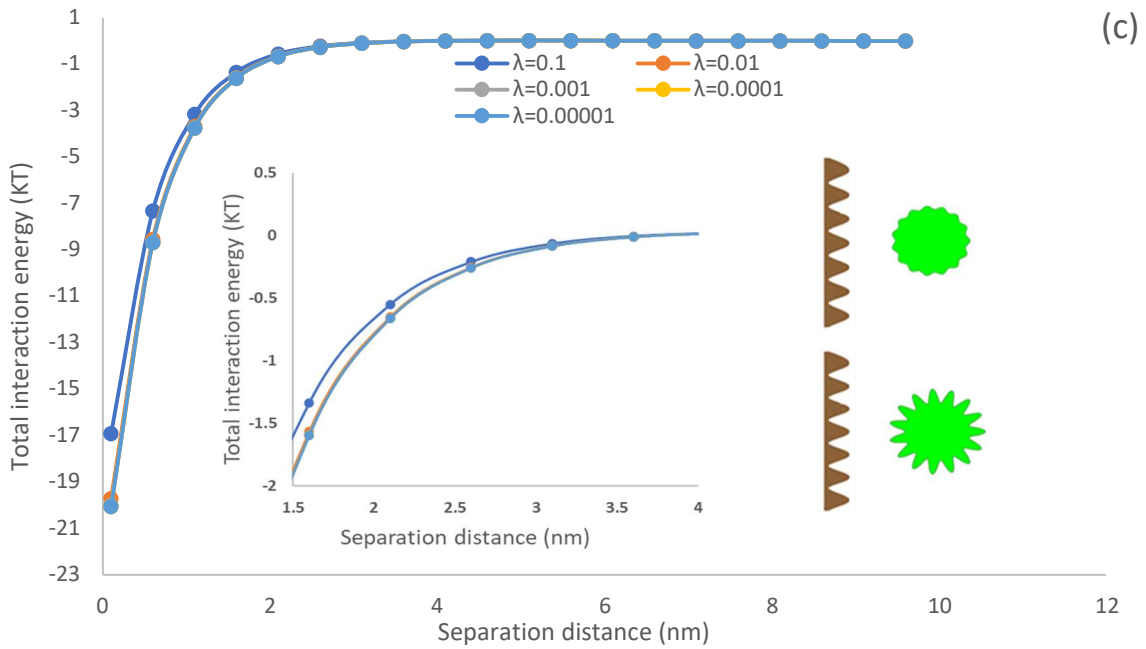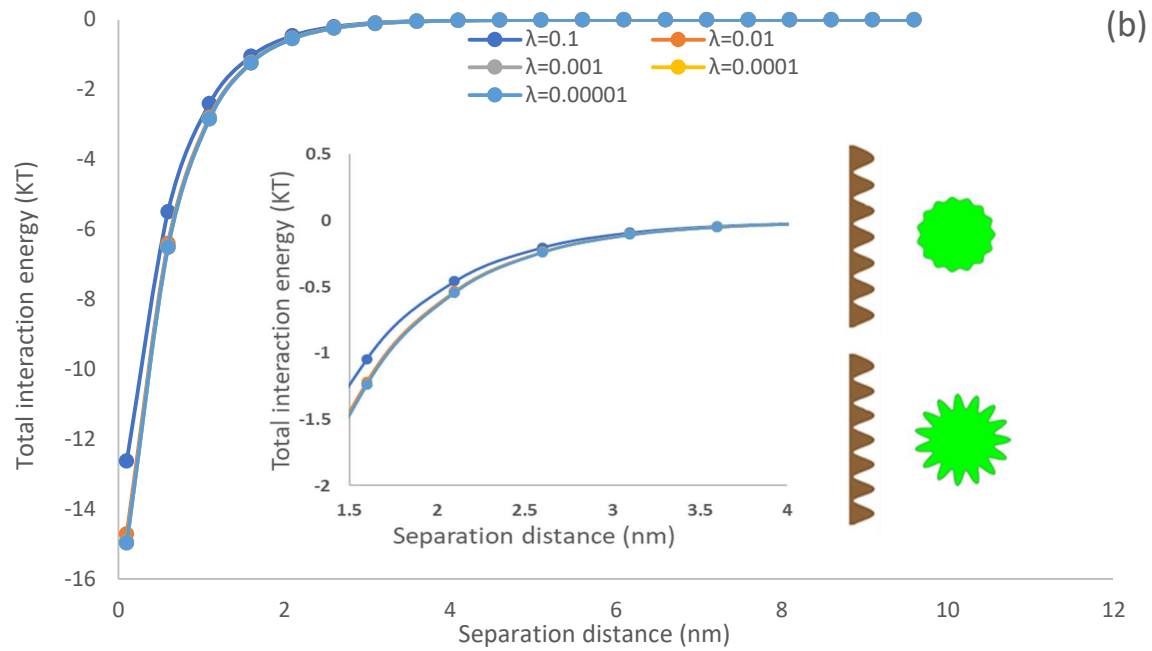
Figure 6.3. The effect of asperity ratio on total interaction energy of particle and membrane surface. (a) PDMS (b) PU (c) PTFE.

6.1.4 Membrane asperity height

Figure 6.4 shows the interaction energy of the particle and membrane surface as a function of membrane asperity height. It is clear that with an increase in the membrane asperity height, the total interaction energy decrease. It is obvious that, with increasing the membrane asperity height (p) the separation distance (h) increase and then the total interaction energy decrease (Erramilli and Genzer 2019; Hoek and Agarwal 2006; Eom et al. 2017; Schmidt et al. 2004; Torkzaban and Bradford 2016). According to this result, membrane asperity height plays an important role in the level of algae adhesion to membrane in wastewater treatment, thus a lower membrane asperity height would lead to fewer algae adhesion. A similar fact that Guven and coworkers discussed was the effect of the surface roughness on the particle-bubble colloidal interaction. The results showed that rising the asperity size is a reason of decreasing in the energy barrier (Posadas et al. 2015). In opposition to the previous analysis, the present model considered two rough surfaces rather than a particle and a bubble. Therefore, the rougher surface is a reason of smaller energy barrier that could affected more readily by van der Waals attraction and hydrophobic interaction forces.
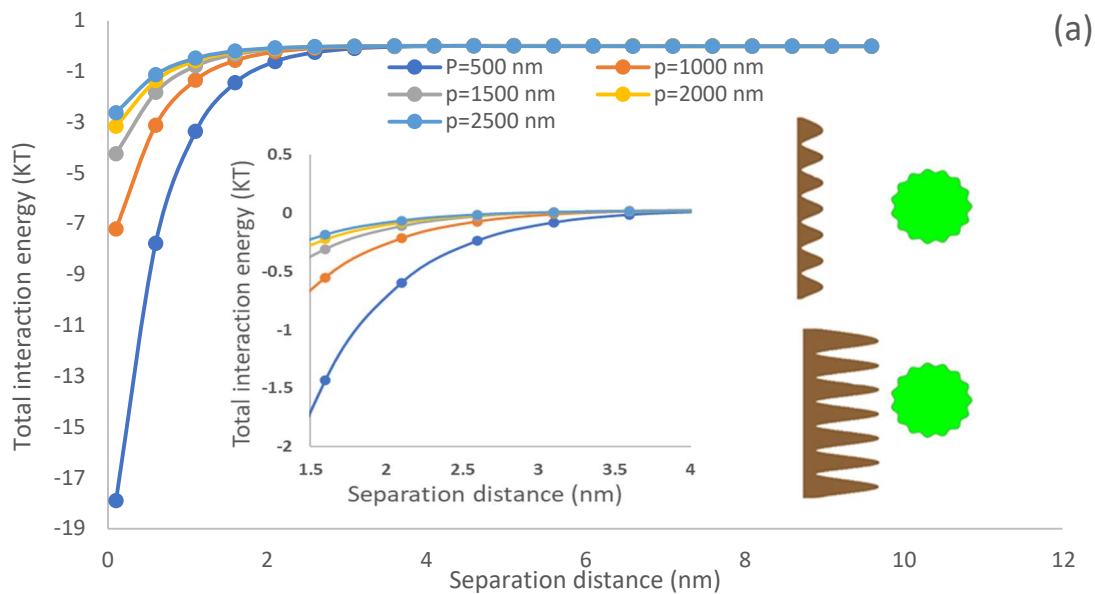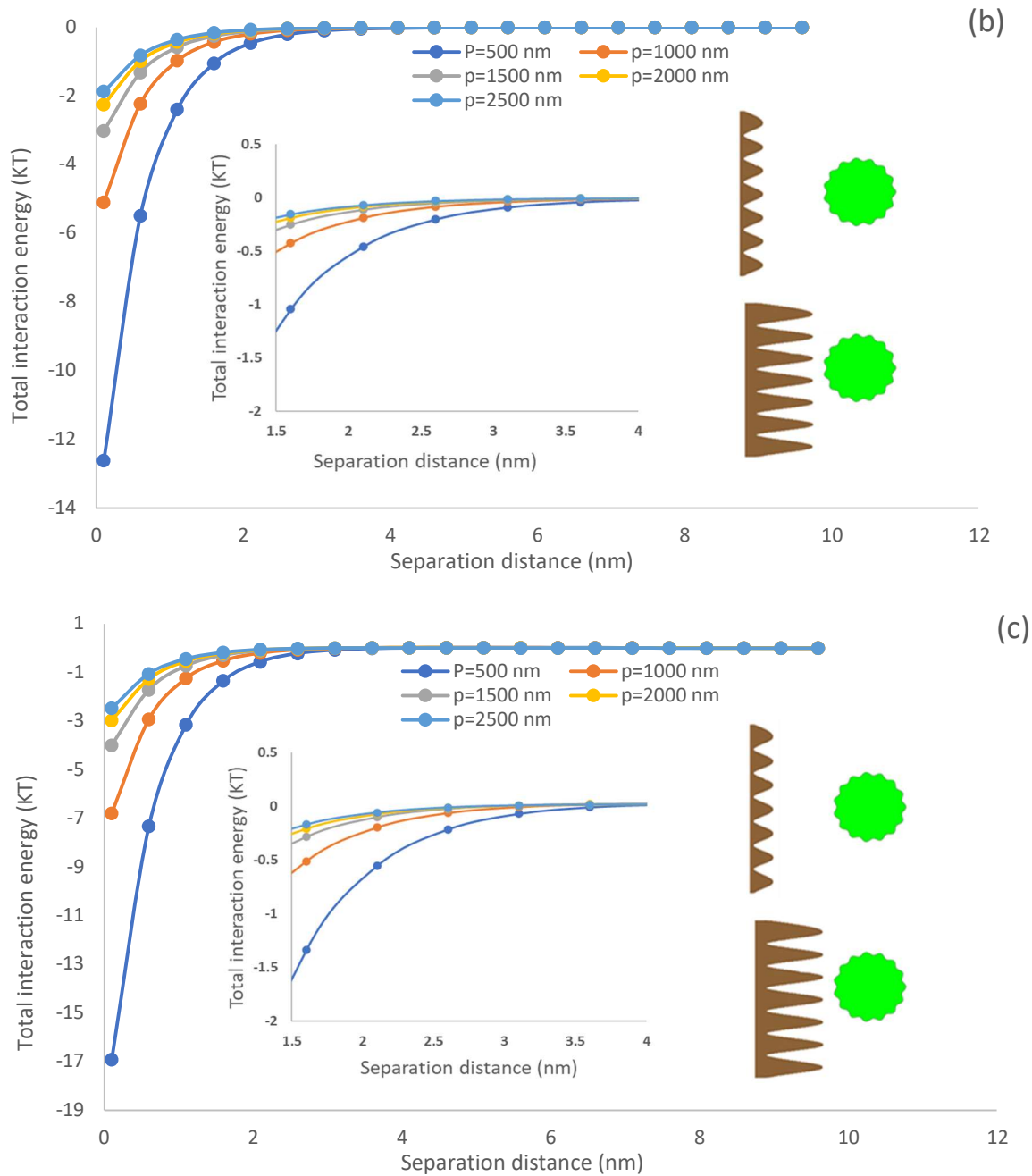
Figure 6.4. The effect of membrane asperity height on total interaction energy of particle and membrane surface. (a) PDMS(b) PU (c) PTFE.

6.1.5 Membrane asperity width

Figure 6.5 shows the effect of membrane asperity width on the total interaction energy of simulated microalgae particle membrane surface. With increasing the membrane asperity width, the total

interaction energy increased (Ozkan and Berberoglu 2011; Kwon et al. 2005; Shen et al. 2012). When the membrane asperity width (w) increases following equation 5.12, the membrane roughness (f(x)) will decrease, and the surface becomes smoother, but the separation distance will not change and thus the total interaction energy increase. Hallab et al. (2001) stated that surface roughness is a critical factor in decreasing the interaction energy. Efforts to produce cell adhesion to biomaterial surface requires the ability to alter surface characteristics for desired cellular proliferation and adhesion. In one study, the surface energy was proportional to cellular adhesion strength (Hallab et al., 2001). It was also discovered that the polymeric materials shown significant improved adhesion strength linked with increased surface roughness (Hallab et al. 2001). Therefore, membrane asperity width plays an important role in the level of algae adhesion to the membrane in wastewater treatment systems.
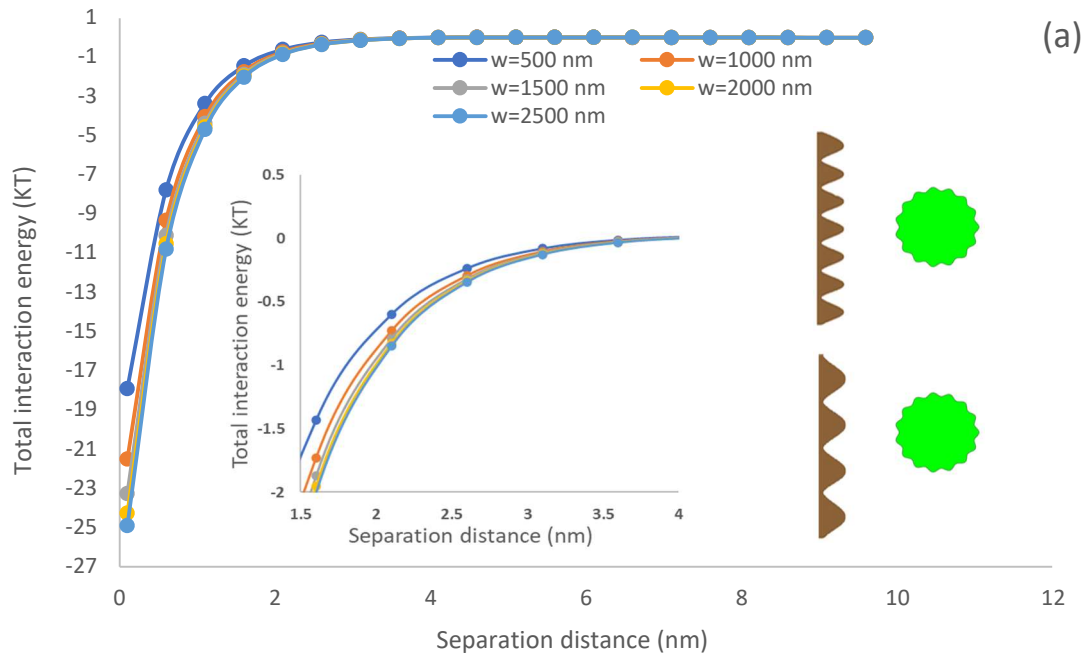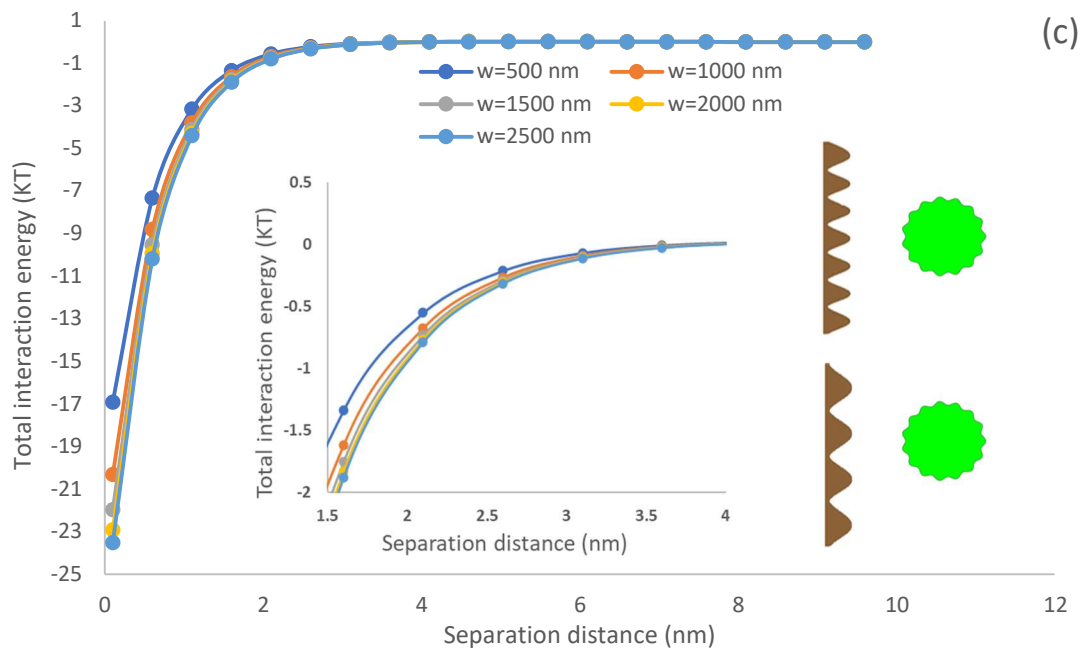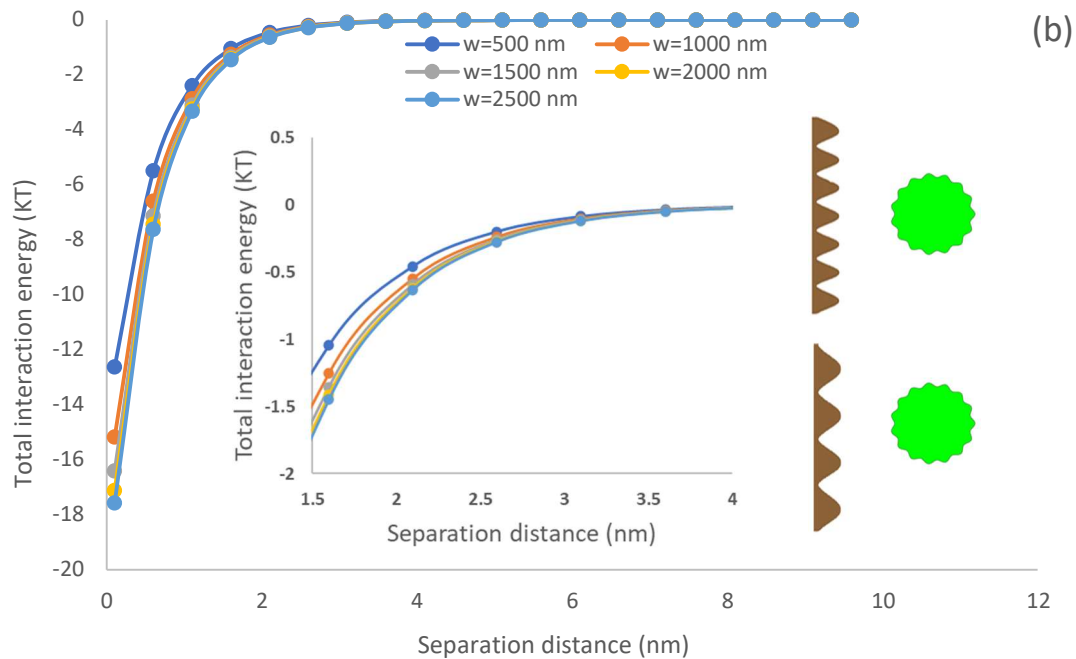
Figure 6.5. The effect of membrane asperity width on total interaction energy of the particle and membrane surface (a)PDMS (b) PU (c) PTFE.

6.2 Results and discussion for the interaction energy of an ellipse particle and membrane surface

6.2.1 Particle size effect

In this set of simulated analysis, the effects of particle size on the total interaction energy developed between the particle and surface were analyzed (Figure 6.6). The radius of ellipse particle was considered to be 1100-1500 nm for radius A and 550-750 nm for radius B. It is seen that by enlarging the particle, the total interaction energy increases slightly as the interaction area between the particle and surface increase. The particle size effect on scheelite flotation and assumed that the total interfacial energy was Yin and Wang studied that elevated by enlarging the particles (Erramilli and Genzer 2019; Bargozin et al. 2015). In another study, as the radius of smooth particle (r) is enhanced, the interaction energy between the particle and surface was empowered. The results in Figures 6.6(a) and 6.6(c) shows that the attraction force between the algae and PDMS and PFTE surface is larger than that on PU membrane as the formers are more hydrophobic.
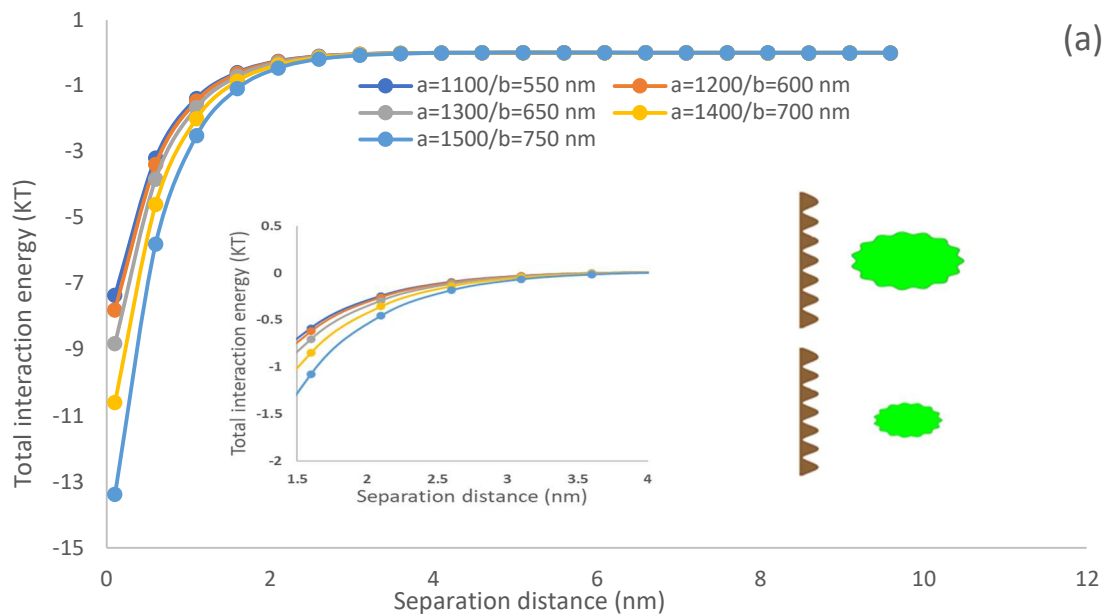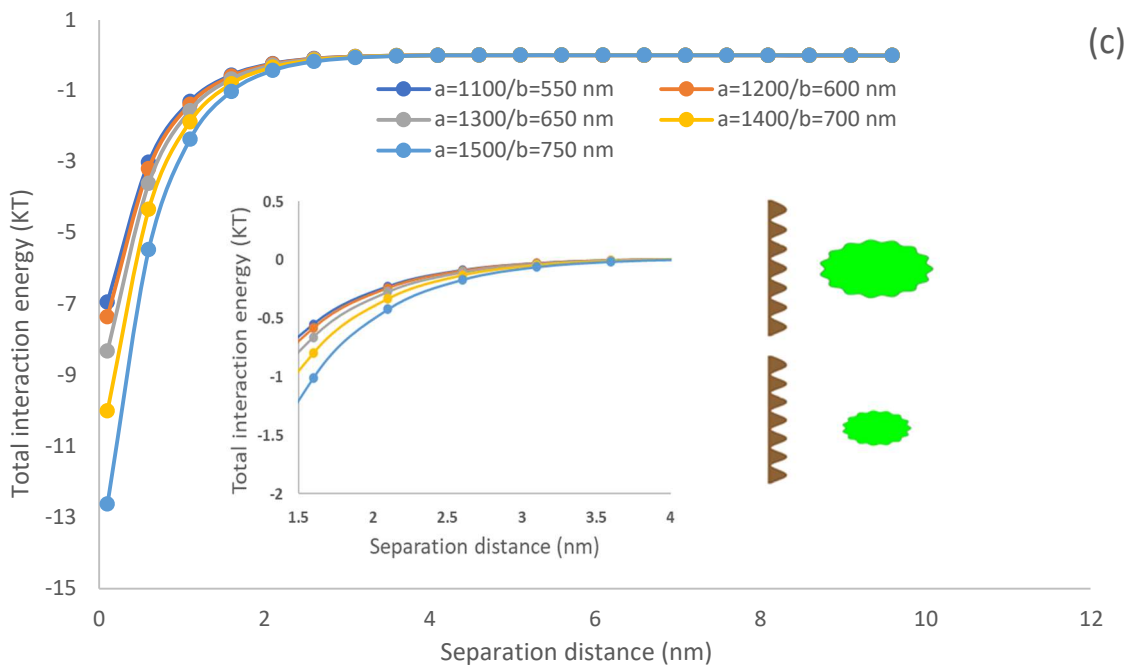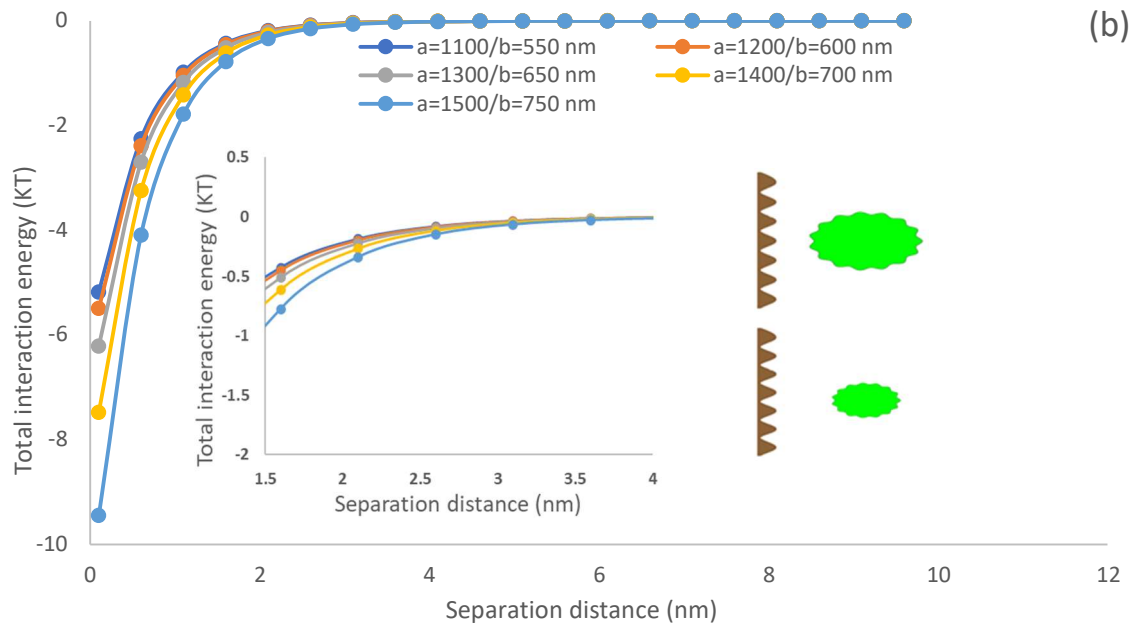
Figure 6.6. The effect of particle size on total interaction energy of the particle and membrane surface (a) PDMS (b)PU (c) PTFE.

6.2.2 Asperity number effects

Figure 6.7 shows the effect of asperity number on the total interaction energy of the ellipsoidal particle and membrane surface. Regardless of the membrane type, with increasing the asperity number of ellipse particle, the total interaction energy slightly decreases, which is similar to the results for the interaction of circular particle and membrane surface (Figure 6.2). With increasing the asperity number (n) in equation 5.17, the particle roughness (Δr) will decrease, the separation distance will also increase, and the total interaction energy will decrease. According to this explanation, particle asperity number have a minimum role on algae adhesion to the membrane in wastewater treatment. Katainen et al. explained that the adhesion force of particles was increased by the surface roughness of particle (Katainen et al. 2006).

(b)

(c)
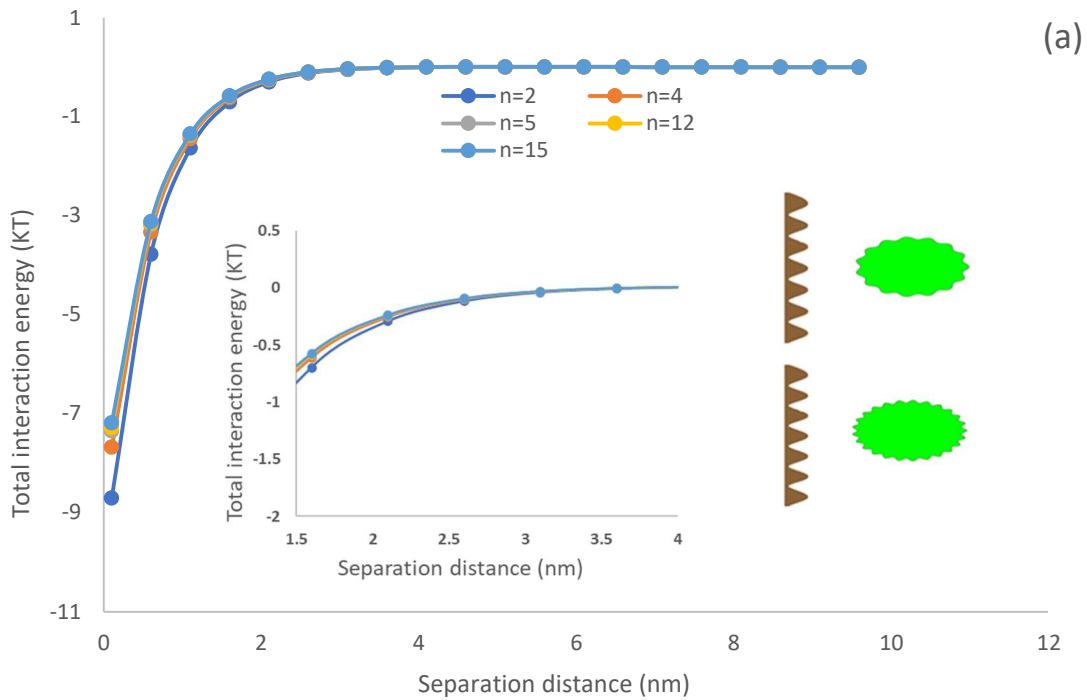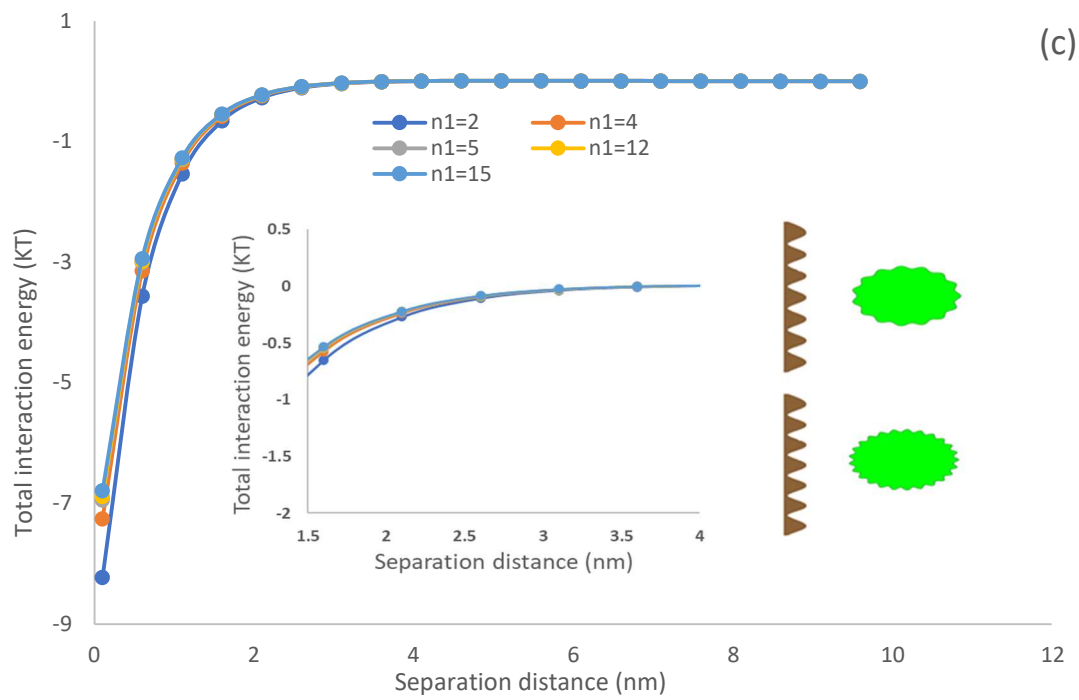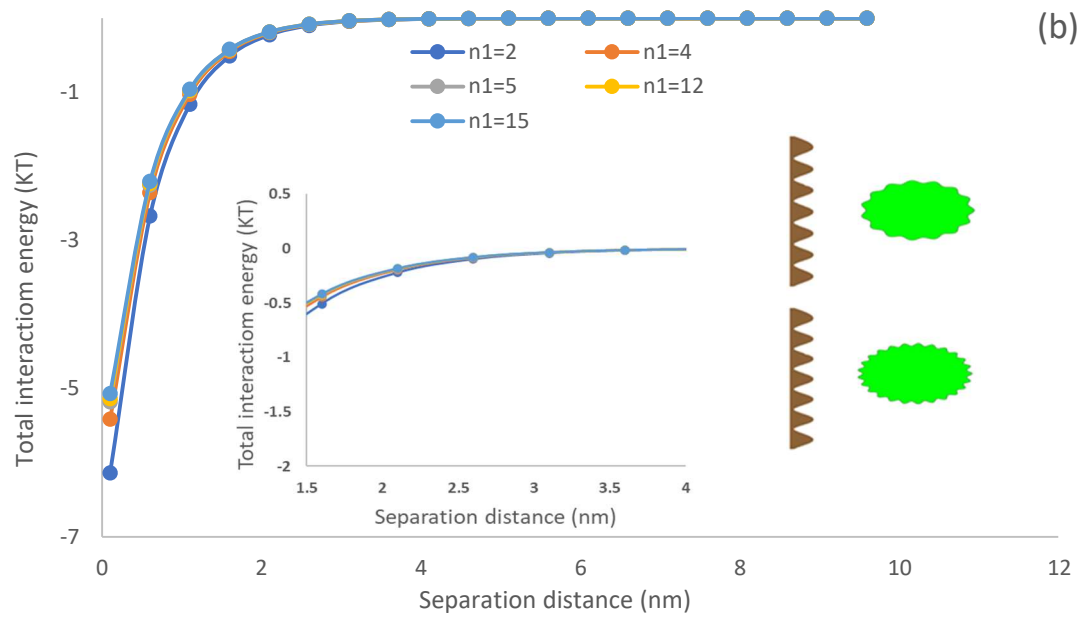
Figure 6.7. The effect of asperity number on total interaction energy of the particle and membrane surface. (a) PDMS (b) PU (c) PTFE.

6.2.3 Asperity ratio effects

Figure 6.8. shows the effect of asperity ratio on the total interaction energy of the ellipsoidal particle and membrane surface. It is seen that with decreasing the asperity ratio of particles, the total interaction energy increases slightly hampering the adhesion of particles on the surface of membrane. A particle with smaller asperity shows stronger total interaction energy (Yin et al. 2020). As the asperity ratio (λ) increases, the separation distance (h) between the particle and surface will increase and hence, the total interaction energy will decrease. According to this result, particle asperity ratio has effect on particle adhesion on the membrane surface.
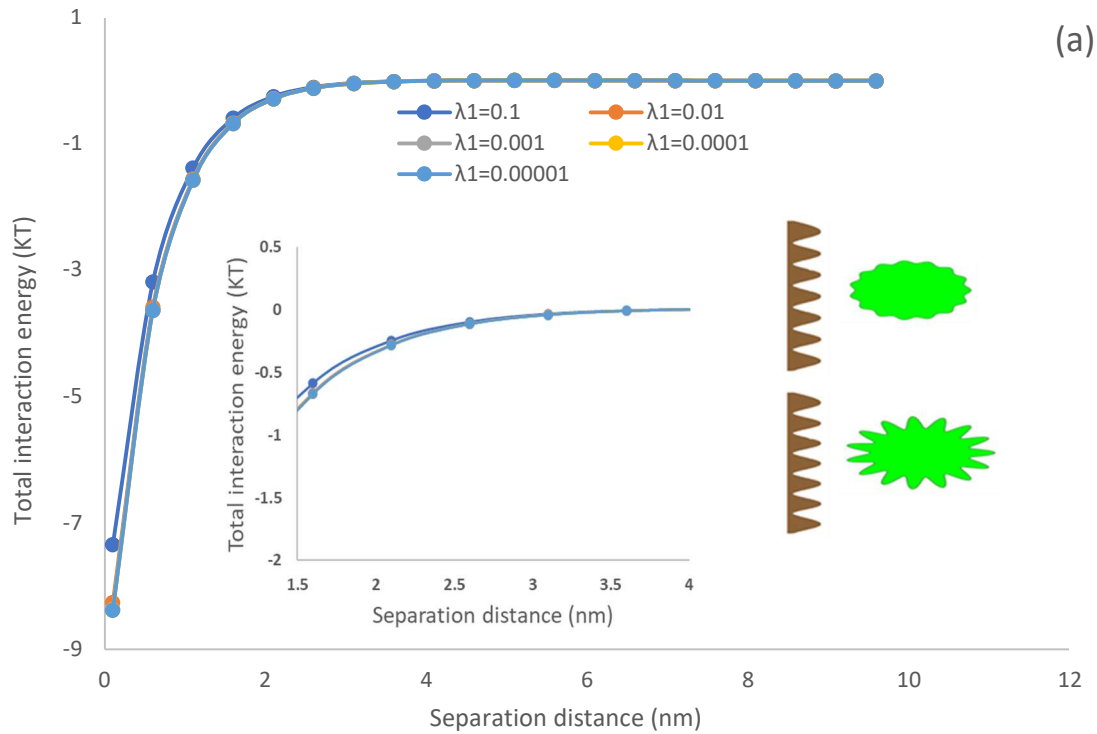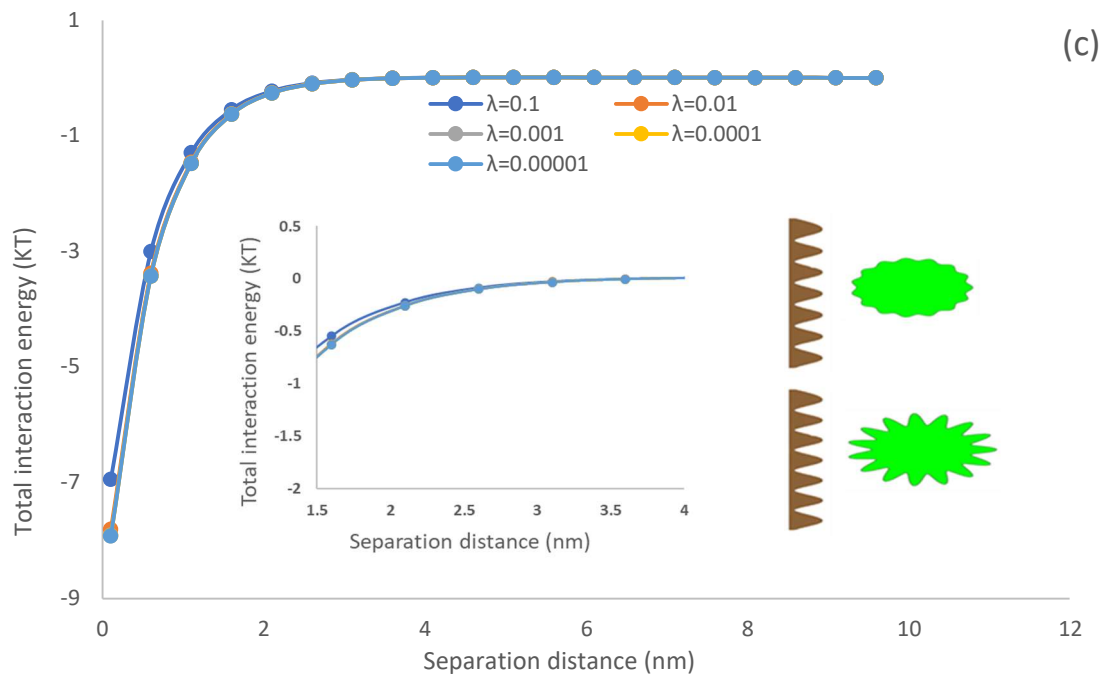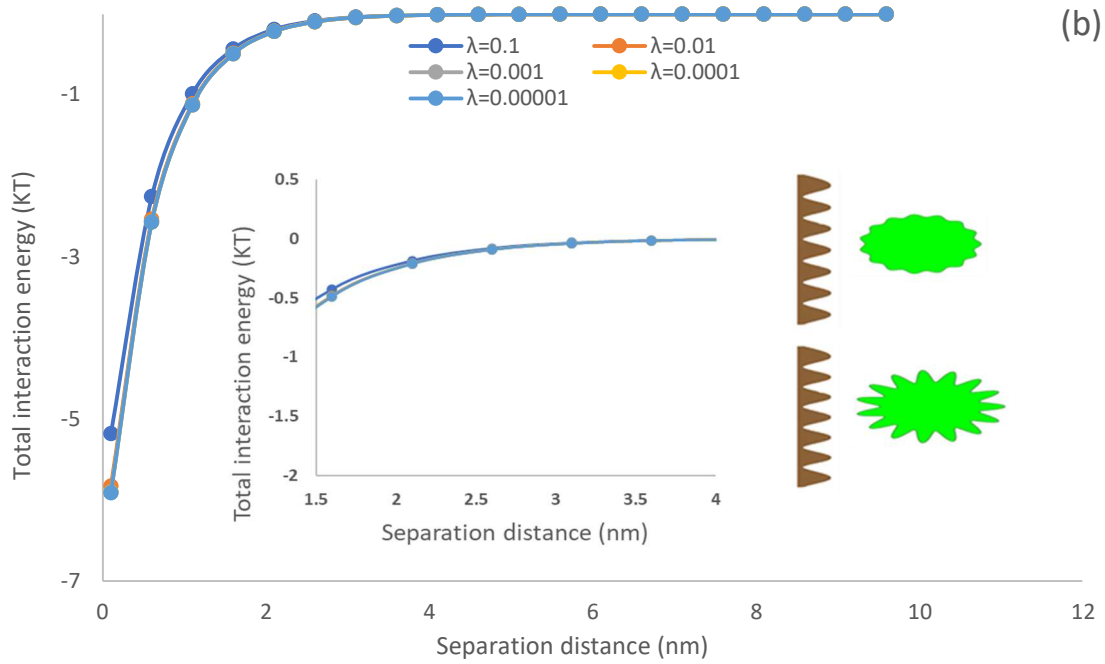
Figure 6.8. The effect of asperity ratio on total interaction energy of the particle and membrane surface (a) PDMS (b) PU(c) PTFE.

6.2.4 Membrane asperity height effect

Figure 6.9 shows the effect of membrane asperity height on the total interaction energy of the ellipsoidal particle and membrane surface. With an increase in the membrane asperity height, the total interaction energy decreases (Hoek and Agarwal 2006; Eom et al. 2017; Torkzaban and Bradford 2016; Erramilli and Genzer 2019). Based on Equation 4.19, as the membrane asperity height (p) increases, the separation distance (h) will increase and thus the total interaction will decrease. As stated by Gross *et al.* (2016), the interaction energy developed between a particle and smooth surface is more remarkable than that and rough membrane surface, and algae attachment on surface is strongly depends on the texture of the membrane. Also, the type of membrane played a significant role in the attachment of particles (Gross et al. 2016). According to the result, membrane asperity height plays a vital role in the level of algae adhesion to the membrane surface in wastewater treatment, thus a smaller membrane asperity height led to more algae adhesion.
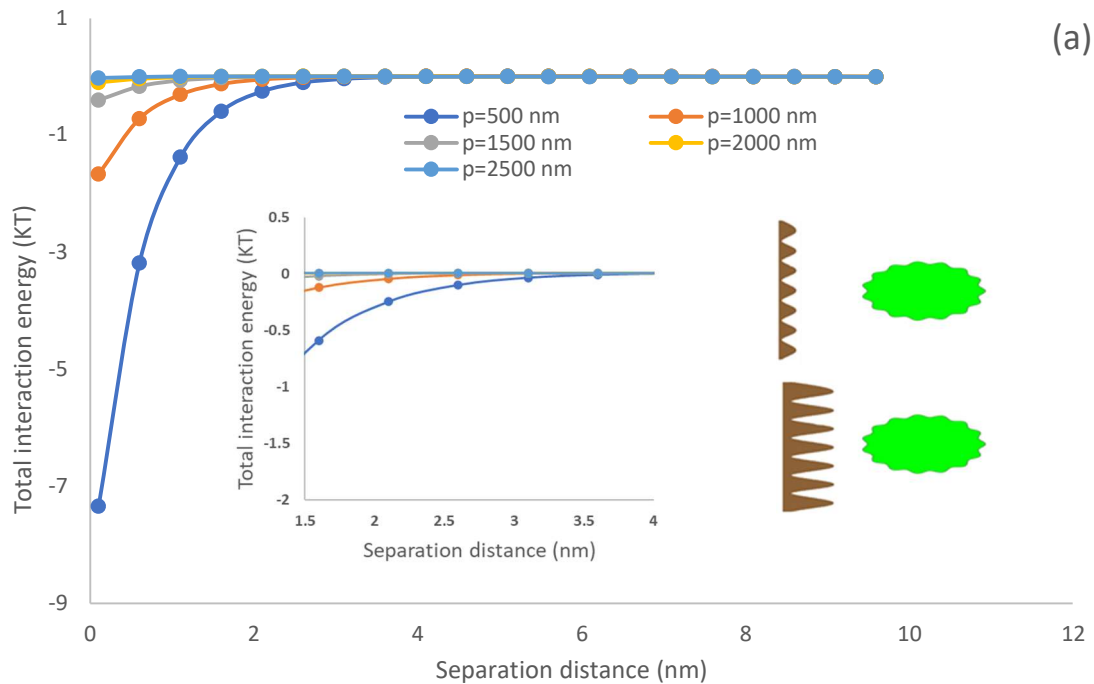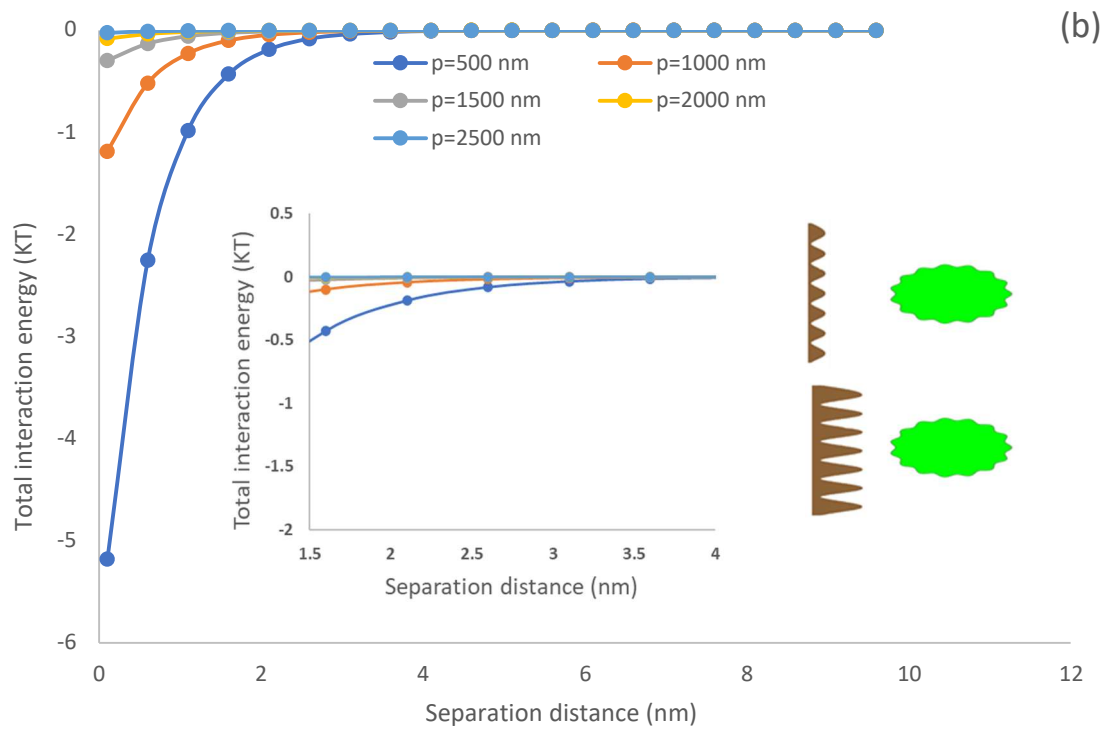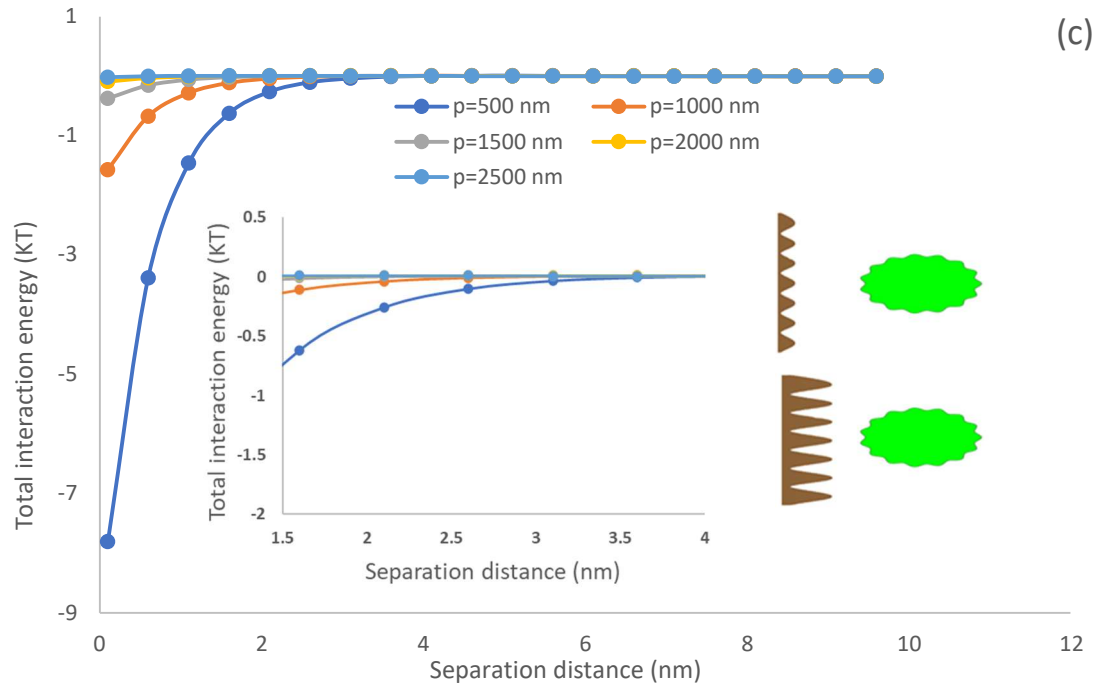
Figure 6.9. The effect of membrane asperity height on total interaction energy of the particle and membrane surface (a) PDMS (b) PU (c) PTFE.

6.2.5 Membrane asperity width effect

Figure 6.10 shows the effect of membrane asperity width on the total interaction energy of an ellipsoidal particle and membrane surface. With increasing the membrane asperity width, the total interaction energy increases (Kwon et al. 2005; Ozkan and Berberoglu 2011; Shen et al. 2012). With increasing the membrane asperity width (w), the separation distance (h) of the particle and membrane surface will decrease, and hence the total interaction energy will increase. It is also clear that with increasing the membrane asperity width, the membrane moves to become smoother and thus the interaction energy increases leading to less adhesion. According to the results, membrane asperity width plays a role in the level of algae adhesion to the membrane in wastewater treatment, regardless of the properties of adhering particles.

(a)

(b)
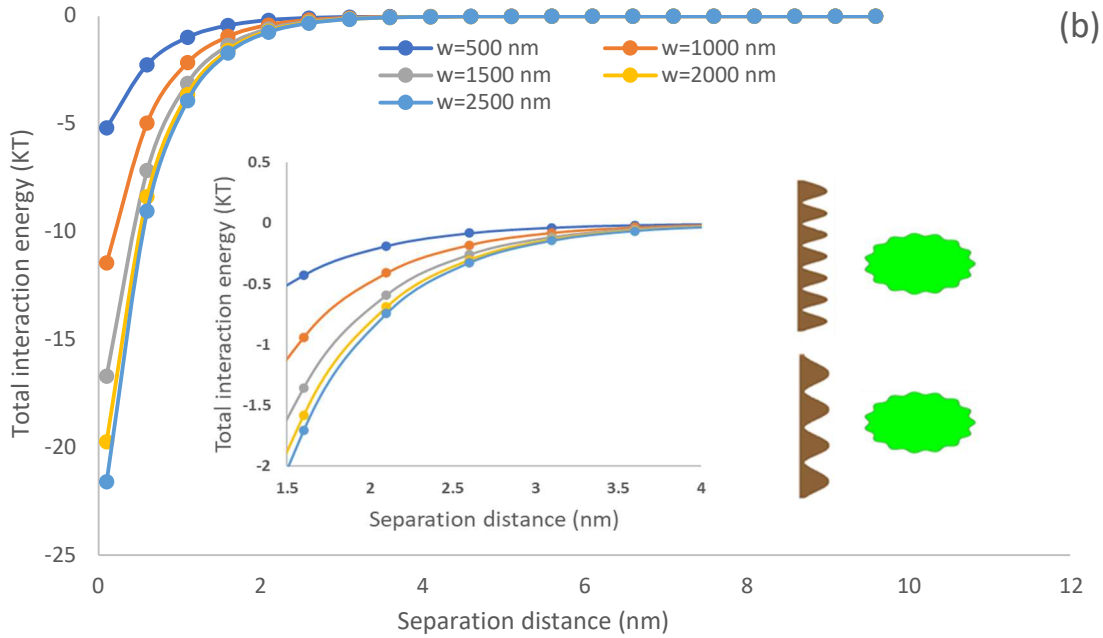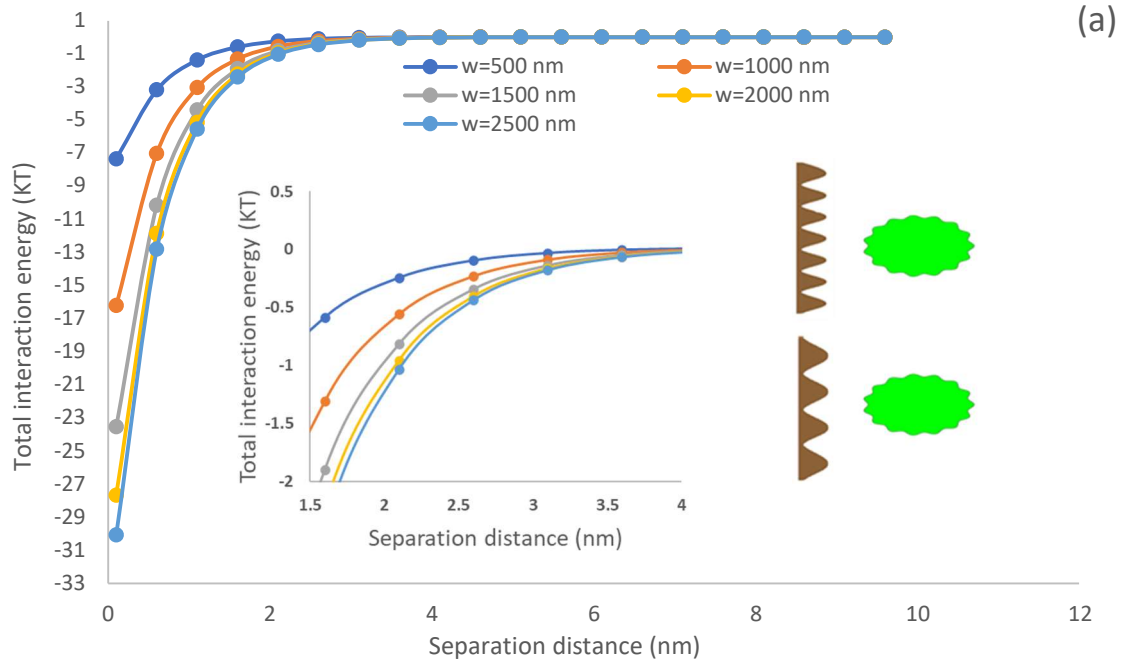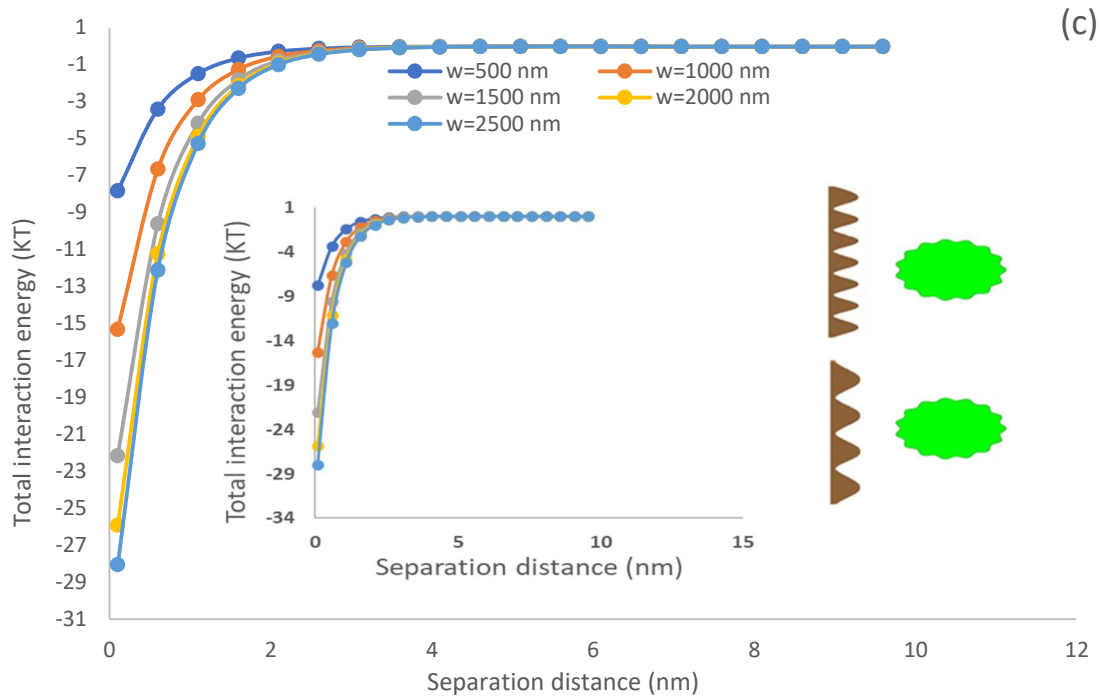
Figure 6.10 The effect of membrane asperity width on total interaction energy of the particle and membrane surface (a) PDMS (b) PU (c) PTFE.

6.3 The orientation angle effect

In Figure 6.11, the effect of orientation angle developed between the ellipsoidal particle and membrane surface is compared. There is more intense interaction between the particle and membrane surface when the particle is oriented parallel to the surface, as the interaction area between the particle and surface is increased (Figure 6.11). Also, like the rippled particle has protrusions and depressions on the surface, if one particle changes its orientation angle in θ direction, the protrusions of this particle can rotate its place and cope with the depressions of the opposite particle instead of the protrusions, for example. Thus, the effect of orientation angle is important in the particle interaction (Ildefonse et al. 1992).
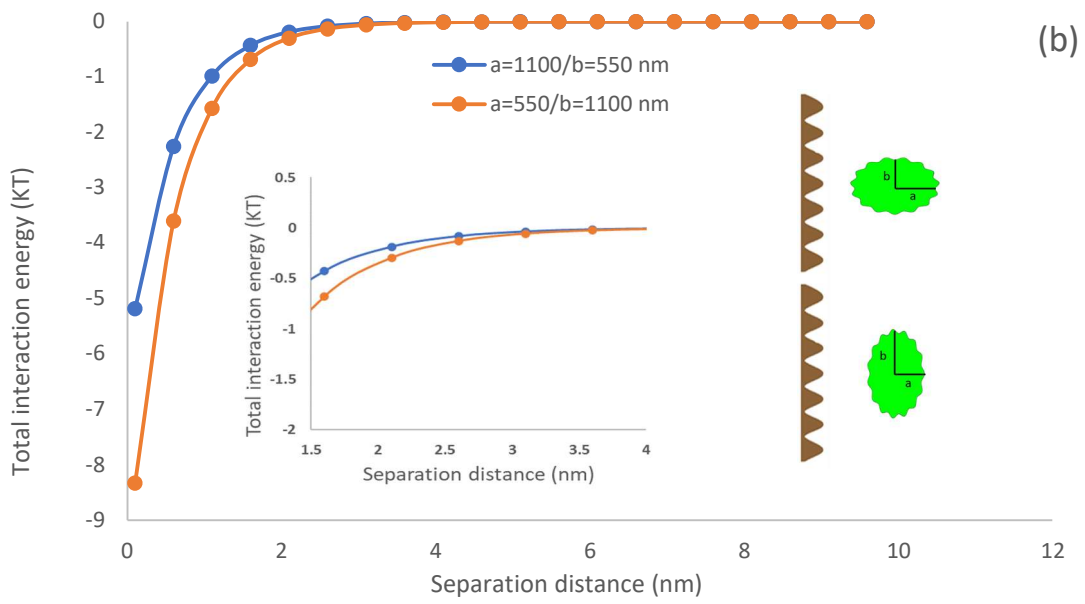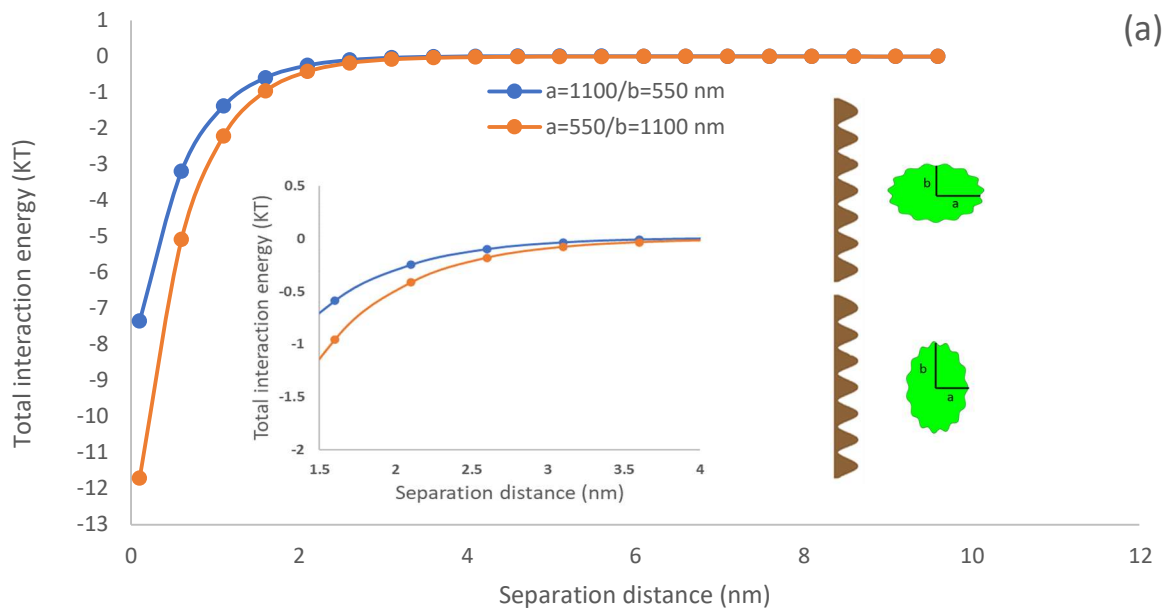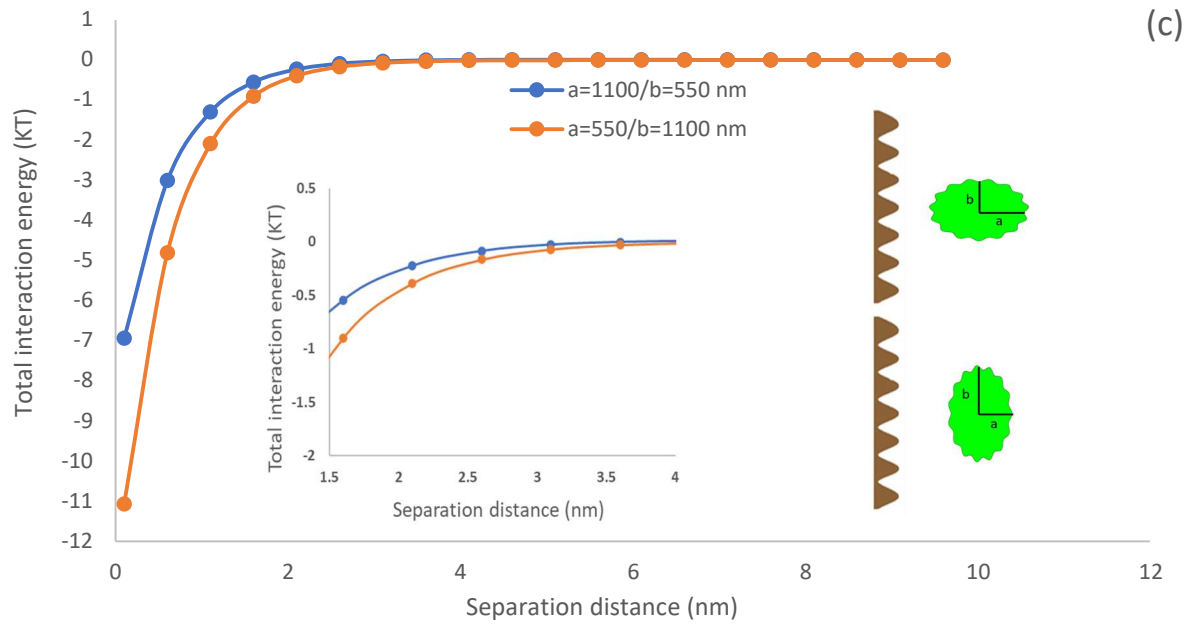
Figure 6.11. The effect of orientation angle of ellipsoidal particle on total interaction energy of the particle and membrane surface. (a) PDMS (b) PU (c) PTFE.

7. Discussion and application

After simulation of all particle and membrane surface properties impact, and comparing of the three figures in each part, it is clear that the most interaction energy in all of simulation is for PDMS sensor and it is completely making sense with comparing the dramatic increase of PDMS in the QCM test. On the other hand, with analyzing the figures of different properties impact in each section, it is clear that the interaction energy of sensors PDMS and PTFE are very close to each other with more interaction energy, and it is completely make sense with the contact angle experimental result that PDMS and PTFE are more hydrophobic than PU.

Microbial adhesion on membrane surfaces is affected by the membrane characteristics, such as membrane hydrophobicity, zeta potential, and surface roughness. The contact angle measurement suggested that the water contact angle of PTFE, PDMS, and PU was 92.7, 89.6 and 55.7 degree, respectively (Table 4.2). The zeta potential of PTFE, PDMS and PU in pure water was -75.2 mV, -83.0 mV, and -18.6 mV, respectively (Liu et al. 2020; Khorasani et al. 2006). It is clear that, PTFE and PDMS are much more hydrophobic and negatively charged than that of PU. The experimental and modeling adsorption analysis confirmed that the more hydrophobic surface of PDMS, PTFE

had the highest adsorption rate and interfacial attraction force (Figures 4.5 and 6.1). Also, the more hydrophilic surface of PU had the slowest adsorption rate and interfacial attraction for algae (Figures 4.5 and 6.1). These results are consistent with the general observation that more hydrophobic and negatively charged surfaces favored the adhesion of microalgae cells (Xia et al. 2015). This is because a larger hydrophobic interaction involving hydrophobic surfaces might induce replacement of attached cell wall components with water molecules repulsed from the membrane surface (Tay et al. 2000). Furthermore, the more negatively charged surfaces might provide more salt binding sites between the membrane surfaces and negatively charged cells to enhance cell adhesion and biofilm formation (Habimana et al. 2014).

The modeling analysis also confirmed that smoother surface promoted the adhesion of algae on the surface, and more influential factor for the adsorption of algae was the surface morphology of membrane rather than that of particles (Figures 6.4, 6.5 and 6.10). This is because smother surface would promote the interaction area of algae and membrane surface. Therefore, the higher overall adsorption of algae at equilibrium on the PTFE than PDMS on the experimental analysis (Figure 4.5) might be due to the smoother surface of PTFE sensor than that of PDMS. However further morphological analysis of sensor is required to prove this hypothesis.

The adhesion of microbial cells to solid materials is often considered to have a prevailing physicochemical character. Several theoretical models are able to quantitatively predict the cell–cell and cell–solid interaction based on physicochemical properties of interacting surfaces, such as the thermodynamic balance of interaction energies, classical (DLVO), and extended DLVO (XDLVO) theory (Sharma and Rao 2003). In this simulation, among all the factors that affect the algae cell adhesion to membrane surface, the morphology of microalgae and the membrane morphology was evaluated. It was observable that the membrane asperity height was the most effective properties on the total interaction energy developed between the particle and membrane surface regardless of the shape of the particle. The results confirm that with increasing the membrane asperity height from 500-2500 nm, the total interaction energy drops from 35 KT to 10 KT. Also, the asperity number of particles had the less effect on the total interaction energy.

The rough particle simulation and extended DLVO theory suggested that the shape of particle (circular vs ellipsoidal) did not affect the adsorption performance of algae on the membrane surface (Figures 6.1 vs 6.4), and only the interaction area of simulated algae and membrane is influential

in the adhesion of algae on the membrane. In the same vein, the size of particle and orientation of ellipsoidal particle (Figure 6.11) would impact its interaction with the membrane surface, and thus the larger algae would adsorb more on the membrane surface as they have more interaction with the membrane surface. This analysis suggests that larger particles would promote the membrane clogging by algae, and non-spherical algae would probably develop a parallel orientation with membrane prior to adhesion.

8   Conclusions and Future Studies

Both experimental and modelling studies were conducted to understand the role of physicochemical properties of membranes and microalgae in determining microalgal biofilm formation. An improved fundamental understanding of microalgal biofilm formation has been achieved. Specific conclusions are summarized below:

1.) Microalgal adhesion kinetic studies using QCM-D shows that more hydrophobic membrane surfaces, in general, favored a faster and larger density of biofilm formation, as compared to a more hydrophilic membrane surface.

2.) Modeling studies on the interaction energy between membrane surfaces and microalgae cells using the extended DLVO theory suggest that a stronger attractive interaction energy associated with a hydrophobic surface favored a faster and larger quantity of biofilm formation and support the experimental observation, in general.

3.) Morphology (shape and size) of the microalgal cell particles has a significant impact on the interaction energy between the membrane surfaces and microalgae cells.

4.) According to the modelling results, membrane asperity height and particle asperity number were more and less effective factors in controlling the range of total interaction energy and adhesion.

This was an initial study on the role of physicochemical properties of membrane surfaces and microalgae in controlling adhesion and biofilm formation of microalgal cells. Further studies should be conducted by using various species of microalgae cells with different properties (hydrophobicity, zeta potential, morphology) to explore the role of microalgae cells on adhesion and biofilm formation. Furthermore, identification and optimization of membrane properties

should be considered to develop a membrane carbonated biofilm reactor (MCBR) for fast biofilm formation and effective nutrients (N and P) removal. This is a new area and worthy of significant research and development, before a full-scale application of the novel concept (MCBR).

References

Adarme-Vega T.C., Lim D.K.Y., Timmins M., Vernen F., Li Y., Schenk P.M, Microalgal Biofactories: A Promising Approach towards Sustainable Omega-3 Fatty Acid Production, *Microbial cell factories,* (2012), 11(96).

Al-Awady., Mohammed J., Gillian M. Greenway., Vesselin N. Paunov. 2015. Nanotoxicity of Polyelectrolyte Functionalized Titania Nanoparticles towards Microalgae and Yeast, Role of the Particle Concentration, Size and Surface Charge. *RSC Advances* (2015). 5(46): 37044–59.

Alcántara, Cynthia, Esther Posadas, Benoit Guieysse, and Raúl Muñoz. Microalgae-Based Wastewater Treatment, *Biotechnology Advances*: (2015) 439–55.

Alsheyab M., Jia-Qian Jiang., Cécile Stanford, Engineering Aspects of Electrochemical Generation of Ferrate: A Step Towards Its Full Scale Application for Water and Wastewater Treatment, *Water, Air, & Soil Pollution* (2010) 210:203–210.

Amaro H.M., Guedes A.C., Malcata F.X, Advances and Perspectives in Using Microalgae to Produce Biodiesel. *Applied Energy* 88(2011)3402-3410.

Arbib Z., Jesús Ruiz., Pablo Álvarez-Díaz., Carmen Garrido-Pérez., Jesus Barragan., José A. Perales, Effect of PH Control by Means of Flue Gas Addition on Three Different Photo-Bioreactors Treating Urban Wastewater in Long-Term Operation. *Ecological Engineering* 57(2013): 226–235.

Austic R.E., Mustafa A., Jung B., Gatrell S., Xin Gen Lei, Potential Limitation of a New Defatted Diatom Microalgal Biomass in Replacing Soybean Meal and Corn in Diets for Broiler Chickens." *Journal of Agricultural and Food Chemistry* (2013) 61, 30, 7341–7348.

Bamba B.S.B., Lozano p., Adjé F., Ouattara A., Vian M.A., Tranchant C., Lozano Y, Effects of Temperature and Other Operational Parameters on *Chlorella vulgaris* Mass Cultivation in a Simple and Low-Cost Column Photobioreactor, *Applied Biochemistry and Biotechnology*, (2015), 1**77**, 389–406.
Bamba B.S.B., Tranchant C.C., Ouattara A., Lozano P, Harvesting of Microalgae Biomass Using Ceramic Microfiltration at High Crossflow Velocity, *Applied Biochemistry and Biotechnology*, (2021), 193, 1147–1169.

Bargozin H., R.A.Hadadhania., H.Faraji., H.Yousefzadeh, Effect of Rough Nanoparticle Orientation on DLVO Energy Interaction, *Journal of Dispersion Science and Technology* (2015), 36(6): 755–764.

Bhave R., Kuritz T., Powell L., Adcock D, Membrane-Based Energy Efficient Dewatering of Microalgae in Biofuels Production and Recovery of Value Added Co-Products, *Environmental Science and Technology* (2012), 46, 10, 5599–5606.

Bilad M.R., Discart V., Vandamme D., Foubert I., Muylaert K., Vankelecom I.F.J, Coupled Cultivation and Pre-Harvesting of Microalgae in a Membrane Photobioreactor (MPBR)." *Bioresource Technology* (2014),155, 410–417.

Blanken W., Janssen M., Cuaresma M., Libor Z., Bhaiji T., Wijffels R.H, Biofilm Growth of Chlorella Sorokiniana in a Rotating Biological Contactor Based Photobioreactor,

Biotechnology and Bioengineering (2014),111(12): 2436–2445.

Boonchai R., Seo G, Microalgae Membrane Photobioreactor for Further Removal of Nitrogen and Phosphorus from Secondary Sewage Effluent, *Korean Journal of chemical Engineering*,(2015), 32,2047-2052.

Borowitzka M.A, High-Value Products from Microalgae—Their Development and Commercialisation. *Journal of Applied Phycology*(2013),25,743–756.

Boutt D.F., Giovanni G., Fredrich J.T., Cook B.K., Williams J.R, Trapping Zones: The Effect of Fracture Roughness on the Directional Anisotropy of Fluid Flow and Colloid Transport in a Single Fracture. *Geophysical Research Letters*, (2006), 33, 21.

Brant J.A., Childress A.E, Assessing Short-Range Membrane–Colloid Interactions Using Surface Energetics, *Journal of Membrane Science* 203(2002): 257–273.

Bamba B.S.B., Lozano P., FéAdjé F., Ouattara A., Maryline Abert Vian., Carole Tranchant ., Yves Lozano, Effects of Temperature and Other Operational Parameters on Chlorella Vulgaris Mass Cultivation in a Simple and Low-Cost Column Photobioreactor, *Applied biochemistry and biotechnology*, (2015)177, 389–406.

Busscher H. J., Weerkamp A.H., Mei H C van der., Pelt AWvan., Jong H Pde., Arends J, Measurement of the Surface Free Energy of Bacterial Cell Surfaces and Its Relevance for Adhesion." *Applied and Environmental Microbiology* (1984), 48, 5, 980–83.

Cabello J., Toledo-Cervantes A., León Sánchez., Sergio Revah., Marcia Morales, Effect of the Temperature, PH and Irradiance on the Photosynthetic Activity by Scenedesmus Obtusiusculus under Nitrogen Replete and Deplete Conditions, *Bioresource Technology,*(2015), 181, 128–35.

Cai T., Y.Park S., Li Y, Nutrient Recovery from Wastewater Streams by Microalgae: Status and Prospects, *Renewable and Sustainable Energy Reviews*, (2013),19,360–369.

Callesen I., Keck H., Andersen T.J, Particle Size Distribution in Soils and Marine Sediments by Laser Diffraction Using Malvern Mastersizer 2000—Method Uncertainty Including the Effect of Hydrogen Peroxide Pretreatment, *Journal of Soils and Sediments,* (2018), 18, 2500–2510.

Carey R.O., Migliaccio K.W, Contribution of Wastewater Treatment Plant Effluents to Nutrient Dynamics in Aquatic Systems, *Environmental Management*, (2009), 44, 205–217.

Chinnasamy S., Ramakrishnan B., Bhatnagar A., C. Das K, Biomass Production Potential of a Wastewater Alga Chlorella Vulgaris ARC 1 under Elevated Levels of CO2 and Temperature, *International Journal of Molecular Sciences,* (2009), 10(2), 518-532.

Chisti Y, Biodiesel from Microalgae, *Biotechnology Advances*, (2007), 25(3), 294–306.

Choi H.J, Lee S.M, Effect of the N/P Ratio on Biomass Productivity and Nutrient Removal from Municipal Wastewater, *Bioprocess and Biosystems Engineering, (2014), 38(4),* 761–766.

Christenson L., Sims R, Production and Harvesting of Microalgae for Wastewater Treatment, Biofuels, and Bioproducts, *Biotechnology Advances,* (2011), 29(6), 686–702.

Chu W.L, Biotechnological Applications of Microalgae, *Review article*, (2012), 6 (Suppl 1), 524-537.

Cieśla J., Bieganowski A., Janczarek M., UrbanikSypniewska T, Determination of the Electrokinetic Potential of Rhizobium Leguminosarum bv Trifolii Rt24.2 Using Laser Doppler Velocimetry — A Methodological Study, *Journal of Microbiological Methods,* (2011), 85(3), 199–205.

Converti A., A.Casazza A., Y.Ortiz E., Perego P., Borghi M.D, Effect of Temperature and Nitrogen Concentration on the Growth and Lipid Content of Nannochloropsis Oculata and Chlorella Vulgaris for Biodiesel Production, *Chemical Engineering and Processing: Process Intensification*, (2009), 48(6): 1146–1151.

Crini G, Lichtfouse E, Advantages and Disadvantages of Techniques Used for Wastewater Treatment, *Environmental chemistry Letters*, (2018), 17, 145–55.

Eom N., Parsons D.F., Craig V.S.J, Roughness in Surface Force Measurements: Extension of DLVO Theory To Describe the Forces between Hafnia Surfaces, *Physical chemistry,* (2021), 24, 79, 135-102.

Erramilli S, Genzer J, Influence of Surface Topography Attributes on Settlement and Adhesion of Natural and Synthetic Species, *Soft MatteR,* (2019), 15(20), 4037–4228.

Fan L.H., Zhang Y.T., Zhang L., Chen H.L, Evaluation of a Membrane-Sparged Helical Tubular Photobioreactor for Carbon Dioxide Biofixation by Chlorella Vulgaris, *Journal of Membrane Science,* (2008), 325(1), 336–345.

Fan L.H., Zhang Y.T., Cheng L.H., Zhang L., Tang D.S., Chen H.L, Optimization of Carbon Dioxide Fixation by Chlorella Vulgaris Cultivated in a Membrane-Photobioreactor, *Chemical Engineering and Technology*, (2007), 30(8), 1094–1099.

Fasaei F., Bitter J.H., legers P.M., Boxtel A.J.B.van, Techno-Economic Evaluation of Microalgae Harvesting and Dewatering Systems, *Algal Research*, (2018), 31, 347–362.

Feng L., Li X., Du G., Chen J, Adsorption and Fouling Characterization of Klebsiella Oxytoca to Microfiltration Membranes, *Process Biochemistry*, (2009), 44(11), 1289–1292.

Gao F., Yang Z.H., Li C., Wang Y.J., Jin W.h., Deng Y.b, Concentrated Microalgae Cultivation in Treated Sewage by Membrane Photobioreactor Operated in Batch Flow Mode, *Bioresource Technology, (2014),* 167, 441–446.

Grau., C.R., Klein., N.W, Sewage-Grown Algae as a Feedstuff for Chicks, *Poultry Science*, (1957), 36(5), 1046–1051.

Gross M., Zhao X., MascarenhasV., Wen Z, Effects of the Surface Physico-Chemical Properties and the Surface Textures on the Initial Colonization and the Attached Growth in Algal Biofilm, *Biotechnology for Biofuels*, (2016), 9, 38.

Guillen-Burrieza E., Ruiz-Aguirre A., Zaragoza G, A. Arafat H, Membrane Fouling and Cleaning in Long Term Plant-Scale Membrane Distillation Operations, *Journal of Membrane Science, (2014),* 468(15), 360–372.

Habimana O., Semião A.J.C., Casey E, The role of cell-surface interactions in bacterial initial adhesion and consequent biofilm formation on nanofiltration/reverse osmosis membranes, *Journal of membrane science*, (2014), 454, 82-96.

Hallab N.J., Bundy K.J, O'Connor K., L. Moses R.L., J. Jacobs J, Evaluation of Metallic and Polymeric Biomaterial Surface Energy and Surface Roughness Characteristics for Directed Cell Adhesion, *TISSUE ENGINEERING, (2004),* 7(1).

Hamadi F., Latrache H., Mabrrouki M., Elghmari A., Outzourhit A., Ellouali M., Chtaini A, Effect of PH on Distribution and Adhesion of Staphylococcus Aureus to Glass, *Adhesion Science and Technology*, (2012), 19(1), 73–85.

He Y.T., Wan J., Tokunaga T, Kinetic Stability of Hematite Nanoparticles: The Effect of Particle Sizes, *Nanoparticle Research*, (2008), 10, 321-332.

Heredia-Arroyo T., Wei W., Ruan R, Hu B, Mixotrophic Cultivation of Chlorella Vulgaris and Its Potential Application for the Oil Accumulation from Non-Sugar Materials, *Biomass and Bioenergy, (2011),* 35(5), 2245–2253.

Hoek.M.V E., K. Agarwal G, Extended DLVO Interactions between Spherical Particles and Rough Surfaces, *Journal of Colloid and Interface Science,* (2006), 298(1), 50–58.

Honda R, Boonnorat J., Chiemchaisri C., Chiemchaisri W., Yamamoto K, Carbon Dioxide Capture and Nutrients Removal Utilizing Treated Sewage by Concentrated Microalgae Cultivation in a Membrane Photobioreactor, *Bioresource Technology,* (2012), 125, 59–64.

Huang Y., Zheng Y., Li J., Liao Q., Fu Q., Xia A., Fu J., Sun Y, Enhancing Microalgae Biofilm Formation and Growth by Fabricating Microgrooves onto the Substrate Surface, *Bioresource Technology*, (2018), 261, 36-43.

Hughes A D., Kelly M.S., Black K.D., Stanley M.S, Biogas from Macroalgae: Is It Time to Revisit the Idea?, *Biotechnology for Biofuels,* (2012), 5(1), 1–7.

Huo S., Wang Z., Zhu S., Zhou W., Dong R., Yuan Z, Cultivation of Chlorella Zofingiensis in Bench-Scale Outdoor Ponds by Regulation of PH Using Dairy Wastewater in Winter, South China, *BioresourceTechnology*, (2012), 121, 76–82.

Ildefonse B., Launeau p., Bouchez J.L., Fernandez A, Effect of Mechanical Interactions on the Development of Shape Preferred Orientations: A Two-Dimensional Experimental Approach, *Journal of Structural Geology,* (1992)*,* 14(1), 73–83.

Irving T.E., Allen D.G, Species and Material Considerations in the Formation and Development of Microalgal Biofilms, *Applied Microbiology and Biotechnology, (2011),* 92(2), 283–294.

Jiang S., Xiao S., Chu H., Zhao F., Yu Z., Zhou X., Zhang Y, Intelligent Mitigation of Fouling by Means of Membrane Vibration for Algae Separation: Dynamics Model, Comprehensive Evaluation, and Critical Vibration Frequency, *Water Research,* (2020)*,* 182,115972.

Karunakaran G., Suriyaprabha R., Rajendran V., Kannan N, Toxicity Evaluation Based on Particle Size, Contact Angle and Zeta Potential of SiO_2 and Al_2O_3 on the Growth of Green Algae,

Advances in nano research, (2015), 3(4), 243–255.

Katainen J., Paajanen M., Ahtola E., Pore V., Lahtinen J, Adhesion as an interplay between particle size and surface roughness, *Journal of colloid and interface science,* (2006), 304(2), 524-529.

Khorasani M.T., Moemenbellah S., Mirzadeh H., Sadatnia B, Effect of surface charge and hydrophobicity of polyurethanes and silicone rubbers on L929 cells response*, Colloids and Surfaces B: Biointerfaces*, (2006), 51, 112–119.

Kwon B., Park N., Cho J, Effect of Algae on Fouling and Efficiency of UF Membranes, *ThermoFisher Scientific,* (2005), 179(1), 203–214.

Li Q., Elimelech M, Organic Fouling and Chemical Cleaning of Nanofiltration Membranes: Measurements and Mechanisms, *Environmental Science and Technology,* (2004)*,* 38(17), 4683–4693.

Liang K., Zhang Q., Cong W, Enzyme-Assisted Aqueous Extraction of Lipid from Microalgae, *Agricyltural Food Chemistry*, (2012), 60, 47, 11771-11776.

Lin T., Lu Z., Chen W, Interaction Mechanisms and Predictions on Membrane Fouling in an Ultrafiltration System, Using the XDLVO Approach, *Elsevier Enhanced Reader*, (2014), 461, 49-58.

Liu Z., Song Y., Li D, Detecting zeta potential of polydimethylsiloxane (PDMS) in electrolyte solutions with atomic force microscope, *Journal of colloid and interface science*, (2020), 578, 116-123.

Low S.L., Ong S.L., Ng H.Y, Characterization of Membrane Fouling in Submerged Ceramic Membrane Photobioreactors Fed with Effluent from Membrane Bioreactors, *Chemical Engineering Journal*, (2016), 290, 91–102.

Lum K.K., Kim J., Lei X.G, Dual Potential of Microalgae as a Sustainable Biofuel Feedstock and Animal Feed, Animal science and Biotechnology, (2013), 4, 53.

Luo Y., Clech P.L., Henderson R.H, ,Simultaneous Microalgae Cultivation and Wastewater Treatment in Submerged Membrane Photobioreactors: *A Review, Elsevier Enhanced Reader*, (2017), 24, 425-437.

Ma Kuixiang ., Chung T.S., Good R.J, Surface Energy of Thermotropic Liquid Crystalline Polyesters and Polyesteramide, Journal of Polymer Science Part B: Polymer Physics, (1998), 36,(13), 2327-2337.

Marbelia L., Bilad M.R., Passaris I., Discart V., Vandamme D., Beuckels A., Muylaert K., Vankelecom Ivo.F.J, Membrane Photobioreactors for Integrated Microalgae Cultivation and Nutrient Remediation of Membrane Bioreactors Effluent, *Bioresource Technology*, (2014), 163, 228–235.

Markou G., Vandamme D., Muylaert K, Microalgal and Cyanobacterial Cultivation: The Supply of Nutrients, *Water Research*, (2014), 65, 186–202.

Massoud M.A., Tarhini A., Nasr J.A, Decentralized approaches to wastewater treatment and management: Applicability in developing countries, *Journal of Environmental Management,* (2009), 90 (1), 652-659.

Mata T.M., Martins A.A., Caetano N.S, Microalgae for Biodiesel Production and Other Applications: A Review, *Renewable and Sustainable Energy Reviews*, (2010), 14(1), 217–32.

Matamoros Víctor., Gutiérrez R., Ferrer I., García J., BayonaJ.M, Capability of Microalgae-Based Wastewater Treatment Systems to Remove Emerging Organic Contaminants: A Pilot-Scale Study, *Journal of Hazardous Materials,* (2015), 288: 34-42.

Mehta S.K., Gaur J.P, Use of Algae for Removing Heavy Metal Ions from Wastewater, Progress and Prospects, *Critical reviews in biotechnology*, (2021), 25(3), 113–152.

Meier B.M., Kayser G.L., Amjad U.Q., Bartram J, Implementing an Evolving Human Right through Water and Sanitation Policy, *Water Policy,* (2012), 15(1), 116–133.

Melin T., Jefferson B., Bixio D., Theeye C., Wilde W.D., Koning J.D., Graaf J van der, Membrane Bioreactor Technology for Wastewater Treatment and Reuse, *Desalination*, (2006), 187(1–3), 271–282.

Moheimani N., P.McHenry M., Boer K de., Bahri P.A, Biomass and Biofuels from Microalgae, *Advances in Engineering and Biology*, (2015), 2, 95–115.

Morra M., Occhiello E., Garbassi F, Surface Characterization of Plasma-Treated PTFE, *Surface and Interface Analysis,* (1990), 16(1–12), 412–17.

Muñoz R., Guieysse B, Algal–Bacterial Processes for the Treatment of Hazardous Contaminants: A Review, *Water Research,* (2006), 40(15), 2799–2815.

Muñoz R., Jacinto M., Guieysse B., Mattiasson B, Combined Carbon and Nitrogen Removal from Acetonitrile Using Algal-Bacterial Bioreactors, *Applied Microbiology and Biotechnology,* (2005) 67(5), 699–707.

Oswald W.J., Gotaas H.B, Photosynthesis in Sewage Treatment, *Transactions of the American Society of Civil Engineers*, (1957), 122(1): 73–97.

Oswald W. J., Golueke C.G, Biological Transformation of Solar Energy, *Advances in Applied Microbiology,* (1960)*,* 2, 223–262.

Ozkan A., Berberoglu H, Adhesion of Chlorella vulgaris on Hydrophilic and Hydrophobic Surface, *IMECE*, (2011), 6 4133, 169-178.

Ozkan A., Berberoglu H, Adhesion of Algal Cells to Surfaces, *Biofouling*, (2013a), 29(4), 469–482.

Ozkan A., Berberoglu H, Adhesion of Algal Cells to Surfaces, *Biofouling,* (2013b), 29(4): 469–482.

Ozkan A., Berberoglu, Cell to Substratum and Cell to Cell Interactions of Microalgae, *Colloids and Surfaces B: Biointerfaces*, (2013c), 112, 302–309.

Ozkan A., Berberoglu, Physico-Chemical Surface Properties of Microalgae, *Colloids and Surfaces B: Biointerfaces,* (2013d), 112, 287–293.

Palmer J., Flint S., Brooks J., Bacterial Cell Attachment, the Beginning of a Biofilm, *J Ind Microbiol Biotechnol* (2007) 34:577—588

Pankratz S., Oyedun A.O., Kumar A, Development of Cost Models of Algae Production in a Cold Climate Using Different Production Systems, *Biofuels, Bioproducts and Biorefining,* (2019), 13(5), 1246–1260.

Park J., Jin H.F., Lim B.R., Park K.Y., Lee K, Ammonia Removal from Anaerobic Digestion Effluent of Livestock Waste Using Green Alga Scenedesmus Sp, *Bioresource Technology,* (2010), 101(22), 8649–8657.

Pearce G, Introduction to Membranes: Fouling Control, *Filtration and Separation, (2007),* 44(6), 30–32.

Ponnusamy T., Lawson L.B., Freytag L.C., Blake D.A., Ayyala R.S., John V, In Vitro Degradation and Release Characteristics of Spin Coated Thin Films of PLGA with a 'Breath Figure' Morphology, *Biomatter,* (2012), 2(2), 77–86.

Pourbozorg M., Li T., W.K.Law A, Effect of Turbulence on Fouling Control of Submerged Hollow Fibre Membrane Filtration, *Elsevier Water Research,* (2016), 99, 101-111.

Posadas E., Morales M del M., Gomez C., Acien G, Influence of PH and CO2 Source on the Performance of Microalgae-Based Secondary Domestic Wastewater Treatment in Outdoors Pilot Raceways, *Chemical Engineering Journal, (2015),* 265, 239–248.

Posten C., Schaub G, Microalgae and Terrestrial Biomass as Source for Fuels-A Process View, *Journal of Biotechnology*, (2009), 142(1), 64–69.

Qin Y., Liu Y., Yuan L., Yong H., Liu J, Preparation and Characterization of Antioxidant, Antimicrobial and PH-Sensitive Films Based on Chitosan, Silver Nanoparticles and Purple Corn Extract, *Food Hydrocolloids, (2019),* 96, 102–111.

Qu J., Fan M, The Current State of Water Quality and Technology Development for Water Pollution Control in China, *Critical Reviews in Environmental Science and Technology*, (2010), 40(6), 519-560.

Razzak S.A., Ilyas M., Ali S.A.M., Hossain M.H, Effects of CO 2 Concentration and PH on Mixotrophic Growth of Nannochloropsis Oculata, *Applied Biochemistry and Biotechnology,* (2015), 176(5), 1290–1302.

Rezakazemi M., Dashti A., Harami Hossein R., Hajilari N, Inamuddin, Fouling-Resistant Membranes for Water Reuse, *Environmental Chemistry Letters*, (2018), 16, 715–763.

Rossignol N., Jaouen P., Robert J-M., Quéméneur F, Production of Exocellular Pigment by the Marine Diatom Haslea Ostrearia Simonsen in a Photobioreactor Equipped with Immersed Ultrafiltration Membranes, *Bioresource Technology,* (2000), 73(2), 197–200.

Ruiz J., Arbib Z., Álvarez-Díaz P.D.,Garrido-Pérez C., Barragán J.,Perales J.A, Influence of Light Presence and Biomass Concentration on Nutrient Kinetic Removal from Urban Wastewater by Scenedesmus Obliquus, *Journal of Biotechnology,* (2014), 178(1), 32–37.

Schmidt D.L., Brady R.F., Lam K., Schmidt D.C., Chaudhury M.K, Contact Angle Hysteresis, Adhesion, and Marine Biofouling, *Langmuir,* (2004), 20(7), 2830–2836.

Schultz M.P., Bendick J.A., Holm E.R., Hertel W.M, Economic Impact of Biofouling on a Naval Surface Ship, *The Journal of Bioadhesion and Biofilm Research,* (2011), 27(1), 87-98.

Schultz M. P., Swain G.W, The Effect of Biofilms on Turbulent Boundary Layers, *Journal of Fluids Engineering,* (1999), 121(1): 44–51.

Schultz M.P., Swain G.W, The Influence of Biofilms on Skin Friction Drag, *Biofouling*, (1999), 15(3), 129–139.

Sekar R., Venugopalan V.P., Satpathy K.K., Rao V.N.R, Laboratory Studies on Adhesion of Microalgae to Hard Substrates, *Asian Pacific Phycology in the 21st Century: Prospects and Challenges*, (1999), 109–116.

Sharma P. K., Rao K.H, Adhesion of Paenibacillus Polymyxa on Chalcopyrite and Pyrite: Surface Thermodynamics and Extended DLVO Theory, *Colloids and Surfaces B: Biointerfaces,* (2003), 29(1), 21–38.

Shen C., Wang L-P., Li B., Huang Y., Jin Y, Role of Surface Roughness in Chemical Detachment of Colloids Deposited at Primary Energy Minima, *Vadose Zone Journal,* (2012), 11(1), 71-78.

Shen Y, Monroy G.L., Derlon N., Janjaroen D., Huang C., Morgenroth E., Boppart S.A., Ashbolt N.J., Liu W.T., Ngugen T.H, Role of Biofilm Roughness and Hydrodynamic Conditions in Legionella Pneumophila Adhesion to and Detachment from Simulated Drinking Water Biofilms, (2015), 49, 7,4274-4282.

Simionato D., Basso S., Giacometti G.M., Morosinotto T, Optimization of Light Use Efficiency for Biofuel Production in Algae, *Biophysical Chemistry,* (2013), 182, 71–78.

Spolaore P., Cassan C.J., Duran E., Isambert A, Commercial Applications of Microalgae, *Journal of Bioscience and Bioengineering,* (2006), 101(2), 87–96.

Spolaore P., Cassan C.J., Duran E., Isambert A, Review Commercial Applications of Microalgae, *Journal of Bioscience and Bioengineering,* , (2006c), 101(2), 87–96.

Sun, Fei Yun, Xiao Mao Wang, and Xiao Yan Li, An Innovative Membrane Bioreactor (MBR) System for Simultaneous Nitrogen and Phosphorus Removal, *Process Biochemistry*, (2006), 48(11), 1749–56.

Sutherland D.L., Williams C.H., Turnbull M.H., Broady P.A., Craggs R.J, The Effects of CO2 Addition along a PH Gradient on Wastewater Microalgal Photo-Physiology, Biomass Production and Nutrient Removal, *Water Research,* (2015), 70, 9–26.

Tang D., Han W., Li P., Miao X., Zhong J, CO2 Biofixation and Fatty Acid Composition of Scenedesmus Obliquus and Chlorella Pyrenoidosa in Response to Different CO2 Levels,

Bioresource Technology, (2011), 102(3), 3071–3076.

Tay J-H., Xu H-L., Teo K-C, Molecular Mechanism of Granulation. I: H$^+$ Translocation-Dehydration Theory, *Journal of Environmental Engineering,* (2000),126(5).

Torkzaban S., Bradford S.A, Critical Role of Surface Roughness on Colloid Retention and Release in Porous Media, *Water Research,* (2016), 88, 274–84.

Travieso L., Benitez F., Weiland P., Sánchez E., Dupeyrón R., Dominguez A.R, Experiments on Immobilization of Microalgae for Nutrient Removal in Wastewater Treatments, *Bioresource Technology,* (1996), 55(3), 181–186.

Ugwu C. U., Aoyagi H., Uchiyama H, Photobioreactors for Mass Cultivation of Algae, *Bioresource Technology,* (2008), 99(10), 4021–4028.

Vandamme D., Foubert I., Muylaert K, Flocculation as a Low-Cost Method for Harvesting Microalgae for Bulk Biomass Production, *Trends in Biotechnology,* (2013), 31(4), 233–239.

Villacorte L.O., Ekowati Y., Calix-Ponce H.N., C.Schippers J., L.Amy G., D.Kennedy M, Improved Method for Measuring Transparent Exopolymer Particles (TEP) and Their Precursors in Fresh and Saline Water, *Water Research,* (2015), 70, 300–312.

Wang B., Q. Lan C., Horsman M, Closed Photobioreactors for Production of Microalgal Biomasses, *Biotechnology Advances,* (2012), 30(4), 904–912.

Wang P., G. Fane A., Lim T-T, Evaluation of a Submerged Membrane Vis-LED Photoreactor (SMPR) for Carbamazepine Degradation and TiO2 Separation, *Chemical Engineering Journal,* (2013), 215–216, 240–251.

Wang P, Lim T-T, Membrane Vis-LED Photoreactor for Simultaneous Penicillin G Degradation and TiO 2 Separation, *Water Research*, (2012), 46(6), 1825-1837.

Wood N. B, A Simple Method for the Calculation of Turbulent Deposition to Smooth and Rough Surfaces, *Journal of Aerosol Science,* (1981) 12(3), 275–290.

Xia L., Li H., Song S, Cell surface characterization of some oleaginous green algae, *J appl phycol,* (2016), 28, 2323-2332.

Xu m., Bernards M., Hu Z, Algae-Facilitated Chemical Phosphorus Removal during High-Density Chlorella Emersonii Cultivation in a Membrane Bioreactor, *Bioresource Technology,* (2014), 153, 383–387.

Yin J., Fan W., Du J., Feng W., Dong Z., Liu Y., Zhou T, The Toxicity of Graphene Oxide Affected by Algal Physiological Characteristics: A Comparative Study in Cyanobacterial, Green Algae, Diatom, *Environmental Pollution,* (2020), 260, 113847.

Yoo C., La H-J., Kim S-C., Oh H-M, Simple Processes for Optimized Growth and Harvest of Ettlia Sp. by PH Control Using CO2 and Light Irradiation, *Biotechnology and Bioengineering,* (2014), 112(2), 288–296.

Yoon S-H., Kim H-S., Yeom I-T, The Optimum Operational Condition of Membrane Bioreactor

(MBR): Cost Estimation of Aeration and Sludge Treatment, *Water Research,* (2004), 38(1), 37–46.

Yuan H., Zhang X., Jiang Z., Wang X., Chen X., Cao L., Zhang X, Analyzing the Effect of PH on Microalgae Adhesion by Identifying the Dominant Interaction between Cell and Surface, *Colloids and SurfacesB: Biointerfaces,* (2019), 177, 479-486.

Zhang X., Jiang Z., Yuan H., Lu Y., Chen L.,Chou A., Yan H., Zhang X, Influence of Surface Zeta Potential on Adhesion of Chlorella Sp. to Substratum Surfaces, *Advanced Materials Research*, (2013), (690–693), 1431–1434.

Zhang X., Zhang Q., Yan T., Jiang Z., Zhang X., Zuo Y, Quantitatively Predicting Bacterial Adhesion Using Surface Free Energy Determined with a Spectrophotometric Method, *Environ. Sci. Technol,* (2015), 49(10), 6164-6171.

Zhang Y., Jia H., Wang X., Ma C., Xu R., Fu Q., Li S, Comparing the Effects of Pre-Deposited and Pre-Mixed Powdered Activated Carbons on Algal Fouling during Ultrafiltration, *Algal Research*, (2019), 44, 101687.

Zhao L., Zhang M., He Y., Chen J., Hong H., Liao B., Lin H, A New Method for Modeling Rough Membrane Surface and Calculation of Interfacial Interactions, *Bioresource Technology,* (2016), 200, 451–457.

Zhen-Feng S., Xin L., Hong-Ying H., Yin-Hu W., Tsutommu N, Culture of Scenedesmus Sp. LX1 in the Modified Effluent of a Wastewater Treatment Plant of an Electric Factory by Photo-Membrane Bioreactor, *Bioresource Technology,* (2011), 102(17), 7627–7632.

Zhongping Y., M.Belu A., Liebmann-Vinson A.L., Sugg H., Chilkoti A, Molecular Imaging of a Micropatterned Biological Ligand on an Activated Polymer Surface, *Langmuir,* (2000), 16(19), 7482–7492.